



UNIVERSITÀ DEGLI STUDI DI MILANO

Ph.D. IN COMPUTER SCIENCE

COMPUTER SCIENCE DEPARTMENT

XXIX CYCLE

MVAR Analysis of iEEG Signals to Differentiate Conscious States

INF/01

Supervisor:

Prof. RITA PIZZI

Candidate:

TERESA RUTIGLIANO

School Director:

Prof. PAOLO BOLDI

A.A. 2016/2017

“Per me l’uomo colto non è colui che sa quando è nato Napoleone, ma colui che sa dove andare a cercare l’informazione nell’unico momento della sua vita in cui gli serve, e in due minuti.”

Umberto Eco.

ABSTRACT

Neuroscience is a highly multidisciplinary and rapidly evolving research field. An important recent challenge of this discipline is the investigation of the so-called connectome. According to its original meaning, connectome is the map of the all brain neural connections. In this framework, the cognitive processes are not seen as localized in specific loci, but stored and processed in a distributed manner. Connectome aims to map and understand the organization of neural interactions trying, at the same time, to explain the role of functional units within the brain system. In particular, one of the most difficult and unsolved tasks in neuroscience is the identification of the areas, connections or brain functions that are called neuronal correlates of consciousness (NCCs).

In this thesis the neural activity was explored by analysing human brain signals acquired during medical procedure. Signals from patients with drug resistant epilepsy were acquired by means of electrodes placed deep in the cortex (intracranial electroencephalography, EEG-iEEG), positioned in order to localize the epileptogenic focus. The technique, called stereotactic EEG (SEEG), guided and flanked by detailed 3D images, also provides for periodical intracranial single-pulse electrical stimulation (SPES) to highlight areas of interest. The continuous recording of the EEG activity took place for several days, and signals were grouped in two datasets: one acquired during wakefulness (WAKE) and the other one during the Non-Rapid Eye Movement sleep (NREM), stage 3.

The signals were processed by means of two methods based on a multivariate autoregressive model (MVAR). The first method was DTF (Directed Transfer Function), that is an estimator of the information flow between structures, depending on the signal frequency; it is able to describe which structure influences another. The second one was ADTF (Adaptive DTF) that permits to study the time-variant signal features, capturing their temporal dynamics. In addition to these connectivity analysis, feature extraction and classification techniques have been employed.

The main aim of the dissertation is to evaluate methods and carry out analyses useful to distinguish between conscious and unconscious states, corresponding to WAKE and NREM respectively, studying at the same time the brain connectivity in response to Single Pulse Electrical Stimulation in intracranial EEG data.

Massimini's group (Department of Biomedical and Clinical sciences "L. Sacco", Università degli Studi di Milano) revealed a different behavior for signals from the two states, WAKE and NREM: they noted a reactivation of the signal around 300 ms after the system perturbation in WAKE and, in contrast, a period of neural silence (down-state) in NREM condition. A hypothesis about the origin of the reactivation phenomenon is a feedback activity, i.e. the result of the activity from the rest of the network. In the thesis, the ADTF method was chosen to shed light on the down-state effect, paying attention to a defined temporal slice of data. The analysis was completed by the application of the DTF procedure, that was chosen to compare the two consciousness states and underline their differences in the frame of network connectivity.

The analysis carried out lead to the following results:

- Indication of useful combinations of features and techniques able to distinguish the states of interest
- Observations of neural connection changes over frequency and time considering causal relationships
- Comparison of connectivity results using different re-referencing styles
- Endorsement of the anatomical-functional importance of some channels corresponding to specialized brain areas.

As conclusion of the analysis it was possible to identify a series of anatomical-functional brain features useful to discriminate the two mentioned states, therefore to speculate on the possibility to differentiate conscious and unconscious states with computational tools.

ABSTRACT (ITALIAN)

Le neuroscienze ricoprono un ambito di ricerca estremamente multidisciplinare e in rapida evoluzione. Un'importante e recente sfida di questa disciplina è l'indagine del connectoma. Secondo il significato originario, il connectoma è la mappa di tutte le connessioni neurali del cervello. Il cervello, in tale contesto, è descritto come una rete dove i processi cognitivi non sono localizzati in una specifica posizione, ma conservati ed elaborati in maniera distribuita. Il connectoma è stato creato con lo scopo di mappare e comprendere l'organizzazione delle interazioni neurali, cercando, allo stesso tempo, di spiegare il ruolo delle unità funzionali del cervello. In particolare, uno dei più difficili e irrisolti sforzi delle neuroscienze è l'identificazione di aree, connessioni o funzioni che sono chiamate NCCs (correlati neurali della coscienza).

Nella tesi l'attività neurale è stata esplorata mediante l'analisi di segnali elettrici cerebrali umani acquisiti durante un intervento medico. I segnali, provenienti da pazienti con epilessia farmaco resistente, sono stati acquisiti mediante elettrodi posti in profondità nel cervello (elettroencefalografia intracranica, EEG-iEEG) con lo scopo di individuare la zona epilettogena. La tecnica, chiamata EEG stereotassica (SEEG), è guidata e affiancata da dettagliate immagini 3D e prevede delle singole, periodiche stimolazioni elettriche (SPES) intracerebrali con lo scopo di evidenziare le aree in esplorazione e di riprodurre alcuni sintomi tipici delle crisi epilettiche. La registrazione continua dell'attività EEG avviene per svariati giorni, il protocollo ha permesso così di raccogliere dati suddivisibili in due datasets: uno acquisito durante i momenti di veglia (WAKE) e l'altro durante la fase 3 del sonno Non REM (NREM).

La rete neurale è stata indagata per mezzo di due tecniche basate su modelli multivariati autoregressivi (MVAR). Il primo metodo impiegato è stato Directed Transfer Function (DTF) ovvero uno stimatore del flusso di informazioni tra strutture, dipendente dalla frequenza del segnale; DTF è in grado di descrivere quale struttura influenza l'altra. Il secondo metodo è stato ADTF (Adaptive DTF) che consente di studiare le caratteristiche del segnale tempo-variante, catturando le dinamiche temporali. Oltre a queste analisi di connettività, sono state considerate e impiegate tecniche di estrazione e classificazione delle caratteristiche (feature extraction techniques).

L'obiettivo principale della tesi è quello di valutare metodi e condurre analisi utili a distinguere gli stati coscienti da quelli non-coscienti, rispettivamente WAKE e NREM, e, allo stesso tempo, studiare la connettività cerebrale in risposta alla stimolazione elettrica in dati provenienti da EEG intracranico.

Il gruppo di ricerca del Prof. Massimini (Dipartimento di Scienze Biomediche e Cliniche "L. Sacco", Università degli Studi di Milano) ha rilevato un comportamento diverso per i segnali dei due stati WAKE e NREM: è stata notata una riattivazione del segnale intorno a 300 ms dopo la perturbazione del sistema in WAKE e, al contrario, un periodo di silenzio neurale (down-state) nella condizione NREM. Un'ipotesi del fenomeno di riattivazione è un'attività di feedback, cioè il risultato dell'attività dalla restante parte della rete. In questa tesi, il metodo ADTF è stato scelto per far luce sull'effetto down-state prestando attenzione ad una fetta temporale definita di dati; mentre il metodo DTF è stato scelto per evidenziare la connettività della rete, confrontando i risultati tra i due stati di coscienza.

L'analisi effettuata ha portato ai seguenti risultati:

- Indicazione di combinazioni di caratteristiche e tecniche utili a distinguere gli stati di interesse
- Osservazioni sulla cambiamenti delle connessioni neurali in base alla frequenza e al tempo considerando i rapporti causali
- Confronto dei risultati di connettività utilizzando diversi stili di montaggio
- Approvazione dell'importanza anatomico-funzionale di alcuni canali corrispondenti a aree cerebrali specializzate.

A conclusione dell'analisi è stato possibile identificare una serie di caratteristiche anatomico-funzionali utili a discriminare i due stati menzionati, quindi a speculare sulla possibilità di differenziare stati consci e inconsci mediante strumenti computazionali.

TABLE OF CONTENTS

ABSTRACT	v
ABSTRACT (ITALIAN)	vii
TABLE OF CONTENTS	ix
LIST OF FIGURES AND TABLES	xi
1 INTRODUCTION	1
1.1 Connectome and Connectivity.....	1
1.2 Connectivity and consciousness	2
1.3 Wakefulness/NREM sleep detection: state-of-the-art	5
1.4 Description of ERP, Cortico-Cortical Evoked Potentials (CCEP), down-state and feedback activity.....	7
1.5 Aims and Methods employed	11
2 CONNECTIVITY ESTIMATORS: THEORY	13
2.1 Multivariate Autoregressive Models	13
2.2 Directed Transfer Function (DTF)	15
2.3 Adaptive Directed Transfer Function (Time Varying) (ADTF).....	16
2.3.1 Kalman Filter	17
2.4 The nonparametric method to assess the significance of the estimated connectivity measures	19
3 CONNECTIVITY ANALYSIS: DTF and ADTF	21
3.1 Data pre-processing and channels selection	23
3.2 Evaluation of Directed Transfer Function results over frequencies in Gamma and Delta bands	31
3.2.1 Results in Gamma band	32
3.2.2 Results in Delta band	37
3.2.3 Comparison between Gamma and Delta	43
3.3 Time Varying Directed Transfer Function results over frequencies in Delta and Gamma bands	46
3.3.1 Statistical Analysis on windowed data	53
3.3.1.1 Delta Band	54
3.3.1.2 Gamma Band	57
3.3.1.3 Original Signals	61
3.4 Conclusions	67
4 ADDITIONAL RESULTS	71
4.1 NREM and WAKE classification by means of feature extraction methods....	71

4.2	How much the re-referencing style can affect the connectivity result? Comparison between three different styles	74
4.3	Conclusions	79
5	SUMMARY AND CONCLUSION	81
	ACKNOWLEDGEMENTS	87
	REFERENCES	89

LIST OF FIGURES AND TABLES

Figure 1. 16 representative seconds of a raw iEEG signal (first channel, subject number one, bipolar montage) in both WAKE and NREM condition. Here 15 stimulation sessions, with the corresponding impulses, are reported. The impulsive signals characterize the instants of the electrical stimulations. Epoch, in our definition, is the signal recorded in the 800 ms after each stimulation..... 24

Figure 2. Representative CCEP from pre-processed signal (first channel, subject number one, bipolar montage) in both WAKE and NREM condition. Minimum and maximum values of the signal in each epoch over time for one channel..... 25

Figure 3. DTF Values in Gamma Frequency Band after average. DTF values are reported in the square matrix 8x8, colour bar indicates the DTF levels (0-1, from Blue to red respectively). On the axes the 8 channels are represented, the information flow goes from j channels (x axis) to i channels (y axis). Left column: the five subjects in WAKE state; right Column: the five subjects in NREM state..... 35

Figure 4. DTF Values in Delta Frequency Band after average. DTF values are reported in the square matrix 8x8, color bar indicates the DTF levels (0-1, from Blue to red respectively). On the axes the 8 channels, where the information flow goes from j (x axis) to i (y axis). Left column: the five subjects in WAKE state; right Column: the five subjects in NREM state. 40

Figure 5. ADTF values in Gamma band for subject 1. DTF values in sink channels 1,2,3. On the x axis the 8 source channels are reported. On the y axis the time series of 800 ms is shown. Column a. for WAKE and column b. for NREM..... 47

Figure 6. ADTF values in Delta band for subject 1. DTF values in sink channels 1,2,3. On the x axis the 8 source channels are reported. On the y axis the time series of 800 ms is shown. Column a. for WAKE and column b. for NREM..... 48

Figure 7. ADTF values in Delta band for subject 1. Only 3 channels are here reported. Panel A shows ADTF values in WAKE, Panel B the ADTF values in NREM. Every coloured lines indicate

a source channel, in x axis a window of the time series is reported: the first 200 ms where the down-state is expected (159 ms).....50

Figure 8. ADTF values in Delta band for subject 2. Only 3 channels are here reported. Panel A shows ADTF values in WAKE, Panel B the ADTF values in NREM. Every coloured lines indicate a source channel, in x axis a window of the time series is reported: the first 200 ms where the down-state is expected (135 ms).....51

Figure 9. ADTF values in Delta band for subject 3. Only 3 channels are here reported. Panel A shows ADTF values in WAKE, Panel B the ADTF values in NREM. Every coloured lines indicate a source channel, in x axis a window of the time series is reported: the first 200 ms where the down-state is expected (108 ms).....52

Figure 10. Normal probability plot of the 4 input groups in Delta band. Group one in Blue, group two in orange, group three in yellow, group four is violet.....55

Figure 11. Boxplot of data into the groups (Delta Band). 4 Groups: 1) means calculated on window before the down-state in WAKE situation; 2) means calculated on window after the down-state in WAKE situation; 3) means calculated on window before the down-state in NREM situation; 4) means calculated on window after the down-state in NREM situation55

Figure 12. Two-way ANOVA Table result in Delta Band55

Figure 13. ANOVA conclusive analysis: multicomparison between groups (Delta band). 4 Groups: 1) means calculated on window before the down-state in WAKE situation; 2) means calculated on window after the down-state in WAKE situation; 3) means calculated on window before the down-state in NREM situation; 4) means calculated on window after the down-state in NREM situation.....56

Figure 14. Dendrogram from MANOVA statistics. (Delta band) Clusters are computed by applying the single linkage method to the matrix of Mahalanobis distances between group means.....57

Figure 15. Normal probability plot of the 4 input groups in Gamma band. Group one in Blue, group two in orange, group three in yellow, group four is violet.....58

Figure 16. Boxplot of data by groups (Gamma Band). 4 Groups: 1) means calculated on window before the down-state in WAKE situation; 2) means calculated on window after the down-state in WAKE situation; 3) means calculated on window before the down-state in NREM situation; 4) means calculated on window after the down-state in NREM situation..... 58

Figure 17. Two-way ANOVA Table result in Gamma Band..... 59

Figure 18. ANOVA conclusive analysis: multicomparison between groups (Gamma band). 4 Groups: 1) means calculated on window before the down-state in WAKE situation; 2) means calculated on window after the down-state in WAKE situation; 3) means calculated on window before the down-state in NREM situation; 4) means calculated on window after the down-state in NREM situation..... 59

Figure 19. Dendrogram from MANOVA statistics (Gamma band). Clusters are computed by applying the single linkage method to the matrix of Mahalanobis distances between group means..... 60

Figure 20. Characteristics of four iEEG signals before (panel A) and after (panel B) the down-state in a representative subject during WAKE 62

Figure 21. Characteristics of four iEEG signals before (panel A) and after (panel B) the down-state in a representative subject during NREM..... 63

Figure 22. Boxplot on windowed data using original signals, not from DTF analysis. The mean values collected after the possible down-state are subtracted to the mean values collected before the possible down-state. The two states WAKE (1) and NREM (2) are considered..... 64

Figure 23. Normal probability plot of the 4 input groups in original signals. Group one in Blue, group two in orange, group three in yellow, group four is violet. 65

Figure 24. Two-way ANOVA table result in original signals..... 65

Figure 25. ANOVA conclusive analysis: multicomparison between groups (Original signals). 4 Groups: 1) means calculated on window before the down-state in WAKE situation; 2) means

calculated on window after the down-state in WAKE situation; 3) means calculated on window before the down-state in NREM situation; 4) means calculated on window after the down-state in NREM situation66

Figure 26. Dendrogram from MANOVA statistics (Original signals). Clusters are computed by applying the single linkage method to the matrix of Mahalanobis distances between group means66

Table 1. For every human subject 8 channels have been selected for the analysis. For every channel the anatomical position is here reported. Anatomical definition is according to the Destrieux Atlas [76]. In the “3D position” column the position in the space (xyz) is calculated for each electrode according to the NMRI data of the subject. In 3D column the relative positions are shown i) between electrodes and ii) between electrodes and the stimulation site (SS).29

Table 2. List of macro areas involved in the project.30

Table 3. Considering the average of the Gamma frequency band, here, some data are reported: i) subject, ii) minimum and iii) maximum of the matrix, iv) threshold (corresponding to 95^opercentile) and v) connections that exceed the threshold. DTF values in WAKE (A) and in NREM states (B).36

Table 4. Connections over 95percentile and anatomical correspondence in WAKE (A) and NREM (B). °indicates the frontal lobe, ^ indicates the Brodmann’s areas, * indicates parietal areas.36

Table 5. Considering the average of the Delta frequency band, here, some data are reported: i) subject, ii) minimum and iii) maximum of the matrix, iv) threshold (corresponding to 95percentile) and v) connections that exceed the threshold. DTF values in WAKE (A) and in NREM states.41

Table 6. Main connections and anatomical correspondence in WAKE (A) and NREM (B). °indicates the frontal lobe, ^ indicates the Brodmann’s areas, * indicates parietal areas.42

Table 7. Main connection directions represented by arrows: yellow for WAKE and blue for NREM	45
Table 8. ANN classification: Average and standard deviation evaluated on the test set, computed over 10 runs (Sensitivity: the true recognition of wakefulness).....	73
Table 9. Average and standard deviation of AUC of the NN outputs computed over 10 runs.....	73
Table 10. DTF analysis in three re-referencing styles BP, CW, MA. In Tables A, B, C results from the three re-referencing styles in WAKE condition. D, E, F results from the three re-referencing styles in NREM condition.....	78

1 INTRODUCTION

1.1 Connectome and Connectivity

One challenge of neuroscience is understanding the complex, physiological and functional mechanisms that may define and recognize complex cognitive tasks [1].

Biologists, physicians, anatomists, biomedical engineers and neuroscientist have investigated the nature of the brain since the most ancient times. Recently, an important step was the first tentative human connectome map generated in 2005 by the computational cognitive neuroscientist Olaf Sporns [2][3][4] 2005, followed in 2008 by the finding of connections linking distinct regions of the cortex noted using MRI [5].

Connectome is of a fundamental importance in cognitive neuroscience and neuropsychology: individual connectomes display unique structural features that might explain differences in cognition and behavior.

The brain connectivity could be analyzed on large scale and on a small-scale level.

- Large-scale level consists of connections between cortical areas,
- Small-scale level consists of connections between neurons, linked by synapses, or of cortical columns, linked by inter-columnar connections.

The anatomical description of brain leads to three distinct levels of organization [4]:

- Single neurons and synapses (microscale),
- Neuronal groups or populations (mesoscale),
- Anatomically distinct brain regions and inter-regional pathways (macroscale).

An advantage of microscale analysis is that single elements are relatively easy to recognize and demarcate, the disadvantage for connectivity studies is that plasticity of cells and variability of connections are not considered. On the other hand, mesoscale does not provide information on functional divisions and processing capabilities, because it reflects the local anatomy functions [6]. The combination of different analysis techniques, such as diffusion-weighted imaging combined with spatially registered high-resolution anatomical and activity data (e.g., electroencephalography, magnetoencephalography) obtained within the

same individual subject, is a good way for mapping the human connectome at the macroscale. The probabilistic connectivity voxel map contains approximately 10^4 – 10^5 elements and 10^5 – 10^7 structural connections. The map permits to provide information not only on the large-scale connection patterns, but also on parcellation of human cortex. This technique permits to generalize the voxel-based connectivity matrix and it can be cross-referenced with existing referencing templates and with published brain atlases (that is not possible at the mesoscale level) [4].

Connections are also distinguished in anatomical (or structural) [7], functional and effective:

- Structural connections typically correspond to white matter tracts between pairs of brain regions. The structural (anatomical) connectome maps the neuronal pathways and it constitutes a major research topic in the neuroscience field, as it is the key to understand both brain physiology and pathology.
- Functional connections coincide with the activity of correlations in time; these kind of connections can be observed also between pairs of anatomically unconnected regions. Functional connectivity might reflect linear or nonlinear interactions; the observation is dependent on the measure applied [8], and refers to a pattern of statistical dependencies.
- Effective connections underline direct or indirect causal influences and may be estimated from observed perturbations of the system [9]. Effective connectivity depends on structural connectivity [7].

In the proposed dissertation we applied causal measures of functional connectivity.

1.2 Connectivity and consciousness

Connectivity model describes statistical or causal relationships measured as cross-correlations, coherence, mutual information. Functional connectivity studies have provided evidences for the organization of functional brain networks, e.g.:

- Matsumoto et al. [10] analysed cortico-cortical evoked potential (CCEP) in electrocorticograms (ECoGs) data revealing important connections in language organization.

- Schrouff et al. [11] noted that functional connectivity was affected in parietal areas and frontal or temporal regions during deep sedation. They computed functional integration and partial correlations on fMRI (Functional Magnetic Resonance Imaging) data.
- Antony et al. [12] analysed intracranial EEG data with a correlation-based measure to identify epileptogenicity and to predict the outcome of epilepsy surgery.
- Brovelli et al. [13] applied to EEG as well as fMRI time series Granger causality. They provided information about directed interactions between neural elements during behavioral and cognitive tasks.

Main aim of the dissertation is to understand neural signatures of consciousness by means of functional connectivity.

In the Cambridge Dictionary it is possible to find the following definition of wakeful: “*not able to sleep, or used to describe a period of time when you are not able to sleep*”. But what does sleep stand for? In a dictionary sleep means “*the resting state in which the body is not active and the mind is unconscious*”. The first philosopher who used the term *conscientia* was René Descartes. Historically philosophers used 'consciousness' with four main meanings: knowledge in general, intentionality, introspection and phenomenal experience. But we have no objective or rational method to evaluate its existence or to measure it. Usually, we evaluate the level of consciousness thinking of the capacity to interact with other people and with the external environment in general. fMRI studies revealed the we are not able to define and detect consciousness when it is not expressed through gestures and words even if we cannot exclude the presence of some kind of consciousness [14][15] also in absence of fMRI evidences. This is also true for some pathological situations when patients cannot communicate.

From a medical point of view, it is known that the removal of cerebral cortex and thalamic nuclei is related to consciousness damage. A cerebellum resection, instead, leads just to coordination problems. We have not a robust way yet to extract from the brain an index for the grade of consciousness, although some first results are emerging. In any case, neuroscience can only investigate the before mentioned neural correlates of consciousness (NCCs), as the nature of our subjective experience is beyond the possible achievements of neuroscience.

Over the last decade many theories on consciousness have been formulated regarding the NCCs. A recent and authoritative one, the Integrated Information Theory (IIT) by Giulio Tononi [16][17], aims to explain the mechanism underlying consciousness as a neural integration within the brain [18][19]. Following this theory, consciousness is due to the brain ability to sustain complex patterns of internal communication; thus it is not only correlated to specific patterns of synchronous activity, or to the ability to respond to inputs, or to the level of its activation. Consciousness is given by the activation of multiple, specialized regions of the thalamo-cortical system able to interact as a single entity (integration) and able to discriminate information [20].

Tononi proposed Phi (Φ , where the vertical bar stands for information and the circle for integration) as a consciousness index. A perturbation induces rapid changes in pattern activity creating information and affecting large portions of the cerebral cortex (integration) in thalamo-cortical system during the conscious state. In the unconscious state, in opposite, a stereotyped (low information) and local (poor integration) activation is detectable [20][21]. The only cerebral structure with high Φ is the thalamo-cortical system, because it is organized in such a way as to emphasize functional specialization and integration [22]. In cerebellum, instead, modules are segregate and give no rise to significant information content.

Casali et al. [23] proposed a theoretically based measure of consciousness (PCI) which provides a data-driven metric that can discriminate the level of consciousness. PCI method considers both the information content and the integration of the corticothalamic system; measuring the complexity of the brain in response to a perturbation. Phi and PCI are just examples of a possible index of consciousness, an index that is really not easy to establish.

It is possible to detect differences between conscious and unconscious states also comparing signal waves in a neural network. In literature, the thalamo-cortical system, in unconscious states, despite being active and reactivated after a perturbation of the network, was observed: i) a breaking down during time or ii) a non-specific response responsible of slow waves. This phenomenon is known as down-state, which correspond to a decrease in signal power and neuronal firing [21][20][24][25]. From a chemical point of view the down-state is characterized by hyperpolarizing potassium currents, as well as by low synaptic activity [26].

The already cited Massimini's group carried out studies by means of two techniques: a

combination of transcranial magnetic stimulation (TMS) and high-density EEG (hd-EEG)[20] [27] [28], and intracranial single-pulse electrical stimulation (SPES) with simultaneous stereotactic EEG (SEEG) recordings, where electrodes are placed deep into the cortex (intracranial EEG-iEEG) [21]. They observed that during wakefulness (WAKE) and REM (Rapid Eye Movement sleep) (that are considered both as conscious states) the brain sustains long-range patterns of activation, whereas during NREM (Non-Rapid Eye Movement sleep) and Midazolam-induced anesthesia (when consciousness fades) this feature is lost (more information on sleep staging are reported in the section 1.3). Pigorini et al [21] compared CCEPs (cortico-cortical evoked potentials) recorded during wakefulness (WAKE) and NREM sleep (NREM) by means of time–frequency analysis. During WAKE, SPES triggers a chain of effects that last for at least 500 ms, while during NREM the same initial activation induces a slow wave and a cortical OFF-period in its cortical targets. The perturbation in WAKE is followed by a composite set of waves, notably a silent down-state upon transient increases in activation; in NREM the reactivation effect is not present.

Massimini et al. [20] hypothesized that the breakdown of complex interactions observed during NREM is not due to the interruption of structural cortico-cortical and/or cortico-subcortico-cortical connections, but rather to changes in the dynamics of neuronal responsiveness. So, a possible explanation of the re-activation, observable in WAKE and not in NREM, could be a trace from the rest of the network that we can call “feedback wave”.

1.3 Wakefulness/NREM sleep detection: state-of-the-art

As above mentioned, stable consciousness is generally intended as the subjective experience during wakefulness (WAKE) and in REM sleep, but this experience is lost during NREM sleep, some kinds of anesthesia and coma [20] [27]. However, there is no general agreement of the meaning of the term “consciousness”. The sleep cycle is an alternation of NREM (non-rapid eye movement, non-REM) and REM (rapid eye movement), this cycle lasts for 90 minutes and occurs 4/6 times in a good night's sleep [29]. NREM is then divided into three stages: N1, N2, and N3 (delta sleep or slow-wave sleep) [30]. The deep sleep (stage N3) is predominant earlier in the night, while REM sleep is just before the natural awakening [29].

Wakefulness and NREM/REM sleep are two different behavioural states and shows different physiological situations: during sleep body temperature and heart rate fall and the brain uses less energy. Wakefulness and NREM/REM sleep stages differ in autonomic nervous system and hemodynamic regulation; changing in pulse amplitude waves and breathing can reflect these differences.

Wakefulness, REM and NREM could be differentiated by the use of [31]:

- Actigraphy.
- Peripheral arterial tone (PAT): a reduction of the PAT amplitude is observable in REM compared to NREM.
- Photoplethysmography (PPG): signal derived from pulse oximetry, the similarity of consecutive breath pattern and the complexity of their rhythm are indicative of the two states.
- PPG associated to Polysomnography (PSG, EEG recordings).
- PSG associated to electrooculography (EOG), respiratory effort, blood oxygen saturation, electrocardiograms (ECG).
- The gold standard for assessing sleep in humans is the analysis of brain-wave patterns (EEG).

In literature, some ways proposed for WAKE/sleep classification used data from wearable disposable. As example: Orellana et al. [32] extracted features and used an Artificial Neural Network (ANN) as classifier on night wrist actigraphic (ACT) data.

Karlen et al. [33] applied a fast Fourier transform to extract features on which applied an artificial neural network as a classifier on cardiorespiratory signals.

Some authors proposed the use of noninvasive techniques to be adopted especially for infants: they explored the possibility of classification by means of techniques applied on electrocardiogram (ECG) data [33]. Conscious states are classified using heart rate variability [34].

Literature on automatic classification of NREM sleep/wakefulness applied to iEEG data is still limited. In fact, iEEG data have been widely used for epileptic seizure detection and prediction. Often, as in our case, the identification of sleep stages is performed by visual inspection of expert neurologists. To the best of our knowledge just two papers reported automatic sleep scoring on iEEG: a very recent one used the vigilance index-based

algorithm [35], while the older one employed spindles activity in iEEG for manual sleep recognition [36].

Moreover, we have few information about the use of connectivity models, employed as feature extraction tool for the distinction between states, on iEEG data. Noteworthy are the following studies: Gaillard et al. [37] identified four markers associated to conscious word processing (pattern of neural activity was characterized by coherence modifications between cortex areas); Chang et al. [38] used the multivariate autoregressive model with exogenous inputs (MVARX) to assess changes in the level of information integration between wakefulness and deep sleep in human subjects (they observed that integrated information is higher in wakefulness than sleep for each subject/condition).

However, iEEG technique has a high resolution in time and space, and the evidence of

- i) a peculiar region, or of
- ii) an interesting channel, or of
- iii) the network behavior in time

could be useful to distinguish the two consciousness states.

In this work we performed connectivity analysis and applied feature extraction (FE) methods on iEEG signals under electrical stimulations to distinguish between NREM sleep and wakefulness statuses in epileptic patients.

1.4 Description of ERP, Cortico-Cortical Evoked Potentials (CCEP), down-state and feedback activity

In an electrophysiology experiment the signal measured by an electrode represents an extracellular field potential obtained from the weighted sum of all current sinks and sources along multiple cells. The extracellular field potentials recorded under these conditions are related both to integrative processes (dendritic events) and to spikes generated by several hundreds of neurons. Two different signal types can be segregated by frequency band separation: a high-pass filter (300-500 Hz) is used to obtain multiple-unit spiking activity, and

a low-pass filter (< 300 Hz) to obtain the so-called local field potentials (LFPs). LFPs reflect the cooperative activity in neural populations. They are represented by slow waveforms and include i) synaptic potentials, ii) after-potentials of somato-dendritic spikes, iii) voltage-gated membrane oscillations. LFPs reflect the input of a given cortical areas as well as its local intra-cortical processing [39].

EEG is an electrophysiological monitoring method to record electrical activity of the brain. Brain electrical potentials can be classified as:

- Potential of spontaneous activity,
- Evoked potential,
- Potential of bioelectric events caused by individual neurons.

Electrocorticography and electroencephalography measure spontaneous activity on cortex or scalp surface, respectively. In spontaneous activity the maximum amplitude of EEG potentials may be $10\text{-}100\ \mu\text{V}$ in electroencephalography or $300\ \mu\text{V}$ in electrocorticography.

Evoked potentials have small amplitude compared to spontaneous activity. Level of activity is comparable to the noise level thus evoked potentials are not easy to detect. Evoked potentials are due to the response to a stimulus (visual, tactile, auditory, electrical...). The evoked brain response is synchronous with the event, while the spontaneous background activity oscillates randomly during and around the event.

The bioelectric events are caused by single neurons and are recorded using microelectrodes implanted directly in the cells of interest. Their resting membrane potential is $-70\ \text{mV}/+35\ \text{mV}$.

In order to allow the study of the evoked potentials, stimulation pulses are typically used so that a multiple record can be performed and the average of these recordings can be done. The average, coming from multiple recordings after the perturbation of the system, is essential to underline the difference between the signal and the noise. The average response is called the event related potential (ERP). Detailed analysis of ERP aims to extract repeatable components related to the event. The ERP components (positive and negative peaks) can be traced back to the various stages of sensory or event-related information processing.

Cortico-cortical evoked potentials [40] (CCEP) are generated by:

1. the activation of the superficial dendritic tree of pyramidal cells in the external granular/pyramidal, internal pyramidal, and/or multiform layers;

2. the downward propagation of local responses through their axons to connected regions through cortico-cortical and cortico-subcortical projections [41].

CCEP are useful to represent cortico-cortical connections. A recent review [41] on CCEP reported that this method has been applied in TMS and SPES study in order to investigate excitatory and inhibitory mechanisms of the cortex in humans. Kunieda et al. [41] reported that this technique is advantageous and capable of evaluating cortical structures, up to 1 cm spatial resolution, in case of subdural electrodes implantation, deep structures with a high spatial resolution (up to 5 mm) in case of SEEG, directional dependence in signal propagation with a high temporal resolution in the order of millisecond, and propagation patterns modulated by external stimuli.

As already mentioned, this dissertation aims to find a possible explanation of re-activation phenomenon that occurs in wakefulness, but not in NREM sleep (N3), hypothesizing that the re-activation is a feedback activity from the rest of the network. For this purpose, a review from literature is reported.

Neurons, electrically excitable cells, respond to the synaptic input producing a local change in the membrane potential. The change in the electric field is due to ion channels (chemically or voltage gated) placed on the membrane, changes in conductance (e.g. caused by potassium currents) induce two possible states: hyperpolarized (down-state) and one more depolarized (up-state). Depolarization and hyperpolarization are departures from the resting potential: in the first condition the interior cell voltage becomes less negative, in the second condition the interior cell voltage becomes more negative.

The cycling ($< \sim 1$ Hz) between up (intense synaptic activity) and down (almost complete silence) states constitutes the *slow oscillation*. Steriade [42] characterized the *slow oscillation* as a global and synchronized network phenomenon in cortical and thalamic network in 1993. Considering the phenomenon in a local cortical network (few tens of millimeters), cortical neurons synchronously depolarize and hyperpolarize with phase delays less than an order of magnitude of the oscillation period [43]. This delay depends upon the activity of horizontal axon collaterals of cortical pyramidal cells [25]. The *slow oscillation* phenomenon is still under investigation.

In the past years the low-voltage fast activity in EEG recordings, performed during attentive tasks, was an electrophysiological marker of consciousness. Nowadays, thanks to intracellular recordings, the transition from the low-voltage fast activity (characteristic of

wakefulness) to the high-voltage slow activity (slow waves), characteristic of sleep and some forms of anesthesia, is another marker of consciousness. The detection of high-amplitude slow waves ($>75 \mu\text{V}$) is an approved method to assess the loss of consciousness in humans. One of the main hypotheses regarding the role of these slow-waves is the memory consolidation.

iEEG signals are composed of repeated waveforms consisting of oscillation between periods of intense firing (up-states) and periods of neuronal silence (down-states), as previously explained. The perturbation of the system in wakefulness induces a composite set of waves, notably a silent down-state upon transient increases in activation; in NREM the reactivation effect is not present (the interested reader can find figures of the phenomenon in [24] [21]). The generally known feature of NREM sleep, differently from wakefulness, is the association of EEG slow waves with a period of down-state. The possible explanation of the up-state termination (and, so, the possible cause of the down-state instauration) is the role of inhibitory interneurons. At the same time, the possible explanation of the up-state re-instauration, only in wakefulness and not in NREM, could be the feedback effect due to the descending connections. Feedback is an instructive signal that could be excitatory or inhibitory, and both these signals participate to the plasticity of the network. Feedback involves the simultaneous exchange of signals among multiple dispersed neuronal populations, and it is the effect of the resultant activity of the network.

In literature, the different signal behaviors according to the two conscious states are reported, among other authors, by Cash et al. [24], that showed the detection of cortical down-state as a significant suppression of high frequency power in the Local Field Potential, and Pigorini et al. [21], that compared CCEPs recorded during wakefulness and NREM by means of time–frequency analysis and PLF (phase locking factor) from SPES-iEEG signals. They observed that PLF measured during wakefulness remained significant up until ~ 500 ms after the perturbation, while during NREM the same initial activation induces a slow wave and a cortical OFF-period after ~ 200 ms.

To try to confirm these hypotheses, we analyzed *in vivo* single-pulse electrical stimulation (SPES) and cortico-cortical evoked potential (CCEP) to track the behavior of brain networks in different states, frequencies, times and subjects, using and comparing a set of different dynamic models analyses.

1.5 Aims and Methods employed

In order to evaluate how the complex brain network changes during different levels of consciousness we worked on intracranial electroencephalographic data (iEEG) in response to single-pulse electrical stimulation (SPES) obtained from human patients, awoken (WAKE), in presence of stable consciousness, and during loss of consciousness, in NREM sleep, stage 3 (NREM). Deeper NREM (stages 3 to 4) is characterized by the predominance of slow waves: *slow oscillation* between periods of intense firing followed by the already explained down-state [44].

In this dissertation NREM and WAKE states are investigated with the aim to shed light on these specific questions:

- ✓ How to define the meaning of the down-state and re-activation phenomena? Is the re-activation a feedback activity as specified above?

We used connectivity measures based on the mathematical properties of the linear autoregressive process (AR) in order to estimate spectral quantities. We joined observations on the path and information flow of iEEG signals by means of Directed Transfer Function (DTF) and Adaptive Directed Transfer Function (ADTF-time varying). DTF/ADTF are a frequency-domain and time-frequency-domain estimators of causal interactions based on the multivariate autoregressive (MVAR) modeling [45] [46]. Through the spectral density they get information on the interdependence between signals and characterized the direction of the interactions between them.

EEG waveforms are subdivided into Alpha, Beta, Theta, Delta and Gamma frequency range; we performed MVAR analysis by examining changes in spectral density across Delta (0.5-4 Hz) and Gamma (30-100 Hz) because these are considered the frequencies most representative of the two different conscious states. In fact, NREM sleep, stage 3, is also called slow wave sleep because Delta waves prevail; and Gamma oscillations have functional role in human episodic memory (which stores spatial and temporal information and can be retraced) [47] and cognitive functions.

- ✓ How to assess parameters that correlate with the level of consciousness?

We explored the brain network by means of time-frequency analysis and wavelet feature extraction to obtain workable instruments to discriminate the two states. We

investigated the performance of such features to distinguish NREM sleep and wakefulness states in epileptic patients. We preliminarily screened the data using standard deviation analysis (STD), then we compared and combined STD values with coefficients from Wavelet decomposition (Daubechies mother wavelet). Parameters were classified using an Artificial Neural Network. MVAR Analysis is the core of the dissertation, but in a parallel investigation we obtained interesting and common results using feature extraction methods (FE) on the same iEEG dataset, although preprocessed in a different way.

✓ How to evaluate differences obtained using several re-reference styles?

In absence of a theoretical way for selecting the correct re-reference style, DTF results coming from three re-reference methods were compared. Three montages methods selected are: i) subtraction of the signal coming from the adjacent contact (bipolar) [24]; ii) subtraction of the signal from the closest electrode placed into the white matter (CW) [48]; iii) subtraction of the average of all contacts (moving average) [49].

The dissertation is organized as follows:

- Introduction of connectivity and consciousness.
- Introduction of down-state and re-activation phenomena.
- Description of iEEG signals.
- Short theoretical review of the principal connectivity estimators; description of MVAR, DTF/ADTF mathematical approaches.
- Application of DTF and ADTF on the dataset and main results.
- Comparison between connectivity results and findings obtained by other Feature Extraction techniques.
- Demonstration of the impact of the re-referencing style on connectivity analysis.
- Reading of the applied methods and results to identify a possible approach to distinguish different conscious states.

2 CONNECTIVITY ESTIMATORS: THEORY

Understanding of mental processes requires not only the localization of the structures involved, but also the comprehension of their mutual relationships. In particular, more biological signals are acquired at the same time: the study of their interdependence could help to understand the role of systems that has created them using Multivariate Analysis (MA). MA takes in consideration not only the observation of some indices (e.g. study of the time series in a particular locus) regarding the activity in exam, but also the interaction between such indices (e.g. how cortex areas work together). MA, that we will use in the form of multichannel autoregressive models, is capable to identify the causal relationships between signals allowing to recognize the direction of propagation [50].

Connectivity estimators can be linear or non-linear. Linear methods (e.g. Directed Transfer Function, Autoregressive models) are very robust to noise [51] , and in the case of EEG signals result to reach good performances even in comparison with non-linear techniques [50].

Autoregressive models (AR) are used to describe stochastic processes and in particular are useful to model time series; they are linear predictors that estimate the variable of interest using past values of the variable.

2.1 Multivariate Autoregressive Models

In a multivariate (MV) autoregressive model (AR) (MVAR) the connectivity pattern is obtained on the basis of a unique model estimated on the whole set of signals, that accounts for all their reciprocal interactions. An MVAR model allows to derive time/frequency domain images by using model coefficients and their spectral properties, respectively [52] [53].

Let be $y(t)$ a vector of stochastic, stationary and ergodic processes with t number of samples per each process. A multivariate autoregressive model of order p is defined as [54]:

$$y(t) = -\sum_{k=1}^p A(k)y(t-k) + u(t) \quad (1)$$

where $y(t) = [y_1(t), y_2(t), \dots, y_N(t)]^T$ is the vector containing the N scalar processes at the time t and T is the transpose operator. p is the model order that represents the number of the previous outputs involved in the description of the current output. $A(k)$ is the matrix $N \times N$ with coefficients from the AR model at the lag k , $u(t)$ is a zero-mean white noise process with non-singular covariance. Element $a_{ij}(k)$ of the $A(k)$ matrix describes the dependence of $y_i(t)$ on $y_j(t-k)$.

The MVAR model describes the value of each time series at the instant t as the weighted linear sum of the $t-1, \dots, t-p$ previous values from all inputs with weights given by the coefficients a_{ij} . Coefficients on the diagonal reflect the weight that each signal has in its future self-description (auto-influence), while other elements describe cross-influences. The input covariance matrix is diagonal because the individual input processes are assumed to be uncorrelated with each other.

The best order number choice is made by i) using the parsimony principle (the order number has to be the lowest possible) then ii) performing the whiteness test of the prediction error to validate the system. The model order p , used in the tests, has been determined using the final prediction error (FPE) criterion [55] and Schwarz Bayesian criterion (SBC) [56].

Two basic conditions, regarding the data y and its association to the MVAR p model, are stability and stationarity. A stochastic process is weakly stationary if its first and second moments (mean and covariance) do not change with time. When causality analysis is based on MVAR non-stationary time series it can produce spurious regression artifact [57]. In order to overcome the problem, time series can often be rendered stationary through transformations [58] such as:

- using the first derivative of the time series rather than the raw values [36].
- modelling the non-stationary components of time series and subtracting them from the observed values (through the linear detrend).
- performing analysis over short windows during which time series may be locally stationary (series of short overlapping or not overlapping windows) [59].

In our analysis DTF analysis AR models were estimated in every short temporal sliding windows where the process is assumed to be (locally) stationary [60] [61]. The stationarity assumption can be neglected if analyses are applied to a point in time (e.g. in Adaptive

Directed Transfer Function): in fact, the causal influence can be calculated at each time point. Possible approaches that permit to observe each time points are:

- Regressive least squares with forgetting algorithm to calculate autoregressive parameter [62][63],
- Kalman filter techniques used for larger models [64][65][45].

2.2 Directed Transfer Function (DTF)

The Directed Transfer Function (DTF) is a frequency–domain estimator of causal interaction based on the MVAR modelling. By the use of spectral density, it is possible to obtain information on the interdependence between signals.

Eq. 1 can be rewritten in the frequency domain as:

$$A_{ij}(f) = \sum_{k=1}^p a_{ij}[k] e^{-j2\pi f T k} \quad (2)$$

that is the Fourier transform of $a_{ij}[k] = [a_{ij}[0], a_{ij}[1], \dots, a_{ij}[p],]$; $a_{ij}[k]$ is the autoregressive parameter related to the couple of signals j, i at the lag k and considering the order p

Eq. 2 is then rewritten in the matrix notation:

$$A(f)Y(f) = U(f) \quad (3)$$

$$A(f) = \begin{bmatrix} A_{11}(f) & \cdots & A_{1N}(f) \\ \vdots & \ddots & \vdots \\ A_{N1}(f) & \cdots & A_{NN}(f) \end{bmatrix} \quad (4)$$

$$Y(f) = \begin{bmatrix} X_1(f) \\ \vdots \\ X_N(f) \end{bmatrix} \quad U(f) = \begin{bmatrix} U_1(f) \\ \vdots \\ U_N(f) \end{bmatrix} \quad (5)$$

$$Y(f) = A^{-1}(f) U(f) = H(f)U(f) \quad (6)$$

where $A(f)$ are the $N \times N$ matrices of model coefficients, $Y(f)$ is the signal dataset and $U(f)$ contains white residues with zero mean, not correlated between them and between the signals. $H(f)$ is the transfer matrix of the MVAR filter, the element i, j of matrix H is the transfer function between the i -th entrance and the j -th exit in the MVAR generator filter, $H_{ij}(f) \neq H_{ji}(f)$.

The spectral density is $S_{xx}(f) = |Y(f)|^2$.

DTF is defined by the elements of the transfer matrix $\vartheta_{ij}(f) = |H_{ij}(f)|^2$ in the spectrum domain and describes the directional causality from channel j to channel i [66]. DTF is expressed by the normalized formula:

$$\vartheta_{ij}^2(f) = \frac{|H_{ij}(f)|^2}{\sum_{m=1}^N |H_{im}(f)|^2} \quad \sum_{n=1}^N \vartheta_{in}(f) = 1 \quad (7)$$

where N is the number of channels. Normalized values of DTF_{ij} are comprised between 0 and 1.

We can say that DTF provides the percentage of power of signal i caused by j [67][68][69] [46].

2.3 Adaptive Directed Transfer Function (Time Varying) (ADTF)

The adaptive DTF (ADTF), a time-varying multivariate method, has been developed for the estimation of rapidly changing connectivity influences between cortical areas of the human brain [70][71].

For each time series, an Adaptive MVAR (AMVAR) process is constructed as:

$$y_t = -\sum_{k=1}^p A(i, t)y(t - i) + u(t) \quad (8)$$

where y_t is the data vector over time, $A(k, t)$ are the matrices of time-varying model coefficients, $u(t)$ is multivariate independent white noise and p is the model order.

The time-varying coefficient matrices of the AMVAR were tracked by using the Kalman filter algorithm [64] that provides instantaneous estimations of the spectral densities in terms of AR coefficient matrices (additional information are in the Section 2.3.1). The Adaptive DTF (ADTF) values are then defined as a function of both time and frequency:

$$\vartheta_{ij}^2(f, t) = \frac{|H_{ij}(f, t)|^2}{\sum_{m=1}^N |H_{im}(f, t)|^2} \quad (9)$$

where $H(f, t)$ is the transfer function obtained by the time-varying transfer matrix. Taking into account that the signals are samples from time-series with varying spectral properties, it is also natural to assume the coefficients to be time dependent. The ADTF measure allows the observation of rapidly changing influences areas and it is suitable for analysis of short duration signals [72] and event-related potentials.

2.3.1 Kalman Filter

A Kalman filter is modelled on a Markov chain, with the difference that the state variables take values in a continuous space and not in the discrete one, and built on linear operators perturbed by errors, e.g. Gaussian noise. Kalman filter uses a system's dynamics model and multiple sequential measurements to estimate the system's varying quantities (the state). The prediction of the system's state and the prediction of the new measurements are obtained using a weighted average, where weights are calculated from the covariance. This process is repeated at every time step: it works recursively and requires only the last "best guess" of a system's state to calculate the new one. This means that only the estimated state from the previous time-step and the current measurement are needed to compute the estimate for the current state (no history of observations is required).

The Kalman filter could be explained in a single equation, however it is most often conceptualized as two linear distinct ones: "Predict or State or *a-priori*" and "Update or

Observation or *a-posteriori*". The state equation uses the state from the previous time-step to produce an estimate of the state at the current time-step; in the second equation the *a-priori* prediction is combined with current observation information to refine the state estimation.

The Kalman filter model assumes the true state at time k is evolved from the state at $(k - 1)$ according to:

$$x_k = F_k x_{k-1} + B_k u_k + w_k \quad (10)$$

where F_k is the state transition model which is applied to the previous state x_{k-1} ; B_k is the control-input model which is applied to the control vector u_k ; w_k is the process noise which is assumed to be drawn from a zero-mean multivariate normal distribution, N , with covariance Q_k such as $w_k \sim N(0, Q_k)$

At time k an observation z_k of the true state x_k is made according to:

$$z_k = K_k x_k + v_k \quad (11)$$

where K_k is the observation model which maps the true state space into the observed space and v_k is the observation noise which is assumed to be a zero-mean Gaussian white noise with covariance R_k such as $v_k \sim N(0, R_k)$

The initial state, and the noise vectors at each step $\{x_0, w_1, \dots, w_k, v_1 \dots v_k\}$, are all assumed to be mutually independent.

Kalman algorithm can be applied in the multivariate case rearranging the elements of the matrices of coefficients in vector form converting the matrix into a column vector [64]. Then, a smoothing procedure is performed: a nonlinear recursive filter is used for each component of the estimated coefficient vector, it is a low pass filter, where the cutoff frequency increases with the value of adaptation constant (0.1). The filter causes an exponential smoothing of the signal where the degree of smoothing reduces as the adaptation constant increases. We used the eConnectome toolbox with an update coefficient of 0.001. Such value limited the variance of the coefficients over time (more smoothness) in our specific application. The interested reader may find further information in [45].

2.4 The nonparametric method to assess the significance of the estimated connectivity measures

To process both DTF and ADTF functions on signals we adopted the MATLAB-based toolbox eConnectome (Electrophysiological Connectome) [45][69], an open-source software package for imaging brain functional connectivity from electrophysiological signals. It provides: i) interactive graphical interfaces for EEG/ECOG/MEG; ii) preprocessing; iii) source estimation; iv) connectivity analysis and visualization. The EcoG module [72] supports a statistical implementation for connectivity: a nonparametric method based on surrogate data is used to assess the significance [73][74]. Surrogate data are used to assess the statistical significance of the causal connectivity estimates both for DTF and ADTF measures. Only statistical significant ($p < 0.05$) connectivity measures coming from the procedure were considered for the following analysis and observations (both for DTF and ADTF).

This nonparametric method is realized in this way:

- The Fourier transform (FT) of the time series is computed (the magnitude of the Fourier coefficients were kept unchanged but phases are randomly).
- The surrogate dataset was created transforming back the FT into the time domain. The phase shuffling maintains the spectral structure of the original time series.
- MVAR model (the estimate connectivity) was fitted to this surrogate dataset.
- The process is repeated for 1000 times for each experiment, yielding a distribution of the DTF and ADTF values under the null hypothesis of the absence of connectivity.

3 CONNECTIVITY ANALYSIS: DTF and ADTF

In the Introduction (Section 1.4) we discussed about the origin of the signals generated by neurons. Potentials recorded by EEG result from extracellular and intracellular flows originated from postsynaptic potentials of several cortical cells.

These postsynaptic potentials, thanks to their relative longer duration (10-40ms) and thanks to the ability to aggregate also in absence of a perfect synchronization, are able to sum up themselves during time, unlike action potentials.

Given that frequency and magnitude of signals are variable and linked to the specific mental states, it is useful to analyze the effect of an external stimulus on brain activity. Signal variations induced by external events are smaller compared to the background brain activity. So, the stimulus must be repeated several times, the average of the events related potential (ERP) is performed, then specific investigations can be done to extract components linked to the event. The evoked activity adds up with respect to the background activity that, being desynchronized across trials, tends to zero. ERP is synchronous with the event, and consists of a phase shifting of the background oscillations with respect to the induced event along with an increase in magnitude.

Analysis of ERP components (positive and negative peaks) permits to identify the cortical area activated by the event. For example, after a visual stimulation, visual cortex activation overlaps with an occipital component at 70 ms after the stimulus. Later, in time, slower components are linked to the activation of a secondary cortex area.

We considered in ERP analysis the two predominant brain rhythms able to provide information about mental states: Gamma and Delta.

High frequency and low amplitude rates are associated to vigilance states, or to REM sleep stages. Gamma rhythms, 30-100 Hz, are features of brain activation and during intense mental activity they have minimum amplitude; the pattern, synchronous oscillations, involves different neuron populations so as to create a network able to carry out a cognitive function [75] [47]. Gamma waves are usually observed at the frontal area, but can also be recorded from other cortical regions.

Low frequency and large amplitude rates are associated with NREM sleep states or a pathological condition (e.g. coma), since when the cortex is involved in re-elaboration of

the information, the activity level of cortical neurons is relatively high, but also relatively non-synchronized over large areas of the cortex. Delta rhythms (called slow waves sleep), up to 4 Hz, are slow with high magnitude, features of NREM stage 3.

In this thesis the effort is directed to localize the neuronal source of the signals and their positions into the cortical area. The aim is to try to identify sources and their dynamics considering the two mentioned conscious states. The use of multiple electrodes aims to reveal a network map. Analysis of nodes behavior (as a source or as a sink for information processes) and analysis of the direction of the information flow have been performed. Interactions between different and differently specialized cortical sites were investigated by means of Directed Transfer Function (DTF) that determines the directional influences between pair of channels in a multivariate data set. Then we repeated the analysis using ADTF, that considers also a time varying parameter. The theory of these methods is reported in Chapter 2.

We evaluated effective (causal) connectivity on matrices composed by 8 channels per each of the five subjects, the analysis was performed considering the two consciousness states (WAKE or NREM) and two frequency bands (Gamma, feature of the brain activation, and Delta, feature of NREM).

Data were divided in time series of 800 ms (equal to 800 samples) and bandpass filtered according to the bands.

Thus the 20 experiments were carried out using 4 conditions:

- 1.** WAKE in Gamma band;
- 2.** WAKE in Delta band;
- 3.** NREM in Gamma band;
- 4.** NREM in Delta band.

Every condition was repeated per each human subject, 5 total.

The accuracy of DTF and ADTF results were confirmed in pilot experiments (not reported in the thesis): even if the test was repeated more than two times the results did not change.

Results are reported in section 3.2 and 3.3.

3.1 Data pre-processing and channels selection

Intracranial recordings (iEEG) were kindly provided by A. Pigorini and M. Massimini, Department of Biomedical and Clinical sciences “L.Sacco”, Università Degli Studi di Milano in collaboration with Niguarda Hospital.

Data were collected during standard clinical routine for epileptic foci detection [21] using the 192-channel recording system EEG Nihon Kohden (NIHON-KOHDEN NEUROFAX-110). The clinical protocol lasted for five days.

Five subjects with drug-resistant focal epilepsy were considered for the present study. During pre-surgical evaluation, stereo-EEG platinum–iridium semi-flexible electrodes were implanted to record signals under electrical stimulation. Electrodes had a diameter of 0.8 mm, the contact length was of 1.5 mm, the inter-contact distance was of 2 mm and the maximum contacts number per electrode was 18 (Dixi Medical, Besancon France).

The dataset, acquired at 1000 Hz, included several acquisition sessions: in each session the stimulation point (channel source of electrical induction) was different, and meanwhile the other contacts (up to 189) were used to collect data. A single stimulation session consisted of 29 impulses at intervals of 1 second, each impulse was 0.2 ms long, the stimulation strength was 5 mA [21]. Stimuli were fired while the subject was awoken and then sleeping (NREM state, N3 stage, as evaluated by expert neurologist [21]). Examples of raw signals, in both conditions, are reported in Figure 1.

The patient gave written informed consent and the procedure was approved by Local Ethical Committee, protocol number: ID 939, Niguarda Hospital, Milan, Italy.

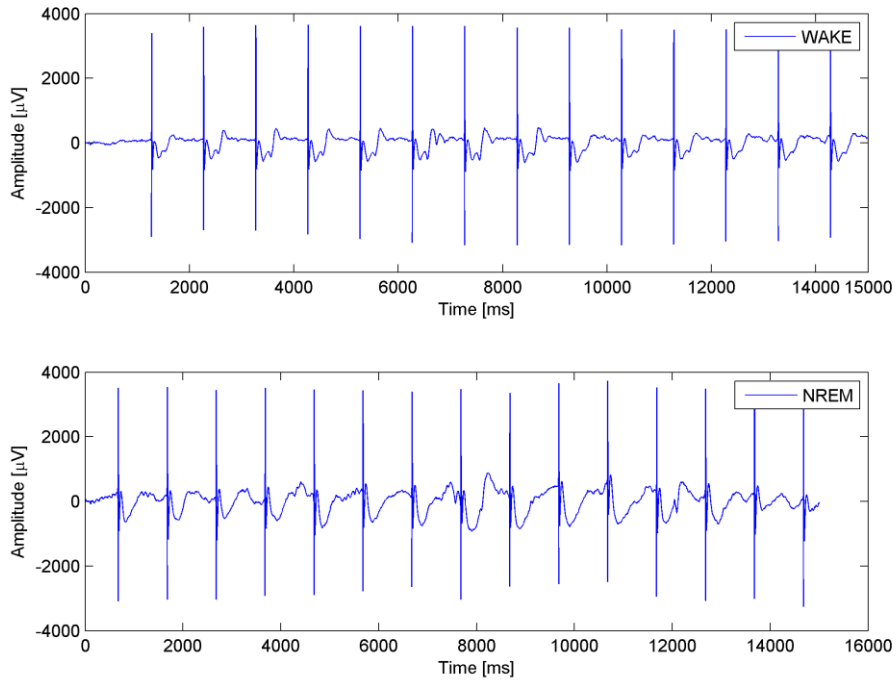


Figure 1. 16 representative seconds of a raw iEEG signal (first channel, subject number one, bipolar montage) in both WAKE and NREM condition. Here 15 stimulation sessions, with the corresponding impulses, are reported. The impulsive signals characterize the instants of the electrical stimulations. Epoch, in our definition, is the signal recorded in the 800 ms after each stimulation.

Raw data were pre-processed as follows:

- Re-referenced as specify below,
- Subjected to epochs creation: 29 windows of eight-hundred milliseconds each,
- Linear detrended and bandpass filtered (third order Butterworth filter, 0.5 – 300 Hz [21] applied in both directions to avoid phase distortion),
- Powerline interference was removed using an IIR notch filter at 50Hz and its main harmonics .

Re-montage was calculated by subtracting the signals from adjacent contacts (each referenced to a common reference located into the white matter), method that is known in literature as bipolar montage, in order to minimize common electrical noise and to maximize spatial resolution [21][24][37]. The assumptions on which the dissertation is based are given by works from literature that used bipolar montage, but we repeated the analyses

using the other re-referencing styles to avoid possible losses of information and to compare the montage methods: the topic will be addressed in the Additional Results Section.

As our intent was to analyse the period following the stimulus, as longer as possible, excluding the stimulus itself, we created a set of windowed time series (also called epochs in the dissertation) to better highlight cortico-cortical evoked potential (Figure 2). Event related time series were obtained extracting 800 ms signal data starting exactly 19 ms after each stimulus (maximum amplitude).

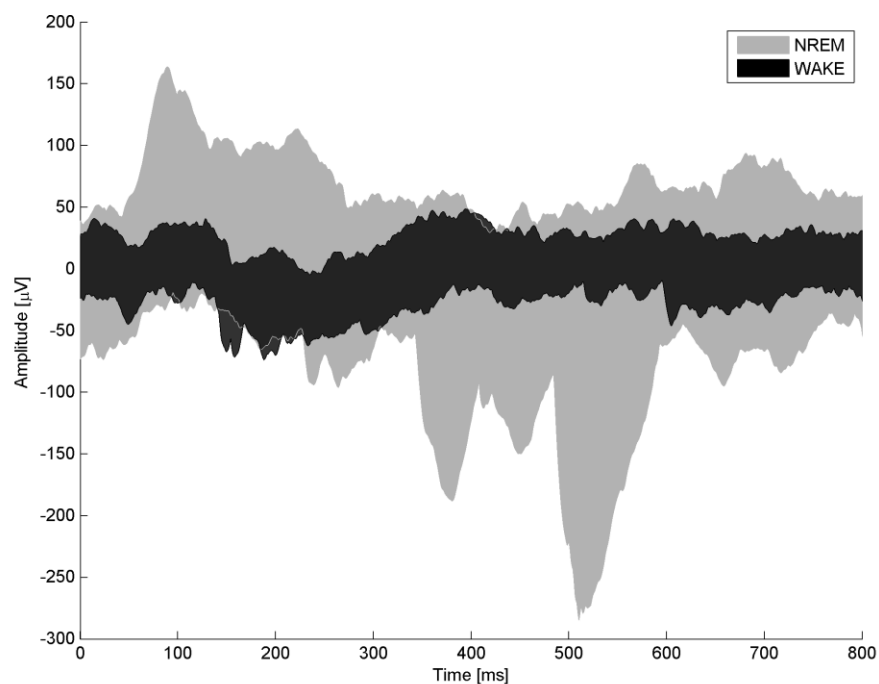


Figure 2. Representative CCEP from pre-processed signal (first channel, subject number one, bipolar montage) in both WAKE and NREM condition. Minimum and maximum values of the signal in each epoch over time for one channel.

The selection of the stimulation session and of the recording sites was based, as in [21], on i) the exclusion of those channels positioned in epileptic areas; ii) the absence of epileptic activity during the session; ii) the absence of artifacts such as muscle twitches, sensations or motor/cognitive effects.

We operated on data of 5 human subjects, selecting 8 channels each, trying to conserve the anatomical positions *inter*-patients. The channels selection criterion was to obtain reproducible *inter*-patients results. The task was not easy because electrode site implantations were chosen purely on clinical needs and based on the suspected seizure locations (e.g. electrodes are often implanted only on one hemisphere, that could not be the same for all the patients).

The spatial coverage (given by coordinates from MRI images co-registered during SPES-iEEG) and anatomical positions of the selected electrodes per patient are summarized in Table 1. As it is possible to observe in the Table 1, coordinates could not be applied to a common atlas. 3D plots are useful just to compare relative positions between channels and in relation to the stimulation site (SS). These plots are also useful to verify the distances between nodes in the network.

The intersection of the anatomical positions (Table 1, column 2) in 5 patients is zero.

Moving to macro areas (Table 2) the channel intersection *inter*-patients comprises:

i) frontal lobe, and ii) Brodmann Areas 24, 25,25, 29, 32.

Channel number	Anatomical position	3D position
Subject 1		
1	G_and_S_cingul_Ant	<p>Subject 1</p> <p>3D scatter plot showing electrode positions (1-8) and Stimulation Site (SS) in a coordinate system with axes x, y, and z. The z-axis ranges from -1 to 5, the x-axis from -4 to 4, and the y-axis from -8 to 2. Electrode 1 is at approximately (2, 0, 2), 2 at (3, 2, 3), 3 at (0, 5, 4), 4 at (1, 0, 0), 5 at (3, -1, -1), 6 at (1, 2, 2), 7 at (-1, 3, 3), and 8 at (-1, -1, -1). The Stimulation Site (SS) is at approximately (0, 1, 1.5).</p>
2	G_front_sup	
3	S_front_sup	
4	S_parieto_occipital	
5	S_oc_sup_and_transversal	
6	G_and_S_paracentral	
7	Medial_wall	
8	G_cingul_Post_dorsal	
Stimulation Site (SS)	S_central	
Subject 2		
1	G_and_S_cingul-Mid-Post	<p>Subject 2</p> <p>3D scatter plot showing electrode positions (1-8) and Stimulation Site (SS) in a coordinate system with axes x, y, and z. The z-axis ranges from 2 to 4.5, the x-axis from -6 to 1, and the y-axis from -6 to 0. Electrode 1 is at approximately (-4, -3, 3), 2 at (-4, -4, 4.5), 3 at (-2, -3, 3), 4 at (-3, -4, 3.5), 5 at (-4, -3, 3), 6 at (-4, -4, 2.5), 7 at (-2, -3, 3.5), and 8 at (-4, -4, 4). The Stimulation Site (SS) is at approximately (-4, -3, 3).</p>
2	G_front_sup	
3	S_subparietal	
4	S_intra-pariet_and_P_trans	
5	S_precentral-inf-part	
6	G_pariet_inf-Supramar	
7	G_cingul-Post-dorsal	
8	G_and_S_cingul-Mid-Ant	
Stimulation Site (SS)	G_and_S_cingul-Mid-Ant	

Channel number	Anatomical position	3D position
Subject 3		
1	G_and_S_cingul-Mid-Ant	<p>Subject 3</p> <p>3D scatter plot showing electrode positions (1-8) and Stimulation Site (SS) for Subject 3. The z-axis ranges from -2 to 4, the x-axis from -2 to 6, and the y-axis from -2 to 6. Electrode 1 is at approximately (1, 1, 0.5), 2 at (3, 2, 1.5), 3 at (5, 2, 1.5), 4 at (1, 2, 2.5), 5 at (2, -1, -1.5), 6 at (4, 1, 1.5), 7 at (1, 2, 2.5), 8 at (4, 1, 1.5). The Stimulation Site (SS) is at approximately (3, 2, 2.5).</p>
2	G_front_middle	
3	G_precentral	
4	S_front_sup	
5	S_circular_insula_ant	
6	G_front_inf-Opercular	
7	S_front_middle	
8	G_precentral	
Stimulation Site (SS)	G_front_middle	
Subject 4		
1	G_and_S_cingul-Mid-Ant	<p>Subject 4</p> <p>3D scatter plot showing electrode positions (1-8) and Stimulation Site (SS) for Subject 4. The z-axis ranges from 1.5 to 5, the x-axis from -6 to 6, and the y-axis from -6 to 6. Electrode 1 is at approximately (-1, 4.5, 4.5), 2 at (1, 2.5, 2.5), 3 at (-1, 5, 5), 4 at (-1, 3.5, 3.5), 5 at (4, 4, 4), 6 at (-2, 3.5, 3.5), 7 at (3, 3, 3), 8 at (4, 1.5, 1.5). The Stimulation Site (SS) is at approximately (-1, 5, 5).</p>
2	G_and_S_cingul-Mid-Post	
3	G_front_middle	
4	G_front_sup	
5	G_postcentral	
6	S_front_sup	
7	S_central	
8	S_intra-pariet_and_P_trans	
Stimulation Site (SS)	S_front_sup	

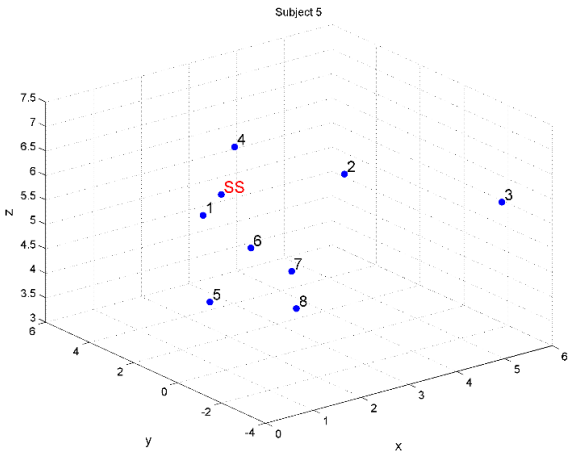
Channel number	Anatomical position	3D position
Subject 5		
1	G_and_S_cingul-Mid-Ant	
2	G_front_sup	
3	G_precentral	
4	S_front_middle	
5	G_and_S_cingul-Mid-Post	
6	G_and_S_cingul-Mid-Post	
7	S_orbital_lateral	
8	S_circular_in-sula_sup	
Stimulation Site (SS)	S_front_sup	

Table 1. For every human subject 8 channels have been selected for the analysis. For every channel the anatomical position is here reported. Anatomical definition is according to the Destrieux Atlas [76]. In the “3D position” column the position in the space (xyz) is calculated for each electrode according to the NMRI data of the subject. In 3D column the relative positions are shown i) between electrodes and ii) between electrodes and the stimulation site (SS).

		BROADMAN AREAS	LOBE
Subject 1	G_and_S_cingul-Ant	32,24,25	Limbic
	G_front_sup		superior frontal
	S_front_sup		superior frontal
	S_parieto_occipital		between occipital and parietal
	S_oc_sup_and_transversal		temporal and occipital
	G_and_S_paracentral	4	Frontal
	Medial_wall		(medial wall)
	G_cingul-Post-dorsal	26,29,30,22,31	
Subject 2	G_and_S_cingul-Mid-Post	26,29,30,22,31	
	G_front_sup		superior frontal
	S_subparietal		medial parietal lobe
	S_intrapariet_and_P_trans		Parietal
	S_precentral-inf-part		close to frontal
	G_pariet_inf-Supramar		(Wernick area)
	G_cingul-Post-dorsal	26,29,30,22,31	
	G_and_S_cingul-Mid-Ant	33,24,25,32	
Subject 3	G_and_S_cingul-Mid-Ant	32,24,25,32	
	G_front_middle		Frontal
	G_precentral	4	
	S_front_sup		Frontal
	S_circular_insula_ant		portion of frontal, parietal and temporal
	G_front_inf-Opercular		Frontal
	S_front_middle		inferior frontal
	G_precentral	4	
Subject 4	G_and_S_cingul-Mid-Ant	32,24,25	(medial wall)
	G_and_S_cingul-Mid-Post	26,29,30,22,31	
	G_front_middle		Frontal
	G_front_sup		Frontal
	G_postcentral	1, 2, 3	
	S_front_sup		Frontal
	S_central		between frontal and parietal(Rolando scissure)
	S_intrapariet_and_P_trans		between parietal lobes
Subject 5	G_and_S_cingul-Mid-Ant	32,24,25	
	G_front_sup		Frontal
	G_precentral	4	
	S_front_middle		Frontal
	G_and_S_cingul-Mid-Post	26,29,30	
	G_and_S_cingul-Mid-Post	26,29,30	
	S_orbital_lateral		Frontal
	S_circular_insula_sup		(circular sulcus of the insula)

Table 2. List of macro areas involved in the project.

3.2 Evaluation of Directed Transfer Function results over frequencies in Gamma and Delta bands

The estimation of functional connectivity from multichannel data are described, with special emphasis, by the direction of estimators. The identification of MVAR model has been possible through the MATLAB ARfit tool, implemented in eConnectome, that, given time series data, estimates the parameters of the model with a stepwise least squares algorithm [77][78]. ARfit includes support for multiple realizations of time series and it estimates multivariate AR models parameters taking all available realizations into account: the resulting model coefficients are based on the correlation matrix averaged over trials.

The input matrix is a 2D array, where the number of rows equals the number of the time series, and the number of columns equals the number of points of each time series (each time series represents 800 ms). The output matrix is in the form `dtf.matrixs (i,j,k)`, where `i` = the sink channel, `j` = the source channel, `k` = the frequency index.

Regarding the Gamma band, the frequency index is composed by 71 points; regarding the Delta band, the frequency index is composed by 4 points.

All data were exported from the eConnectome toolbox and the analysis was performed off-line using the software package MATLAB (MATLAB, The MathWorks Inc., Natick, MA, 2000).

Plots in Figure 5 and 4 are created using the *imagesc* and *contour* functions.

- *imagesc* permits to display the DTF matrix with scaled colors (from blue to red). Each element of the matrix specifies the color for 1 pixel of the image. The resulting image is an m-by-n grid of pixels where m is the number of columns and n is the number of rows in the DTF matrix. The row and column indices of the elements determine the centers of the corresponding pixels. The function is used to create the plot scales the color limits, so that image uses the full range of the colormap, where the smallest value in the matrix maps to the first color in the colormap and the largest value maps to the last color.
- *contour* function defines the white curves in the picture; the isoline function joins points of equal value and the curve represents a constant function values.

3.2.1 Results in Gamma band

In Figure 3 the matrix from DTF analysis is displayed, averaging the frequency band (30-100Hz). Figure 3 is organized in two columns (the first for WAKE state and the second for NREM state) and five rows, one per subject.

First of all, we compared the presence *vs* the absence of consciousness comparing columns. As expected from literature, in Gamma band a higher activity is observable as well as, in WAKE, a higher number of connections. The second main observation is that in NREM the source channels (vertical lines in matrices of Figure 1) are very well distinguishable: this gives the idea that only some source channels are really important during NREM and that only some source channels are able to influence many sink channels. So, again, this information suggests that during the NREM state (during the brain re-elaboration processes that occur during the night) some channels play a firm role.

Trying to compare channels commonly expressed in both states, it is notable that, often, the channels involved are the same, but the number of sink channels involved is different and, above all, the level of information flow diverges. Looking at the channels involved differently in the two consciousness states, channels that emerge are:

- 8 for subject 2,
- 1 for subject 3,
- 8 for subject 5,

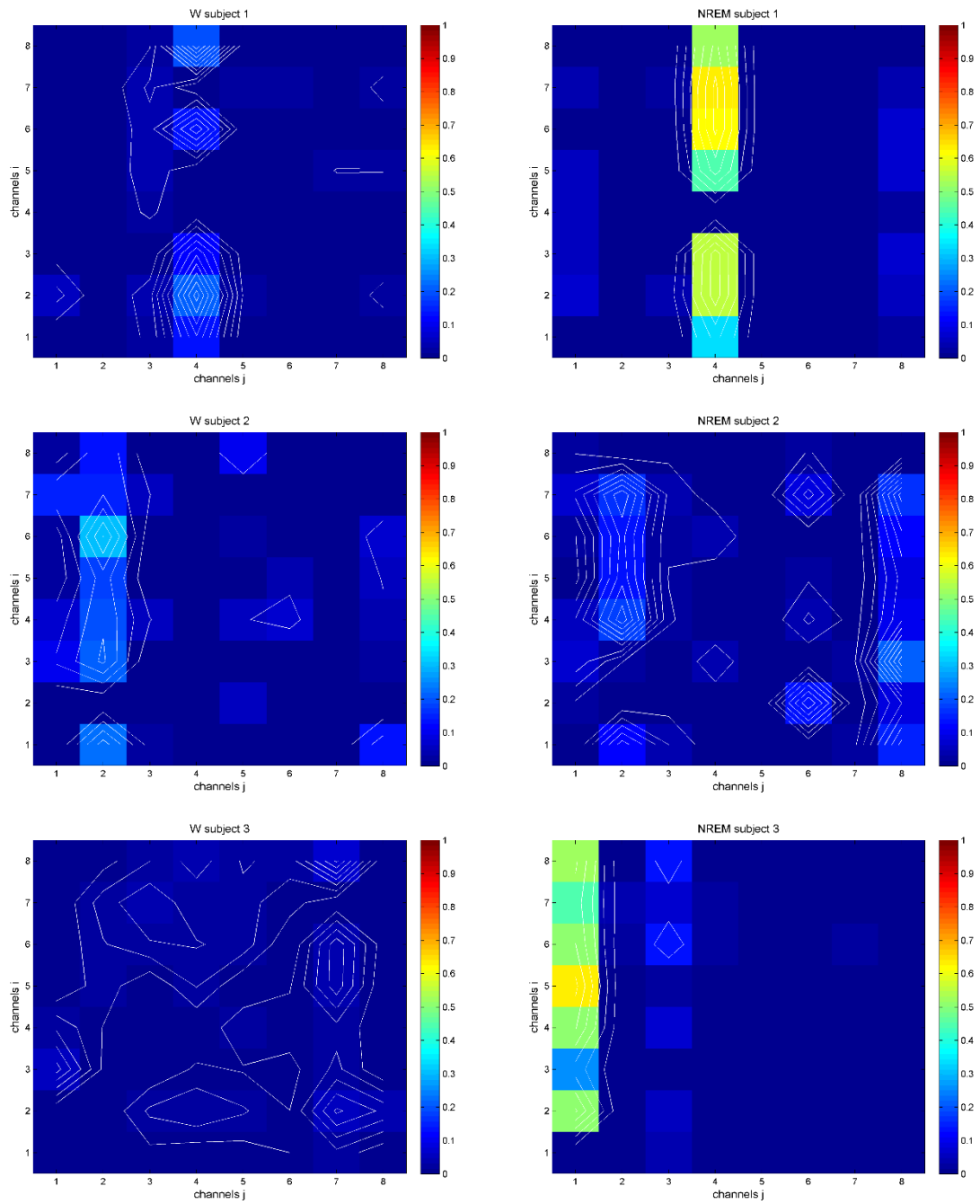
respectively: “G_and_S_cingul-Mid-Ant”, “G_and_S_cingul-Mid-Ant”, “S_circular_insula_sup”. “Cingulate Girus and Sulcus middle anterior” (Brodmann’s area) could be an interesting micro areas. This information is visualized also in Table 4.

Moving to the quantitative analysis we created the Tables 3 and 4. The DTF values are normalized between 0 and 1. We calculated the minimum and maximum value of the matrix (Table 3), and noted that the DTF value range is higher in NREM than in WAKE. The data are valid and reproducible for 4 subject over 5. In order to visualize the main connections (with higher DTF values) we applied a threshold at 95° percentiles. In Table 3 the DTF values of these main connections are reported.

In Table 4 the DTF values of the main connection, their matching channel numbers and anatomical positions are reported. In Table 4 panel A, in WAKE, there is a predominance

of frontal area both in source channels and in sink, but especially in sinks. In NREM, Table 4 panel B, the involvement of parietal, frontal and Brodmann areas is pretty evenly spread.

DTF Matrix in Gamma Band



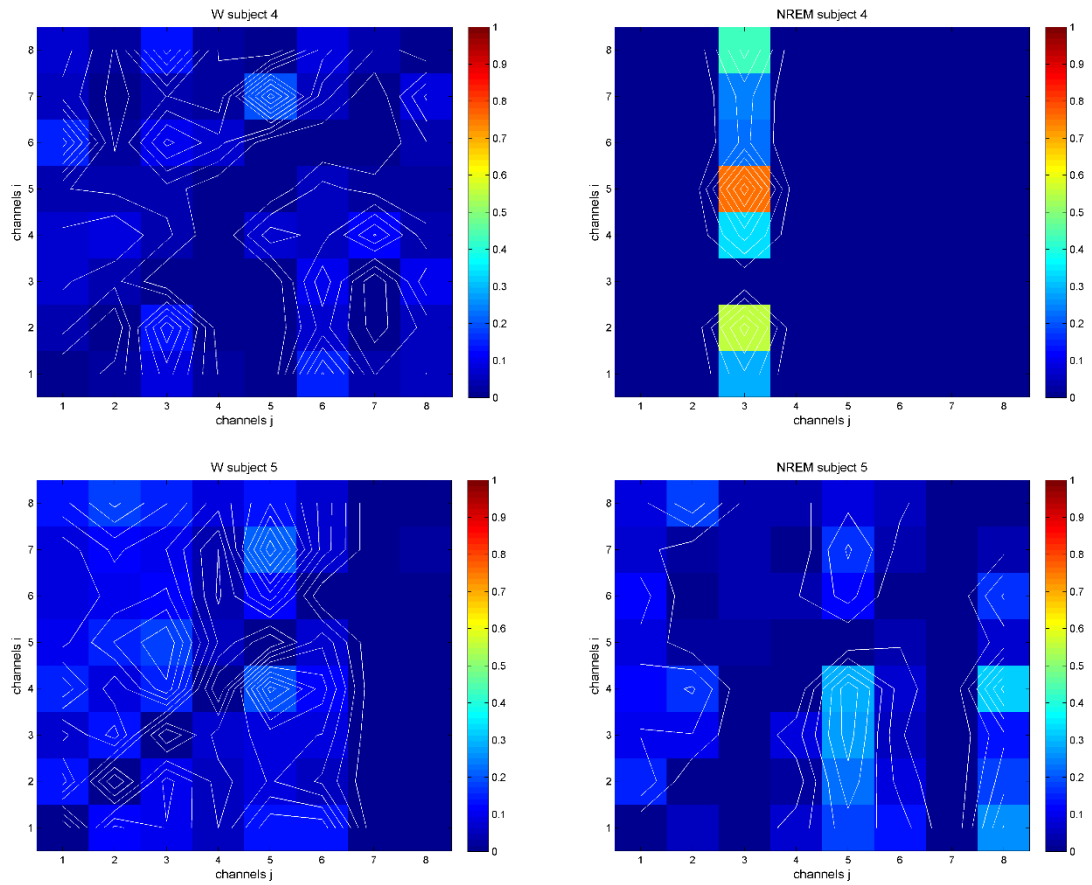


Figure 3. DTF Values in Gamma Frequency Band after average. DTF values are reported in the square matrix 8x8, colour bar indicates the DTF levels (0-1, from Blue to red respectively). On the axes the 8 channels are represented, the information flow goes from j channels (x axis) to i channels (y axis). Left column: the five subjects in WAKE state; right Column: the five subjects in NREM state.

Subject	Min	Max	Threshold	Main Connection
1	0	0,210214	0,199703195	0,210213889
2	0	0,301177	0,286118148	0,301176997
3	0	0,071934	0,068336917	0,071933596
4	0	0,190279	0,180765005	0,190278952
5	0	0,214859	0,204115666	0,214858596

A. WAKE

1	0	0,625411	0,594140116	0,624134704 0,625410649
2	0	0,213903	0,20320743	0,213902558
3	0	0,627116	0,595760294	0,627116098
4	0	0,758964	0,721015383	0,758963561
5	0	0,315229	0,299467831	0,315229296

B. NREM

Table 3. Considering the average of the Gamma frequency band, here, some data are reported: i) subject, ii) minimum and iii) maximum of the matrix, iv) threshold (corresponding to 95°percentile) and v) connections that exceed the threshold. DTF values in WAKE (A) and in NREM states (B).

Subject	Main Connection	Channels involved	Anatomical position
1	0,210213889	4>2	*S_parieto_occipital> °G_front_sup
2	0,301176997	2>6	°G_front_sup>*G_pariet_inf-Supramar
3	0,071933596	7>8	°S_front_middle> °G_precentral
4	0,190278952	5>7	^G_postcentral> °S_central
5	0,214858596	5>7	^G_and_S_cingul-Mid-Post>°S_orbital_lateral

A. WAKE

1	0,624134704	4>6	*S_parieto_occipital> °G_and_S_parietocentral
	0,625410649	4>7	*S_parieto_occipital> Medial_wall
2	0,213902558	8>3	^G_and_S_cingul-Mid-Ant>* S_subparietal
3	0,627116098	1>5	^G_and_S_cingul-Mid- Ant>°S_circular_insula_ant
4	0,758963561	3>5	°G_front_middle >^G_postcentral
5	0,315229296	8>4	S_circular_insula_sup> °S_front_middle

B. NREM

Table 4. Connections over 95percentile and anatomical correspondence in WAKE (A) and NREM (B). °indicates the frontal lobe, ^ indicates the Brodmann's areas, * indicates parietal areas.

3.2.2 Results in Delta band

Matrices displayed in Figure 4 come from the average of the DTF values over the frequency range 0.5-4Hz. Actually, due to technical reasons, the slowest frequency observed is 1.25 Hz (in fact, sampling frequency is 1000 Hz and the chosen windowed time series length is 0.8 second). One of the aims of the project was to propose an alternative method able to detect the slow waves because it is known that during NREM the brain cortex is bi-stable (a slow-wave is generated after electrical stimulation) and during WAKE the response to a pulse of stimulation does not show the presence of slow waves. It took us to the limits of what was feasible to appreciate also a part of slow wave range.

The details about the pictures creation and parameters settings have been previously explained.

Connections are organized in an orderly manner both in WAKE and in NREM: this is the same behaviour observed in NREM of Gamma band that could be caused by: i) the lower number of frequencies considered with respect with to Gamma band, or ii) characteristics of Delta band.

Comparing NREM and WAKE (Figure 3), the activity is again mainly in conscious state (left column). Comparing the common channels involved, a situation opposite to the Gamma band is reported: very few channels are in common between NREM and WAKE. It seems that channels involved in Delta band are peculiar of the conscious states. And, again, one source channel is able to induce effects in many sink channel. The sink channel 6, in subject 2, WAKE, is induced by many source channels; this channel, G_pariet_inf-Supramar, is positioned into the parietal lobe.

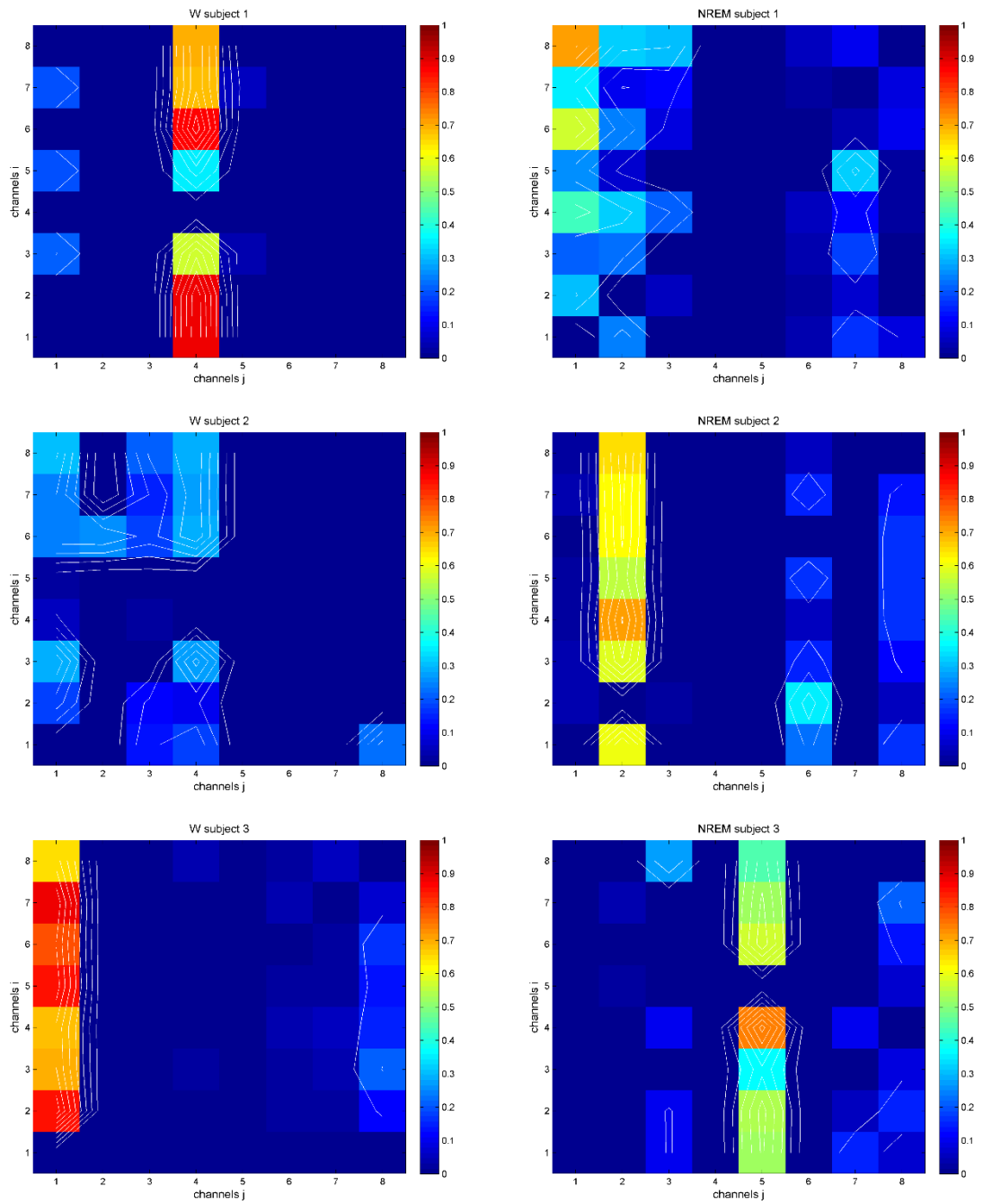
The DTF values range in WAKE is larger: DTF measures have higher maximum values compared to the NREM. This happens for 4 patients over 5. The subject 2 has always an opposite behaviour. Since this situation is often reported, the iter regarding loading of data, preprocessing, DTF matrix creation for subject 2 was double checked to be sure that no swapping between NREM and WAKE was occurred.

In WAKE many connections are above the threshold (Table 5).

In Table 6 anatomical locations of the main connection are reported and, noteworthy, in conscious state the source channels are positions into Brodmann and parietal areas, sink

channels are mainly in frontal ones. In unconscious state a smaller number of connections are underlined and the main source channels are in Brodmann area and in frontal, not in parietal areas. The connection 5 > 6 in subject 5 is present in both conscious state, where both 5 and 6 are G_and_S_cingul-Mid-Post positioned in Brodmann's areas 26, 29, 30.

DTF Matrix in Delta Band



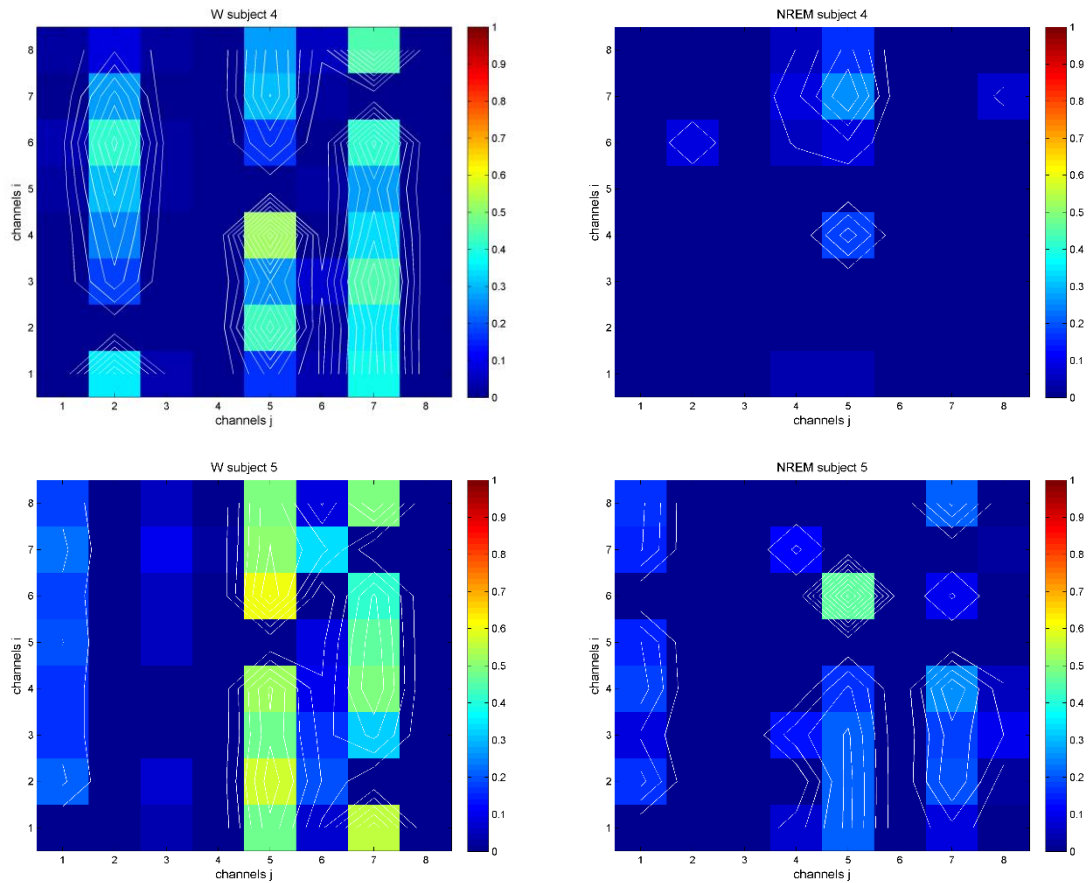


Figure 4. DTF Values in Delta Frequency Band after average. DTF values are reported in the square matrix 8x8, color bar indicates the DTF levels (0-1, from Blue to red respectively). On the axes the 8 channels, where the information flow goes from j (x axis) to i (y axis). Left column: the five subjects in WAKE state; right Column: the five subjects in NREM state.

Subject	Min	Max	Threshold	Main Connection
1	0	0,88789	0,843496	0,88789
				0,877503
				0,860168
2	0	0,308642	0,29321	0,308642
3	0	0,876004	0,832204	0,854535
				0,858587
				0,876004
4	0	0,524675	0,498441	0,524675
5	0	0,603169	0,57301	0,603169
A. WAKE				
1	0	0,711174	0,675616	0,711174
2	0	0,712129	0,676523	0,712129
3	0	0,741091	0,704036	0,741091
4	0	0,25	0,2375	0,25
5	0	0,46574	0,442453	0,46574
B. NREM				

Table 5. Considering the average of the Delta frequency band, here, some data are reported: i) subject, ii) minimum and iii) maximum of the matrix, iv) threshold (corresponding to 95percentile) and v) connections that exceed the threshold. DTF values in WAKE (A) and in NREM states.

Subject	Main Connection	Channels involved	Anatomical position
1	0,88789	4>1	*S_parieto_occipital> ^G_and_S_cingul-Ant
	0,877503	4>2	*S_parieto_occipital> °G_front_sup
	0,860168	4>6	*S_parieto_occipital> °G_and_S_para-central
2	0,308642	1>8	^G_and_S_cingul-Mid-Post> ^G_and_S_cingul-Mid-Ant
3	0,854535	1>2	^G_and_S_cingul-Mid-Ant> °G_front_middle
	0,858587	1>5	^G_and_S_cingul-Mid-Ant> °S_circular_insula_ant
	0,876004	1>7	^G_and_S_cingul-Mid-Ant> °S_front_middle
4	0,524675	5>4	^G_postcentral> °G_front_sup
5	0,603169	5>6	^G_and_S_cingul-Mid-Post> ^G_and_S_cingul-Mid-Post
A. WAKE			
1	0,711174	1>8	^G_and_S_cingul-Ant> ^G_cingul-Post-dorsal
2	0,712129	2>4	°G_front_sup> *S_intra-pariet_and_P_trans
3	0,741091	5>4	°S_circular_insula_ant> °S_front_sup
4	0,25	5>7	^G_postcentral> S_central
5	0,46574	5>6	^G_and_S_cingul-Mid-Post>^G_and_S_cingul-Mid-Post
C. NREM			

Table 6. Main connections and anatomical correspondence in WAKE (A) and NREM (B). ° indicates the frontal lobe, ^ indicates the Brodmann's areas, * indicates parietal areas.

3.2.3 Comparison between Gamma and Delta

It is interesting that Gamma and Delta connections involve quite the same channels. In Table 7 the connections exceeded the threshold are indicated with arrows: in yellow the connections in conscious state, in blue the connections in unconscious state.

Subject 1 has the 4>2 connection in common between Gamma and Delta band. Channel 4 (S_parieto_occipital, between occipital and parietal lobes) seems to have an important role both in NREM and in WAKE (Gamma band) or only in WAKE (Delta band). The connection 4>6 is important during NREM in Gamma, and during WAKE in Delta. Channels 2 (G_front_sup) and 6 (G_and_S_paracentral) are both in frontal lobe. The direction of these connections are from occipital to frontal and these occur in both states.

In patient 2 the two mainly involved channels, in different ways, are 2 (G_front_sup) and 8 (G_and_S_cingul-Mid-Ant).

In patient 3 the three mainly involved channels are 1,5,8. Interestingly, the common connection 1 (G_and_S_cingul-Mid-Ant) > 5 (S_circular_insula_ant) is observable in WAKE in Delta and in NREM in Gamma.

In patient 4 the common connection between bands is 5 (G_postcentral) >7 (S_central) with, again, opposite behaviour considering NREM and WAKE.

In patient 5 the common channel is the 5 (G_and_S_cingul-Mid-Post).

Comparing states, we did not find a common path able to explain different behaviour in conscious or unconscious states. Also considering the macro areas, it is not possible to identify a common direction of the information flow (e.g. from frontal to Brodmann areas in WAKE). As well as we did not find a relevant difference in connection.

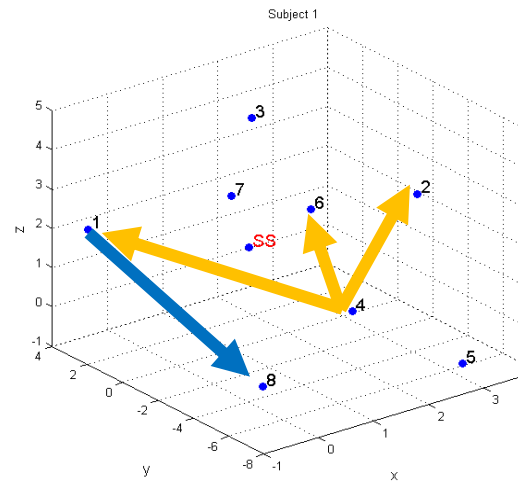
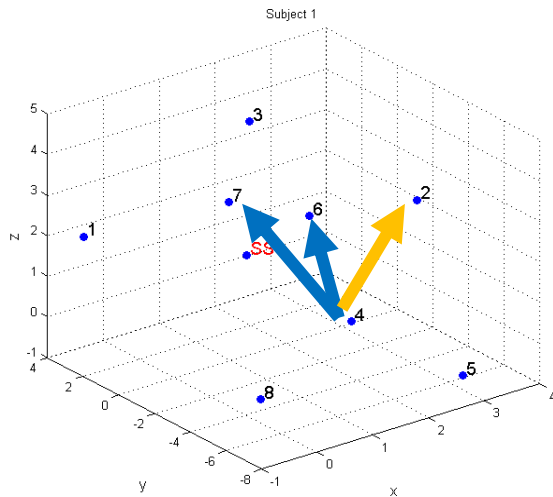
Interestingly, comparing bands, in every subject the arrows indicating connections in NREM and WAKE have the same direction in Gamma band. In 3 over 5 subject the arrows indicating connections in NREM and WAKE have opposite direction in Delta. The information in Gamma goes in the same direction, the information in Delta seems to move in the opposite way.

In the network, the distances between connected nodes can be long or short: in the same system both kinds of length may be present. The paths, the distance between connected

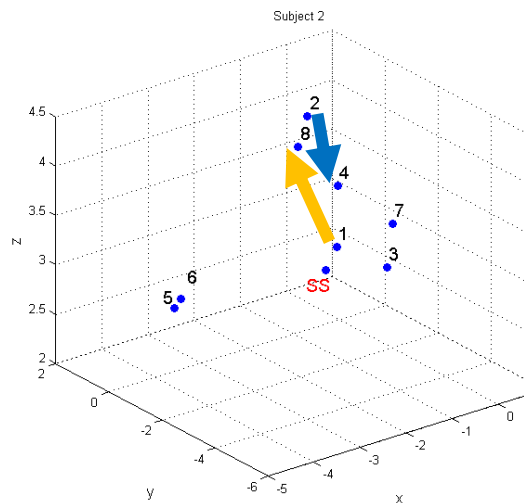
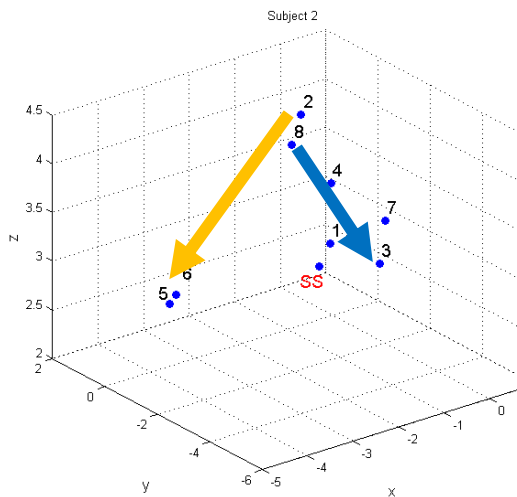
nodes, the positions in relation to the stimulation site (SS) seem not to be affected by parameters.

Connections in Gamma Band	Connections in Delta Band
---------------------------	---------------------------

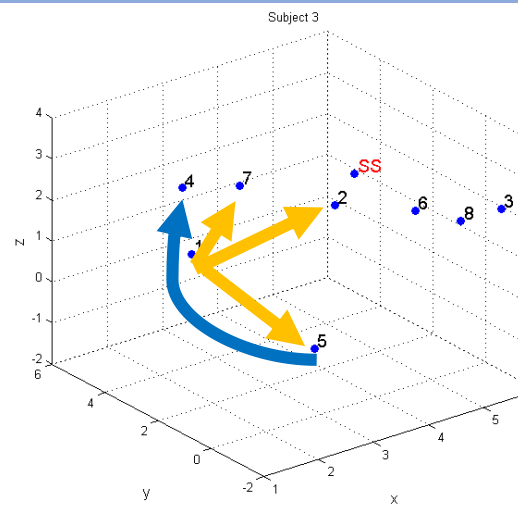
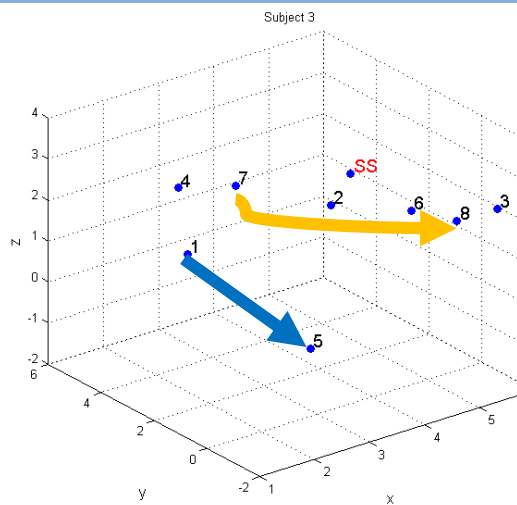
Subject 1



Subject 2



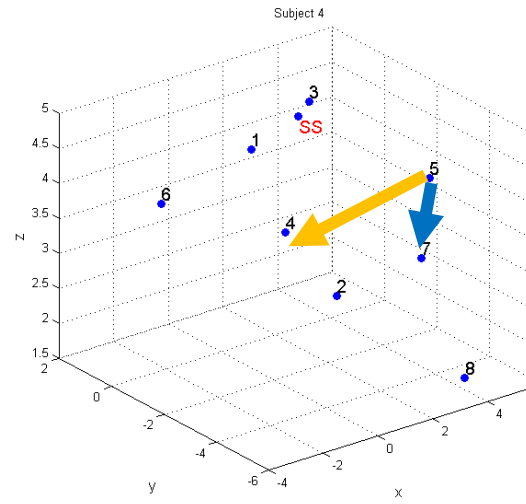
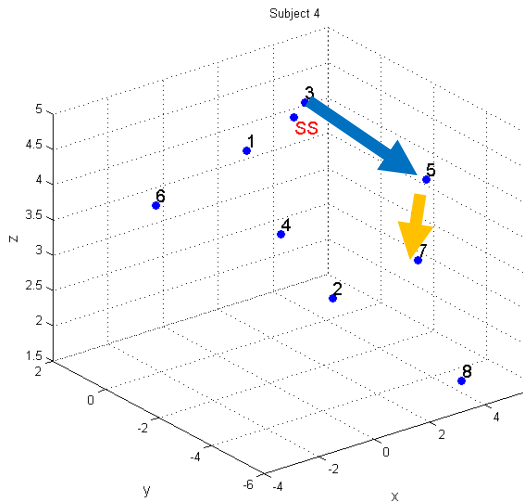
Subject 3



Connections in Gamma Band

Connections in Delta Band

Subject 4



Subject 5

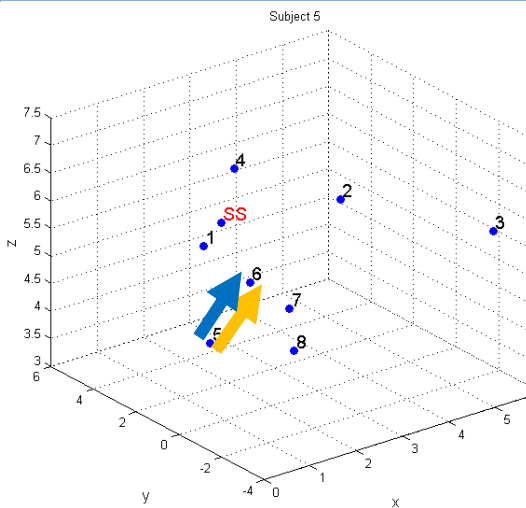
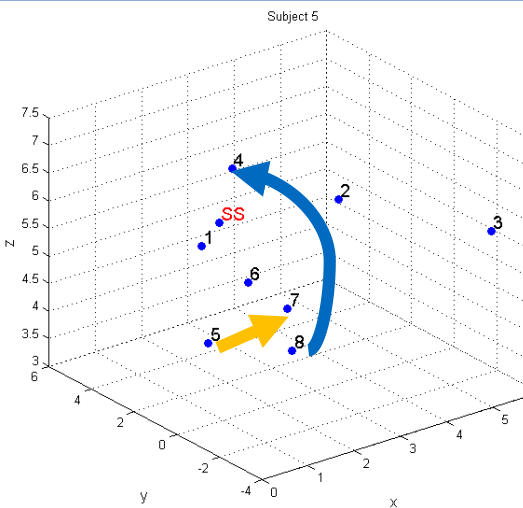


Table 7. Main connection directions represented by arrows: yellow for WAKE and blue for NREM

3.3 Time Varying Directed Transfer Function results over frequencies in Delta and Gamma bands

As described above, Adaptive Directed Transfer Function analysis [70] among multi-channel windowed time series (800 ms) has been performed. The function performs ADTF analysis on each time series using an Adaptive MVAR model (MVAAR) that generates an updated coefficient matrix for each time point, which is then used in the DTF calculations. The time-varying coefficient matrices on each time series is obtained using the Kalman filter algorithm [70] as detailed in Section 2.3.1.

In Section 3.2 the input matrix has been introduced: the output is in the form ADTF.matrix (a,b,c,d), where a = time point, b = sink channel, c = source channel, d = index for the frequency value.

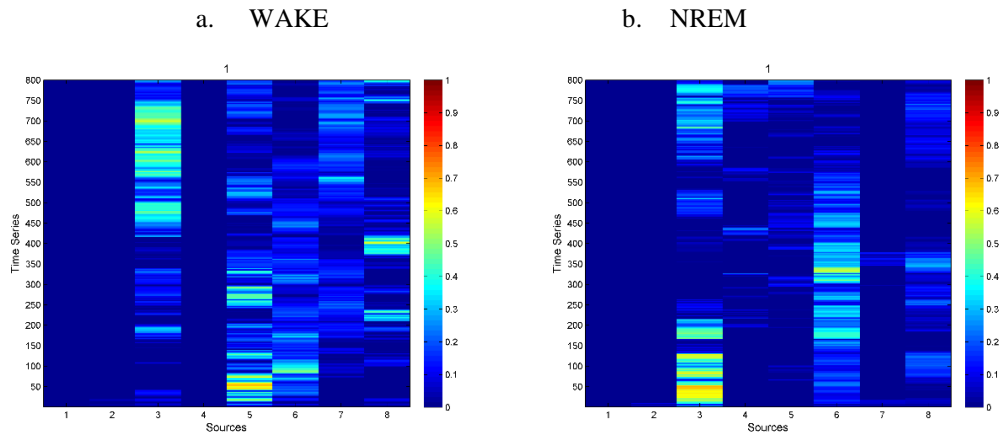
With the aim to find, underline and explain the down-state effect and the re-activation phenomenon, we decided to observe DTF values considering also the time as a parameter. So, we obtained a 4D matrix with information about time and frequency changes for every combination of sink and source channels. Considering the hypothesis that the re-activation is given by a feedback activity from the network, we considered the information inflow of every channels.

If a feedback activity is present, we expected to visualize information flow coming in, followed by a period of virtually no information flow, then the information flow coming in again. Below some examples of DTF activity in some channels and for some subjects are reported.

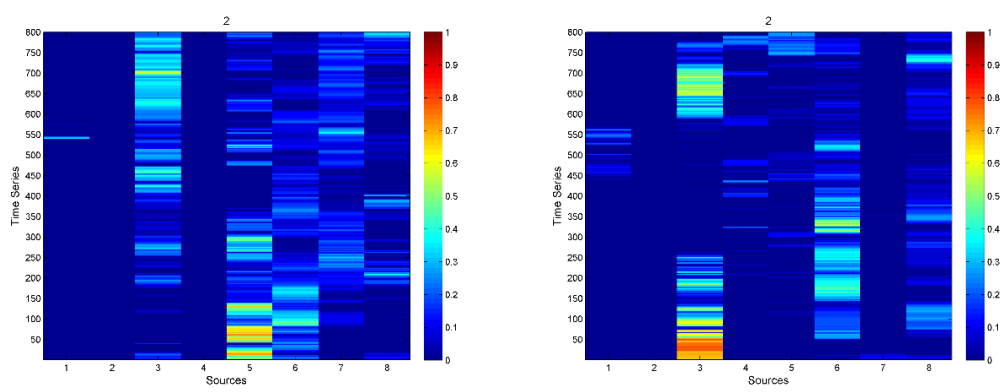
In Figure 5 the inflow activity in sink channels 1, 2, 3 of subject 1 is observable. Data are obtained after frequency averaging. In the Figure 5, it is possible to visualize the time points (into the range of 800 ms) where each source channel influences the observed sink channel. In Gamma band (Figure 3), both in WAKE and in NREM, the inflow in a single sink channels always exists due to the influence of many source channels.

Sink

1



2



3

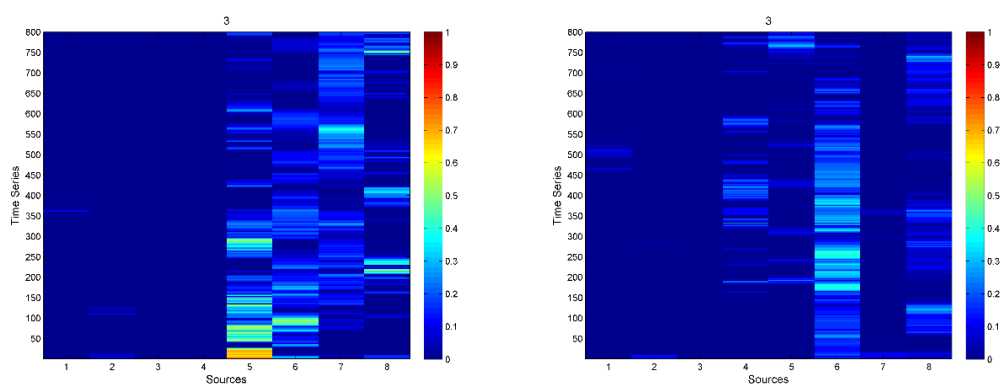


Figure 5. ADF values in Gamma band for subject 1. DTF values in sink channels 1,2,3. On the x axis the 8 source channels are reported. On the y axis the time series of 800 ms is shown. Column a. for WAKE and column b. for NREM.

Now, moving to Delta waves (Figure 6), the immediate observation is that the fragmentation of the information flow present in the Gamma situation is here completely absent. In opposite, the information from one channel to the other is here flowing, stable and with conserved intensity.

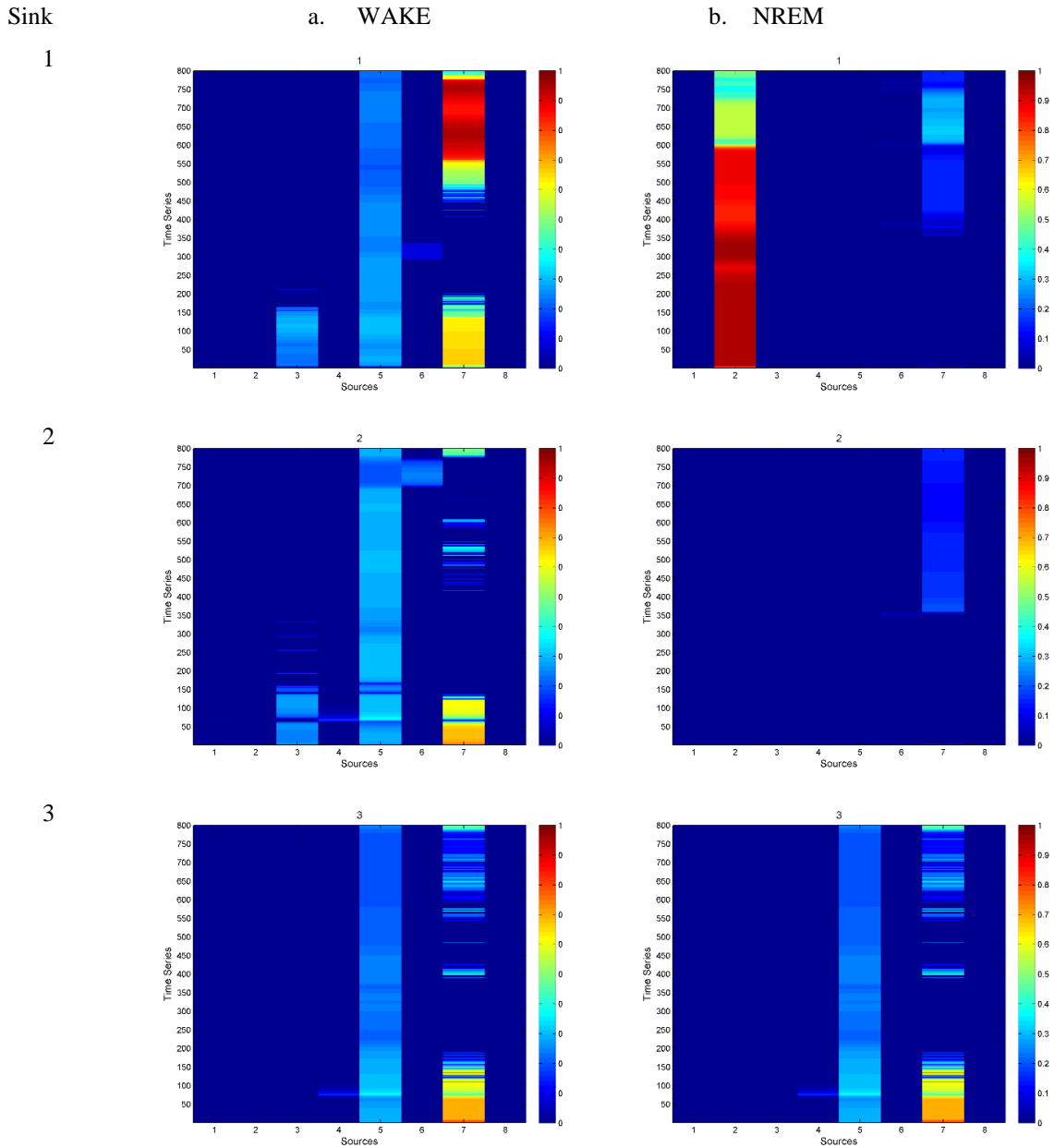


Figure 6. ADTF values in Delta band for subject 1. DTF values in sink channels 1,2,3. On the x axis the 8 source channels are reported. On the y axis the time series of 800 ms is shown. Column a. for WAKE and column b. for NREM.

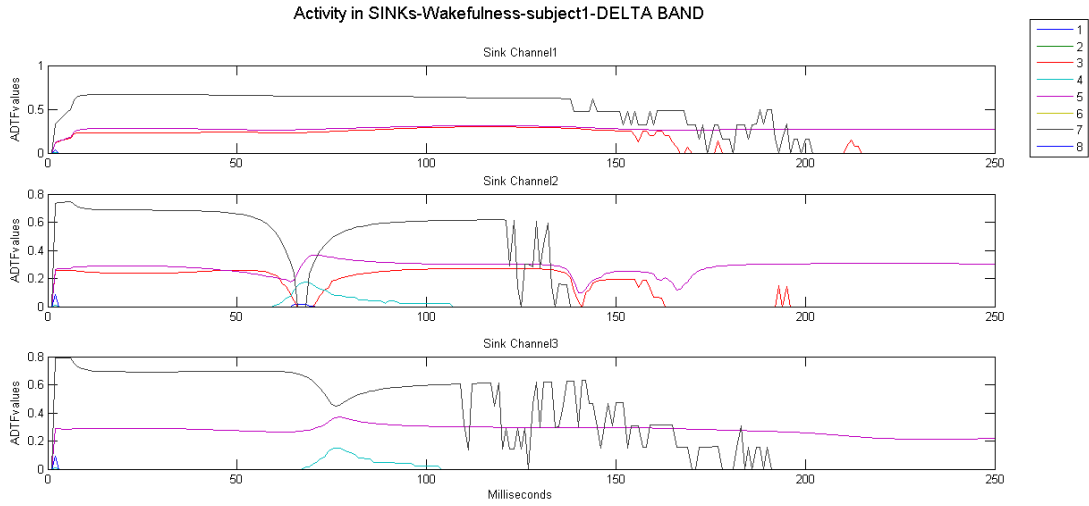
Pigorini et al. [21] reported that the possible down-state time for this patient is around 159 ms after the perturbation, that coincides with 159 ms of the mentioned time series.

Observing one channel per time (Figure 7) we can say that the sink channel receives information in different time points from many channels until 200 ms, then the total amount of information decrease but it is never zero (panel A, Figure 7). We have to consider, in fact, the contribution from many source channels (coloured lines in Figure 7).

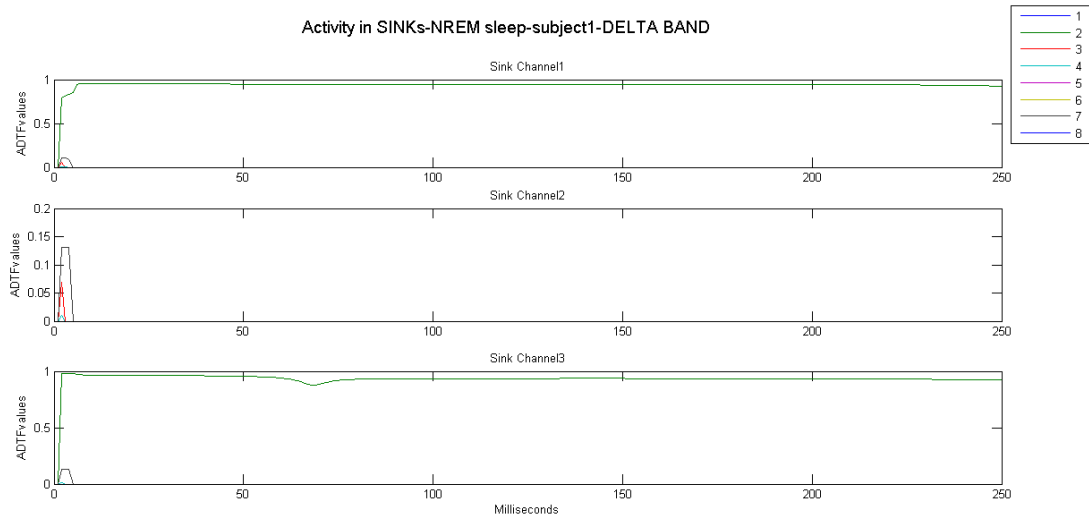
Pigorini et al. reported also a breakdown of the signal in NREM situation after the down-state. In Figure 5 and 7, panel B, we cannot observe a silencing of information flow.

Figures 8 and 9 are reported just as examples to demonstrate the discussed results. In the subject 2 (Figure 8) the down-state, according to the work [21], is expected 135 ms after the perturbation; in the subject 3 (Figure 9) the down-state is expected 108 ms after the perturbation.

We observed a common feature between subjects: WAKE shows two different activities (due to the influence of source channels) in respect of the time point 200 ms, in NREM the activity exhibits an unvaried trend.

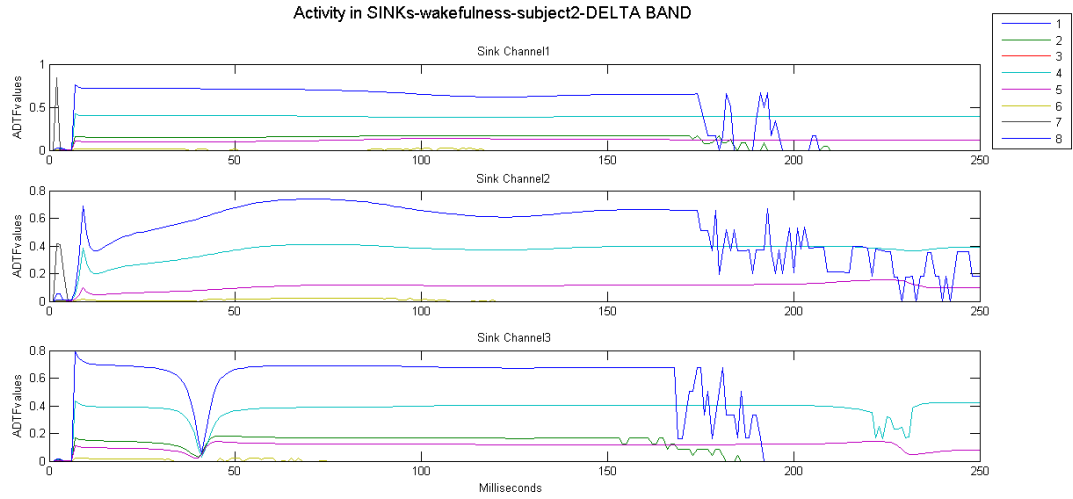


A. WAKE

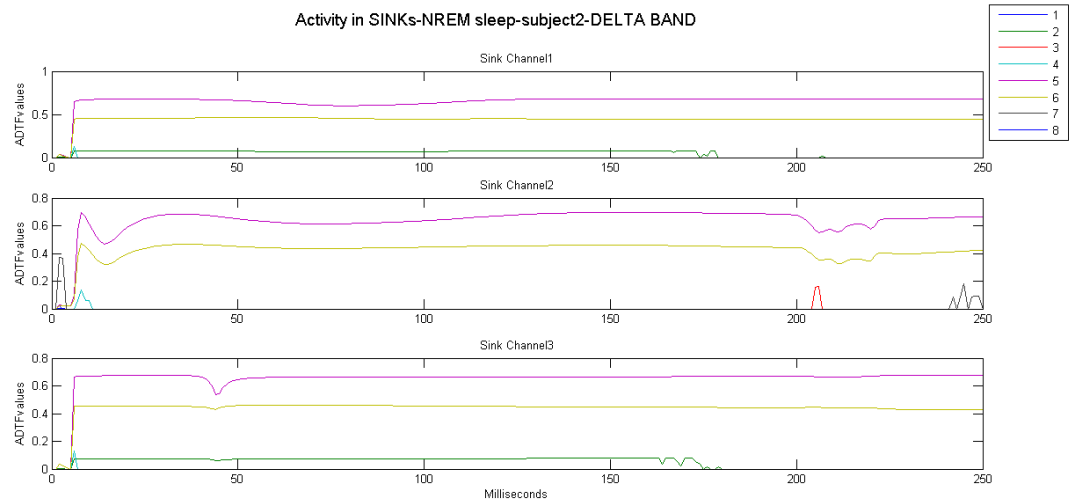


B. NREM

Figure 7. ADTF values in Delta band for subject 1. Only 3 channels are here reported. Panel A shows ADTF values in WAKE, Panel B the ADTF values in NREM. Every coloured lines indicate a source channel, in x axis a window of the time series is reported: the first 200 ms where the down-state is expected (159 ms).

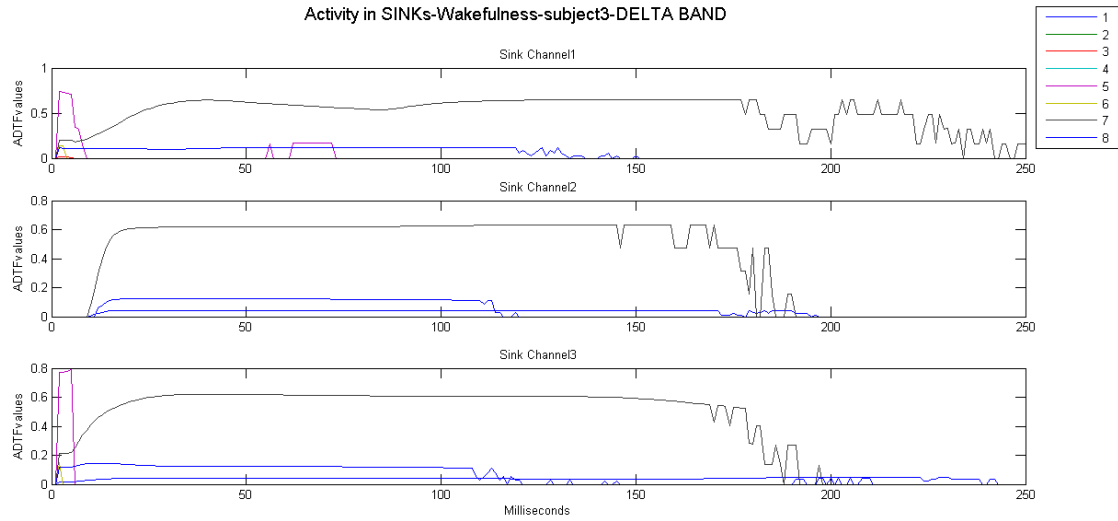


A. WAKE

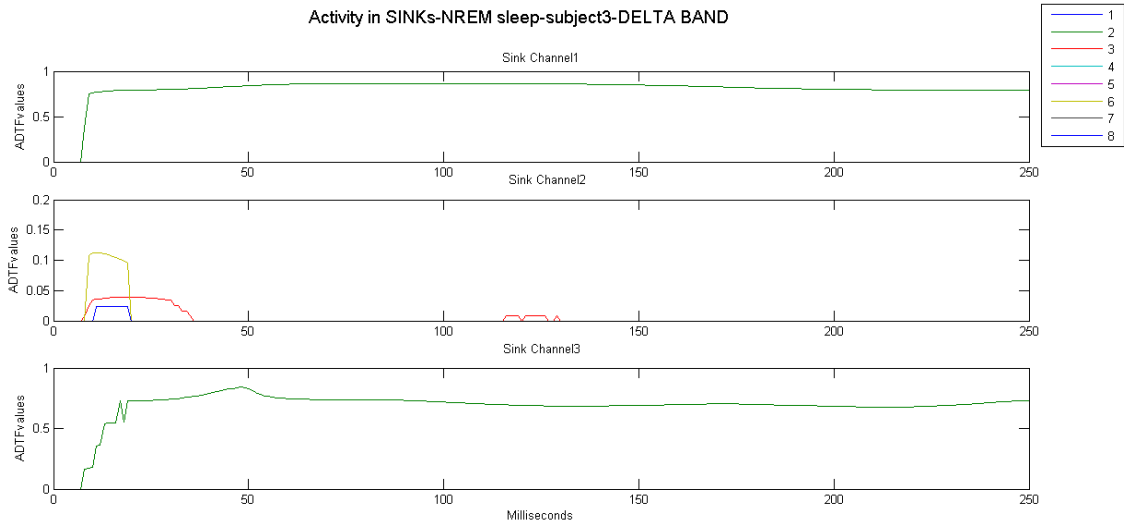


B. NREM

Figure 8. ADF values in Delta band for subject 2. Only 3 channels are here reported. Panel A shows ADF values in WAKE, Panel B the ADF values in NREM. Every coloured lines indicate a source channel, in x axis a window of the time series is reported: the first 200 ms where the down-state is expected (135 ms).



A. WAKE



B. NREM

Figure 9. ADTF values in Delta band for subject 3. Only 3 channels are here reported. Panel A shows ADTF values in WAKE, Panel B the ADTF values in NREM. Every coloured lines indicate a source channel, in x axis a window of the time series is reported: the first 200 ms where the down-state is expected (108 ms).

3.3.1 *Statistical Analysis on windowed data*

We proceeded creating two windows containing ADTF values (4-D ADTF.matrix (time, sink, source, frequency)): one immediately before the known down-state point and the other one immediately after. So, we selected and extracted ADTF values from windows lasting 100 milliseconds. We calculated the frequency mean obtaining a 3D matrix (ADTF.matrix (time, sink, source)), then we calculated the influence of all source channels in each sink channel obtaining a 2-D matrix (one ADTF values per every millisecond). As last step, the mean was extracted from values in time, and this mean for each sink channel was considered as a descriptive feature and utilized in statistical analysis.

Given that the down-state is not peculiar of i) a single subject or ii) some particular channels or iii) particular position of the channels, but is peculiar of NREM situation, we pooled data of all patients and all electrodes. The only distinction taken into account was the conscious state. We designed the experiment considering 4 groups of 40 elements each (40 means of ADTF values). The four groups (later called INPUT groups) were:

1. Means of ADTF values calculated on the window BEFORE the down-state in WAKE situation;
2. Means calculated on the window AFTER the down-state in WAKE situation;
3. Means calculated on the window BEFORE the down-state in NREM situation;
4. Means calculated on the window AFTER the down-state in NREM situation.

We aimed to test if some conditions (BEFORE/AFTER the down-state corresponding to a particular conscious state) have significantly higher means than others.

For the significance evaluation we applied Analysis of variance (ANOVA), where the null hypothesis was that all the averages do not differ from each other. The simplest model of variance analysis (one-way ANOVA) uses only one classification criterion comparing the means between groups and determining whether any of those means are statistically significantly different from each other. The limitation of this procedure is that it cannot determine which specific groups were statistically significantly different from the other groups. The two-way ANOVA compares the mean differences between groups that have been split on two independent variables (factors). In two-way ANOVA the effects of two

factors, on a response variable, are of interest. The two-way ANOVA tests hypotheses about the effects of factors A and B , and their interaction on the response variable.

In our case, the columns of the INPUT matrix must correspond to groups of the column factor, B : these indicate Status (WAKE/NREM) and Situations (BEFORE/AFTER the down-state), groups previously named 1:4. The rows of the INPUT matrix must correspond to the groups of the row factor, A : which include all channels (8 per each subject) and all subjects (five) from datasets.

We first applied ANOVA, after we used MANOVA to visualize differences due to the *inter*-patients variability. ANOVA and MANOVA analysis have been used to underline different characteristics from our dataset. Multivariate analysis of variance (MANOVA) is an extension of ANOVA test: the second tests the difference in means between two or more groups, while the first evaluates the difference in two or more vectors of means (it tests multiple dependent variables). MANOVA is applied on means of the columns of X , grouped by groups. X is an m -by- n matrix of data values, and each row is a vector of measurements on n variables for a single observation. Two observations (that represent a sample from a population) are in the same group if they have the same value in the group array.

In our dataset, X is the same Table INPUT used in ANOVA previously explained; the group variable contains repeated number from 1 to 5 which represent the patient 1:5.

In both analyses (ANOVA and MANOVA) we used multiple comparison procedures: pairwise comparison of the group means.

3.3.1.1 *Delta Band*

Starting from Delta waves, using the two-way ANOVA procedure we obtained the following results.

The data distribution of the four groups is reported in Figure 10 and 11. The p -value for the condition (WAKE /NREM, BEFORE/AFTER) effects (columns) is very low; the p -value for the *inter*-patient variability (rows) is under the threshold of 0.01 (Figure 12). This indicates that one factor (in the row or in the column) is out-performing the other, so we proceeded to the multicomparison with MANOVA in order to find the different element.

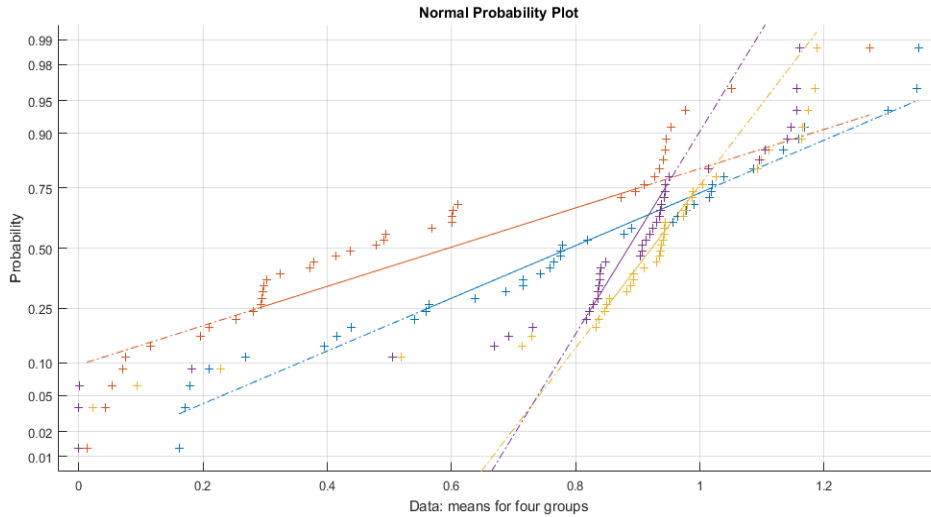


Figure 10. Normal probability plot of the 4 input groups in Delta band. Group one in Blue, group two in orange, group three in yellow, group four is violet

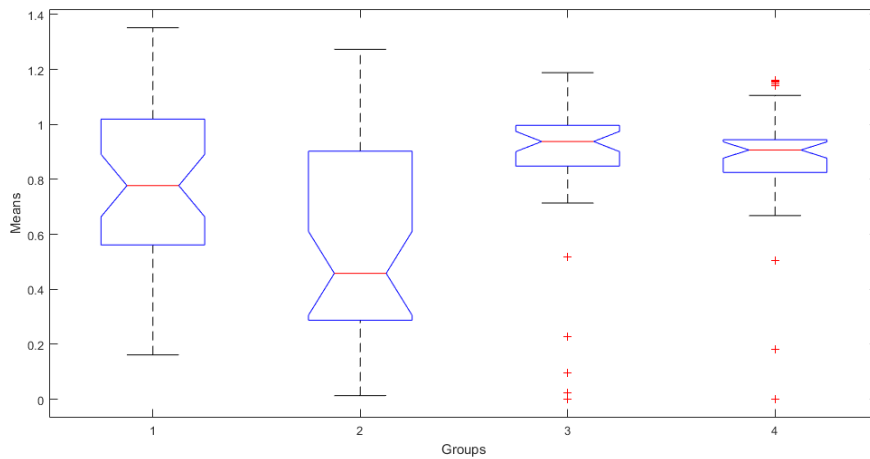


Figure 11. Boxplot of data into the groups (Delta Band). 4 Groups: 1) means calculated on window before the down-state in WAKE situation; 2) means calculated on window after the down-state in WAKE situation; 3) means calculated on window before the down-state in NREM situation; 4) means calculated on window after the down-state in NREM situation

ANOVA Table					
Source	SS	df	MS	F	Prob>F
Columns	2.9462	3	0.98206	15.74	1.15244e-08
Rows	8.3741	39	0.21472	3.44	1.39322e-07
Error	7.2982	117	0.06238		
Total	18.6184	159			

Figure 12. Two-way ANOVA Table result in Delta Band

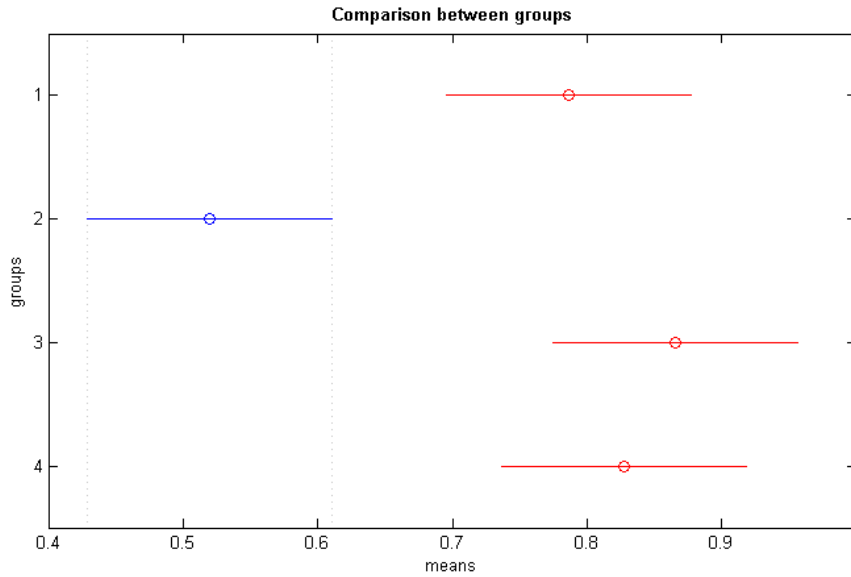


Figure 13. ANOVA conclusive analysis: multicomparison between groups (Delta band). 4 Groups: 1) means calculated on window before the down-state in WAKE situation; 2) means calculated on window after the down-state in WAKE situation; 3) means calculated on window before the down-state in NREM situation; 4) means calculated on window after the down-state in NREM situation

In Figure 13, the blue bar shows the interval of comparison for the mean of the selected group: Group 2 (means in WAKE condition calculated in the window following the down-state) differs from all the other three groups ($p < 0.00001$ in all the comparisons). Group 2 is peculiar of the consciousness state: in fact, the means are calculated from the windowed data where the re-activation phenomenon is awaited. As expected, Group 2 differs from Group 4 where a completely different behaviour of the network is forecast.

Proceeding with MANOVA, we meant to underline differences between subjects. In fact, as shown in the cluster dendrogram (Figure 14), subject one has a completely different response in comparison with the others.

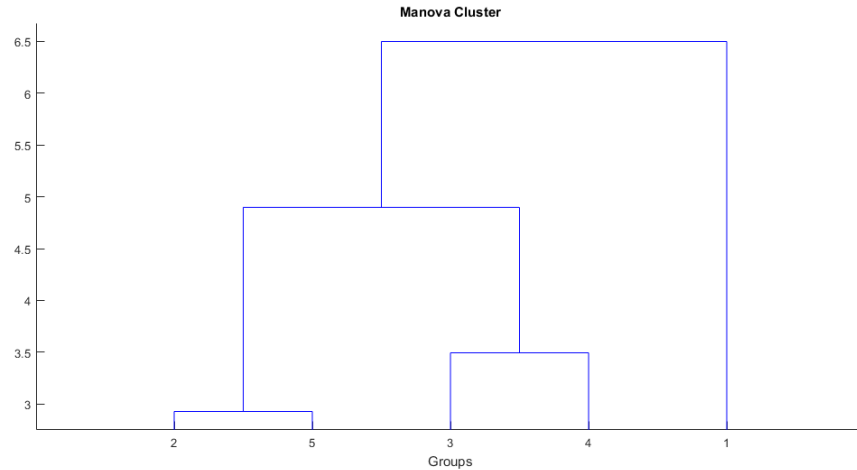


Figure 14. Dendrogram from MANOVA statistics. (Delta band) Clusters are computed by applying the single linkage method to the matrix of Mahalanobis distances between group means.

3.3.1.2 Gamma Band

If down-state is peculiar for the slow waves, analysing the Gamma band a differ statistics is not expected. The above mentioned statistical analysis scheme was applied also on data from Gamma band. Input Matrix and Groups vector were the same.

The data distribution of the four groups is reported in Figure 15 and 16.

Two-way ANOVA results are the following:

- the p -value for the condition (WAKE /NREM, BEFORE/AFTER) (shown in columns) is very low (0.0012),
- the p -value for the *inter*-patient variability (in rows) is < 0.00001 (Figure 15).

This indicates that one element of row and one of the column is out-performing the other: thus we proceeded to the multicomparison and MANOVA in order to find the different elements.

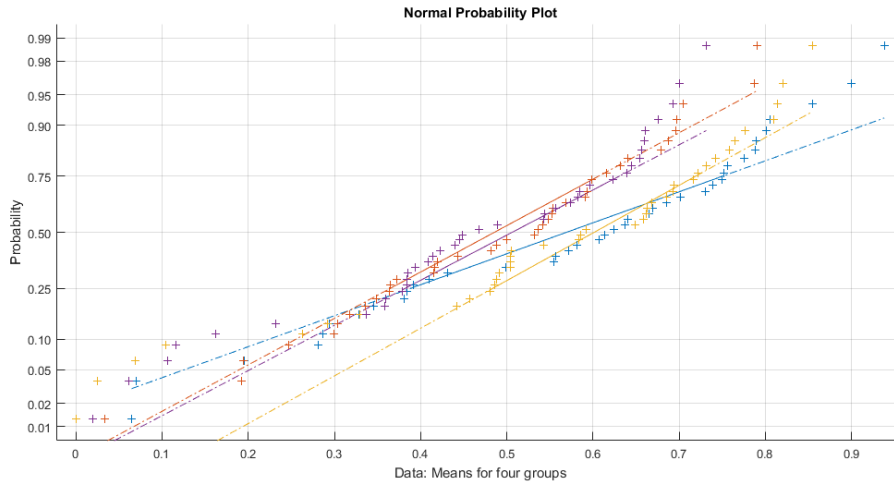


Figure 15. Normal probability plot of the 4 input groups in Gamma band. Group one in Blue, group two in orange, group three in yellow, group four is violet

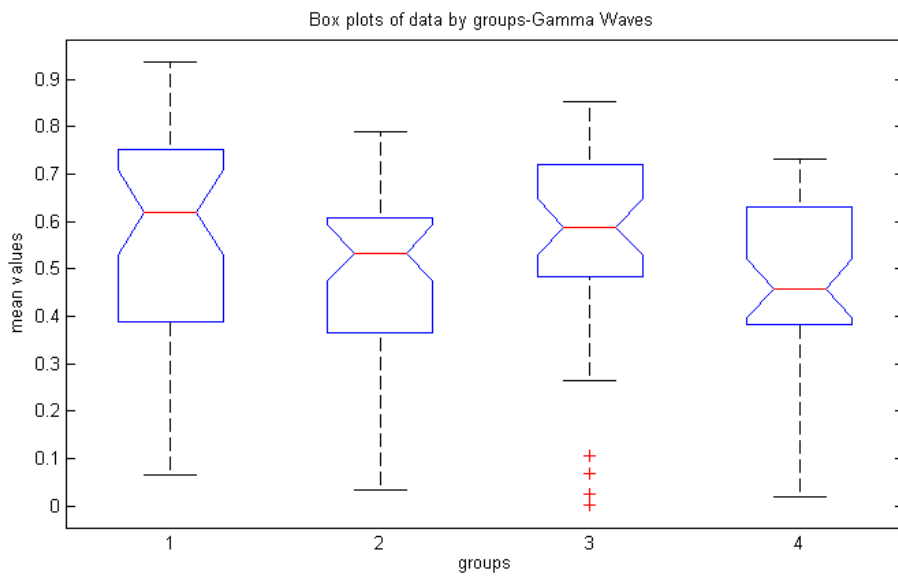


Figure 16. Boxplot of data by groups (Gamma Band). 4 Groups: 1) means calculated on window before the down-state in WAKE situation; 2) means calculated on window after the down-state in WAKE situation; 3) means calculated on window before the down-state in NREM situation; 4) means calculated on window after the down-state in NREM situation

ANOVA Table					
Source	SS	df	MS	F	Prob>F
Columns	0.30875	3	0.10292	5.67	0.0012
Rows	4.29356	39	0.11009	6.06	0
Error	2.12439	117	0.01816		
Total	6.72669	159			

Figure 17. Two-way ANOVA Table result in Gamma Band

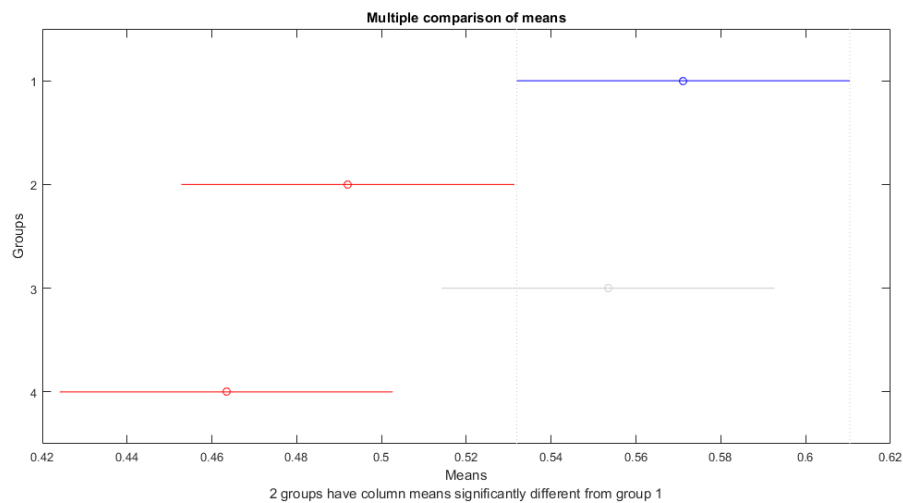


Figure 18. ANOVA conclusive analysis: multicomparison between groups (Gamma band). 4 Groups: 1) means calculated on window before the down-state in WAKE situation; 2) means calculated on window after the down-state in WAKE situation; 3) means calculated on window before the down-state in NREM situation; 4) means calculated on window after the down-state in NREM situation

In Figure 18 the blue bar shows the comparison interval for the selected group mean: Group 1 (means in WAKE condition calculated in the window before the down-state) differs from the Group 2 ($p=0.0477$) and from the Group 4 ($p= 0.0028$). But also Group 3 differs from 4 ($p=0.0178$) (data not shown in the picture).

These results can be described in this way: in Gamma band, connectivity that occurs before the expected down-state is completely different from the connectivity after the down-state, considering both the WAKE and the NREM conditions.

Connectivity before and after the down-state changes in WAKE but also in NREM state. The network connectivity in both conscious states changes according to the position of the down-state.

There is also a difference between WAKE before the down-state and NREM after the down-state: this indicates that differences in this network parameters are not due to the presence of consciousness.

Thanks to these connectivity and statistics analyses we can achieve interesting information on differences between the networks in the conscious states.

Results in Gamma band are not directly linked to the re-activation phenomenon, that occurs only in WAKE condition; in fact, not only the Group 2 differs from the other, but also we did not find differences between the Group 3 and 4. We confirmed the presence of an effect/phenomenon able to affect the network, and this effect can be identified with the down-state: in fact, differences occur always between two periods of the same dataset.

MANOVA test showed that, in Gamma band, the subject that differs is the number 4 (Figure 19), differently from the number 1 as in Delta analysis. These data reinforce the idea that analysis is subjected to many factors and we must observe a wide variability in results.

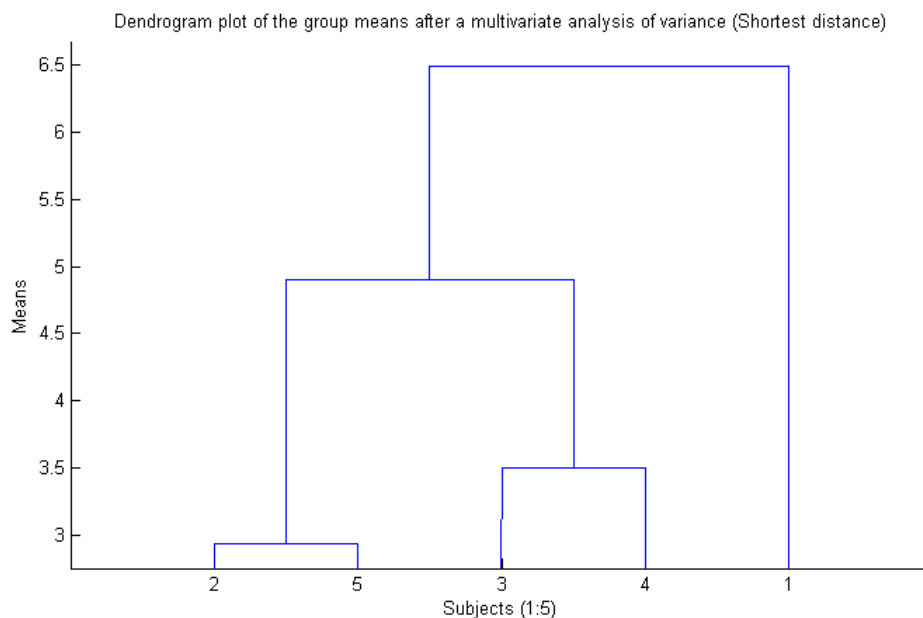
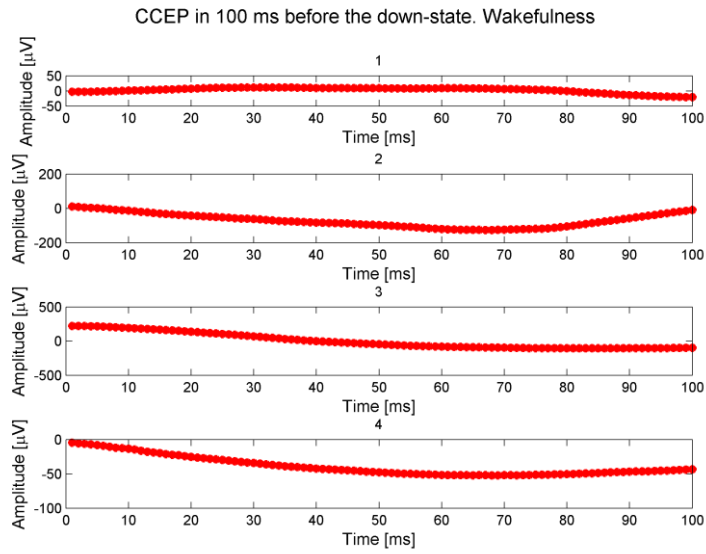


Figure 19. Dendrogram from MANOVA statistics (Gamma band). Clusters are computed by applying the single linkage method to the matrix of Mahalanobis distances between group means

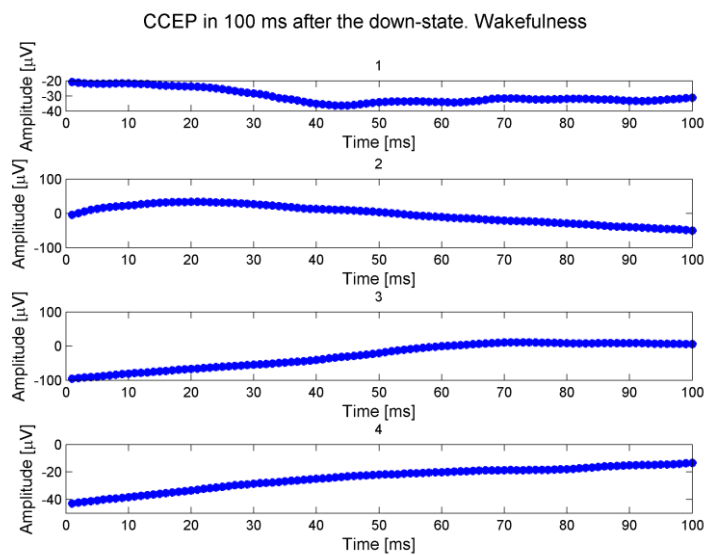
3.3.1.3 *Original Signals*

The described results outline that we did not visualize the down-state and the re-activation phenomena in our connectivity results, but we observed differences in connectivity. In order to confirm the unicity and validity of the connectivity analysis, we compared results from this technique with results coming from raw data.

We decided to better investigate the original signals as resulting from the only preprocessing step. We created the same windows containing 100 samples, samples extracted exactly before and after the down-state time. We calculated CCEP (100 samples per 29 stimulations for each signal) then the mean for each time window (Figure 20 and 21). We performed ANOVA as previously explained.

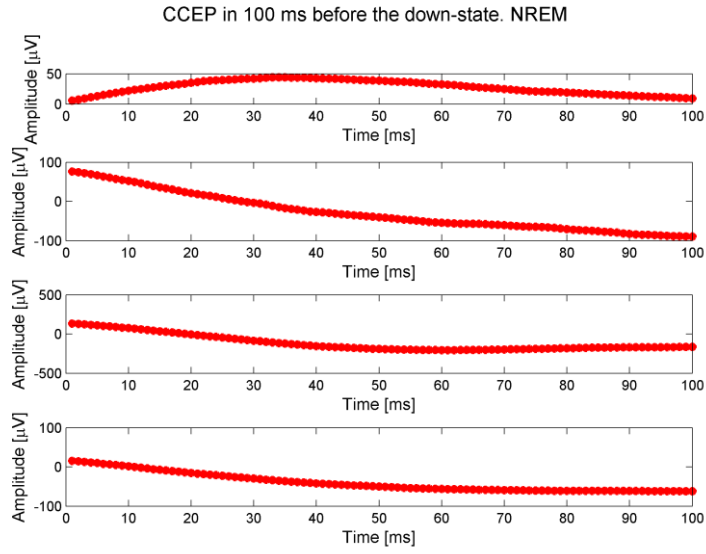


A.

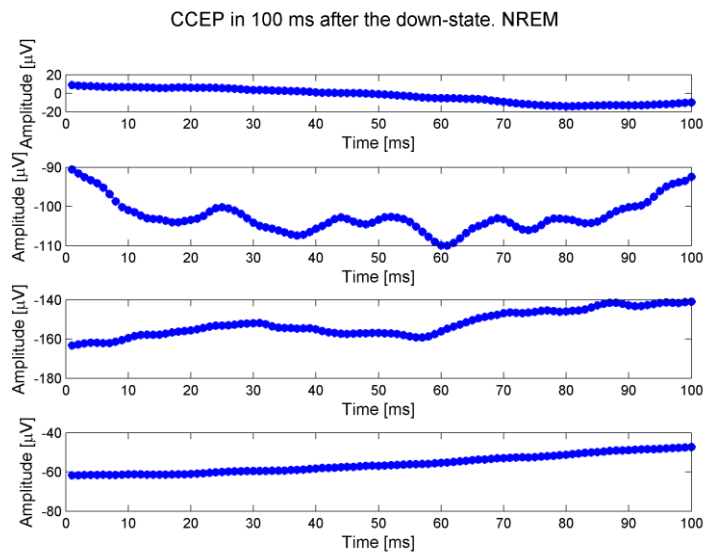


B.

Figure 20. Characteristics of four iEEG signals before (panel A) and after (panel B) the down-state in a representative subject during WAKE



A.



B.

Figure 21. Characteristics of four iEEG signals before (panel A) and after (panel B) the down-state in a representative subject during NREM

The data distribution of the four groups is reported in Figure 22 and 23.

Unfortunately, we could not apply the Fourier Transform because the frequency resolution into the window is 10 Hz (Sample Frequency/Number of samples=1000/100).

A simple subtraction of means revealed an opposite behavior with respect to the re-activation phenomenon: the difference between the mean after and before the down-state is positive in the NREM condition (Figure 22).

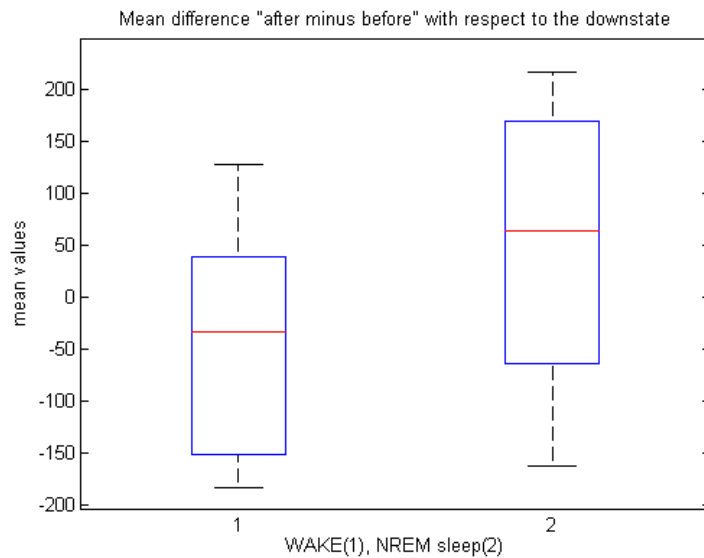


Figure 22. Boxplot on windowed data using original signals, not from DTF analysis. The mean values collected after the possible down-state are subtracted to the mean values collected before the possible down-state. The two states WAKE (1) and NREM (2) are considered.

Two-way ANOVA shows no differences between the four groups (Figure 25), but differences between subjects (rows in Figure 24). And, again, we observed a result different from the previous analysis: the main difference is between subject 3 and the others (Figure 26).

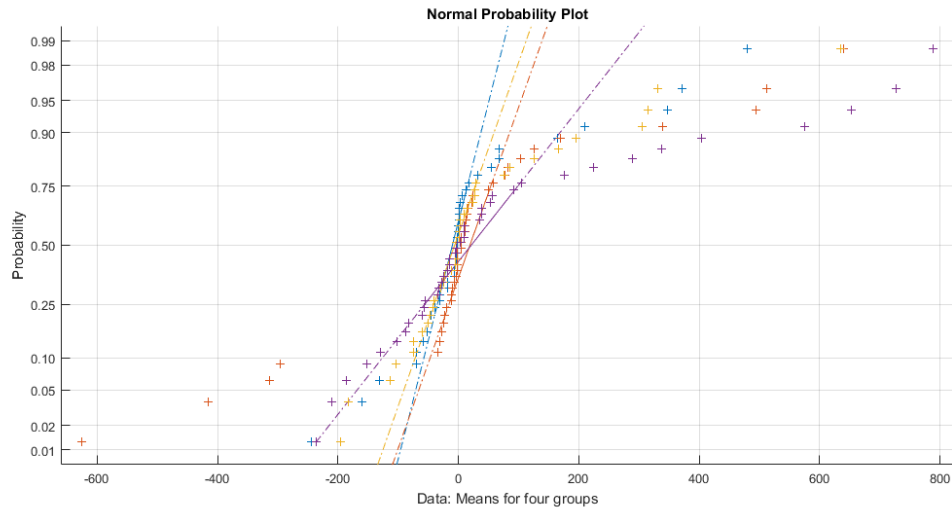


Figure 23. Normal probability plot of the 4 input groups in original signals. Group one in Blue, group two in orange, group three in yellow, group four is violet.

ANOVA Table					
Source	SS	df	MS	F	Prob>F
Columns	85802.6	3	28600.9	2.19	0.093
Rows	4234345.2	39	108573	8.31	0
Error	1528619.9	117	13065.1		
Total	5848767.7	159			

Figure 24. Two-way ANOVA table result in original signals

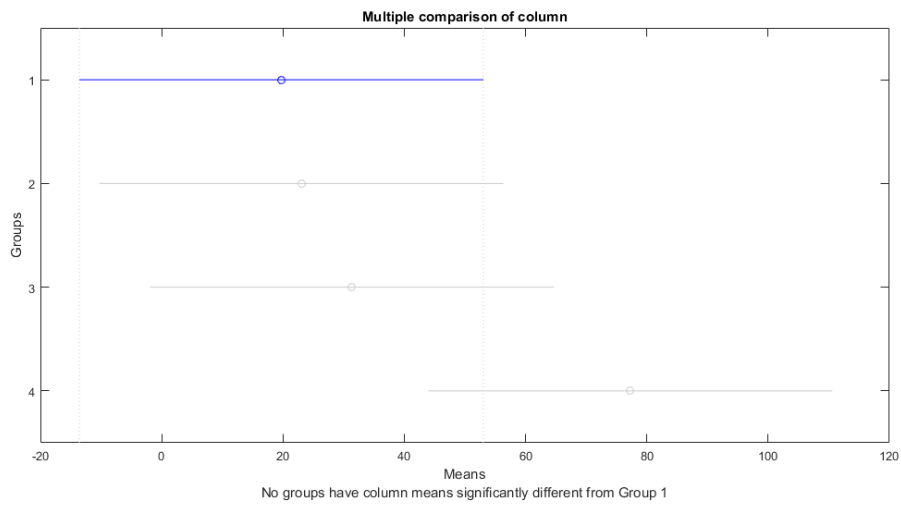


Figure 25. ANOVA conclusive analysis: multicomparison between groups (Original signals). 4 Groups: 1) means calculated on window before the down-state in WAKE situation; 2) means calculated on window after the down-state in WAKE situation; 3) means calculated on window before the down-state in NREM situation; 4) means calculated on window after the down-state in NREM situation

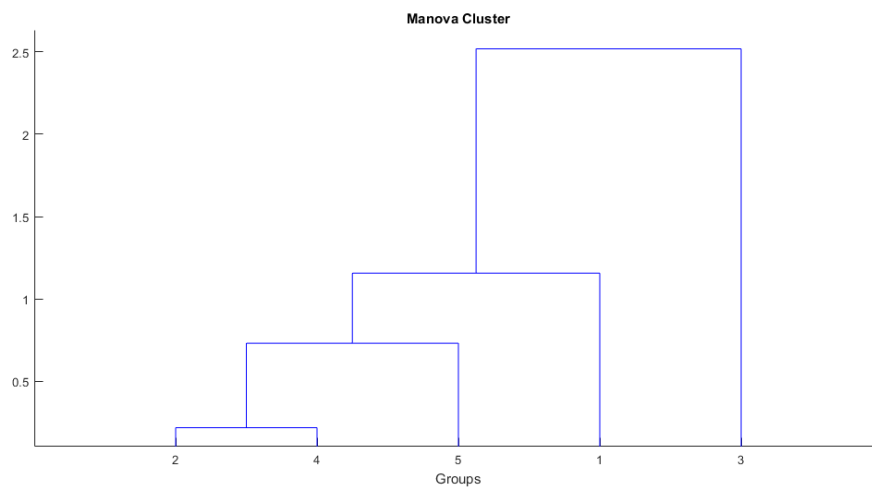


Figure 26. Dendrogram from MANOVA statistics (Original signals). Clusters are computed by applying the single linkage method to the matrix of Mahalanobis distances between group means

3.4 Conclusions

DTF and ADTF analysis allowed to get many observations able to introduce new issues to the opened questions of the dissertation. DTF analysis allowed to analyze the path and the direction of the information flow into the network. On the other hand, the ADTF procedure shed light on information flow considering the time parameter, thus it was able to inquire on the down-state effect as known in literature.

DTF has been helpful to localize sinks, sources, and locations of the major players of the network. ADTF has been useful to extract data to be submitted to statistics in order to prove the existence of a different behavior of the two networks after the expected down-state.

Conclusions regarding the DTF analysis could be summarized as follows:

1. As reported in literature, connections coming from and in the frontal area are predominant in Gamma band. This is particular evident in WAKE state where frontal area is mainly involved as sink. In NREM, instead, other macro areas are involved.
2. In Gamma band the number of connections is higher in WAKE, but the intensity of connection is higher in NREM.
3. Differences in connectivity numbers between Delta and Gamma could be explained considering the role of High-Gamma oscillations, often considered to be largely local.
4. In Delta band a restricted number of connections is involved, probably due to the smaller range of frequencies.
5. Main source channels are better underlined in Delta band: these are mainly positioned in Brodmann's areas.
6. WAKE shows a higher connection intensity in Delta band, in contrast to what observed in Gamma band.
7. We can observe some common connections between the two frequency bands.
8. We did not find common paths able to explain the presence or absence of consciousness. The network seems to be not influenced by the electrode position.

9. It is of interest to observe the direction of the information flow:
 - a. in Gamma band, WAKE and NREM connections have the same direction;
 - b. in Delta band, WAKE and NREM connections have opposite direction.

Conclusions regarding the ADTF analysis could be summarized as followed:

1. Delta band shows a continuous and ordered information flow: the opposite is observable in Gamma band, where the information flow shows to be fragmented.
2. Thanks to the ADTF analysis it is possible to observe which channels are involved considering the time after the perturbation. Given that, the cortex area directly involved with the stimulus is perturbed immediately after the stimulation, and later we can observe the activation of the secondary cortex; thanks to the ADTF analysis we can visualize which is the cortex region is involved after a precise perturbation able to induce a response.
3. The down-state is not observable by means of a summary quantitative analysis: in fact, the total amount of inflow per channel is never close to zero.
4. Applying statistics to data extracted from the windows before and after the down-state point, we can visualize in Delta waves a difference between the behavior of WAKE and NREM in the period after the down-state in Delta waves. This result can be explained by the re-activation phenomenon.
5. Analyzing the differences *inter*-subjects, we visualized shorter paths and clustering trees between some of them: *inter*-patient variability is an element to be considered. This variability is also linked to the frequency band.
6. We visualized different behaviors of the network before and after the down-state in both conscious states also in Gamma band. We can confirm the presence of an effect, probably the down-state, able to change the connectivity network. This down-state shows to be not only related to the slow waves.
7. Connectivity analysis has been the right choice to reveal differences in the network: in fact, these differences are not presence in raw signals.

Thanks to the connectivity analysis we observed how the information flow moves into the network and changes in time and frequency.

Using DTF we observed differences in band frequency and we focused our attention on the local position of the electrodes.

Using ADF we collected observations also regarding the time: thanks to this additional information we extrapolated data from specific windows in the neighbourhood of the expected down-state. By means of statistics, we confirmed that something really happens after a certain time in WAKE and not in NREM. But this is peculiar only of some frequency ranges and, above all, visible in a broad range of frequencies or with higher oscillation.

4 ADDITIONAL RESULTS

4.1 NREM and WAKE classification by means of feature extraction methods

Polysomnography (PSG) with multichannel electroencephalograms (EEGs), surface electromyography, multichannel electrocardiograms, photoplethysmogram and actigraphy are the techniques employed for sleep investigation. But the understanding of the brain functionality and its connectivity during sleep is still limited. In fact, the mentioned instrumentations are not able to capture all the modifications happening in the cortex areas.

We obtained data from a powerful technique: iEEG is the gold standard technique to analyse differences between signals in brain cortex (with millisecond time resolution and centimetre spatial resolution) [37] and it allows to visualize the signals network [79] .

The most interesting results were obtained using connectivity analysis, specifically with the time varying Directed Transfer Function, that evaluates DTF values in each millisecond. We focused our attention to the presence of the down-state and the re-activation phenomena. We did not confirm the presence of these events, but underlined a difference in means between data slices positioned before and after the expected down-state. Means from ADTF values, in Delta band, extracted after the down-state and compared using ANOVA have proven to be a feature able to distinguish between NREM and/or WAKE.

By means of the performed analysis we never visualized the down-state effect. As it would be very useful to find a way to detect the down-state, a possible approach could be using feature extraction techniques (FE). We applied FE techniques on the same iEEG signals, in particular on the subject 1, performing another pre-processing method. Our paper [80] presents a detailed description of this procedure .

We investigated and compared the performance of different methods able to distinguish between WAKE and NREM states. Furthermore, we evaluated anatomical regions capable of differentiating the two physiological conditions.

For this purpose, we made the following steps:

1. We determined the most meaningful channel:
 - a. Signals were divided in epochs 600 ms long with the same method applied in Section 3.1.
 - b. We computed the standard deviation (STD) for each epoch and channel, then we selected the two channels with maximum absolute difference, considering the median STD values, between the two WAKE and NREM conditions. The two channels resulted to be “Superior Temporal Sulcus” (STS) and “Intraparietal-Sulcus and Parietal Transverse” (IPS). Performing Pearson’s correlation, the two channels resulted to have a moderate-to-high correlation, so we decided to continue the analysis only with STS.
2. We performed Wavelet decomposition (Daubechies mother wavelet, level 6, order 4) to increase the frequency resolution; both the approximation (Ca) and detail coefficients (Cd6) of the last level were considered for the analysis.
3. We employed an Artificial Neural Networks (ANN) as a classification method. We applied the ROC (Receiver Operating Characteristic) curve to further evaluate the performance of the classifier.
4. We tested with the ANN a combination of features (STD, Ca, Cd6) in order to detect which one was capable of differentiating NREM and WAKE. Sensitivity (Se), Specificity (Sp) and Accuracy (Acc) were computed for each combination.

We obtained the following results:

- STD values were greater in NREM compared to WAKE for both STS and IPS.
- Ca, Cd6 got similar accuracy performances in ANN classification, 95.71% and 92.85% respectively; the accuracy resulted to be higher when Ca and Cd6 are combined with STD or between them (98.57%) (Table 8).
- *t*-test on AUC values gave the following information (Table 9):
 - there was no significant difference between Ca and Cd6 performances;
 - the associations of Ca with Cd6 and of Ca with STD did not improve the classification performances with respect to Ca or Cd6 alone.
- The STD analysis was able to identify channels (STS and IPS) that could be defined as peculiar sites for consciousness. Further tests (Wavelet classified with ANN)

demonstrated the importance of the STS channel (Superior Temporal Sulcus). Studies from literature report multisensory processing capabilities of STS, whose activation shows to be linked to specific social inputs (speech and hearing) [81][82][83]. The STS main function is the cross-modal integration, as it receives input from sensory areas.

- STS is positioned into the temporal lobe, whereas IPS is posteriorly from postcentral sulcus toward occipital lobe. These areas are not in frontal lobe: Koch et al. [84] reported that the anatomical areas correlated to consciousness are primarily localized in the posterior cortical area rather than in the fronto-parietal one.

Performance (%)			
Features	Accuracy	Specificity	Sensitivity
STD	82,84±13,14	70,87±33,81	87,51±16,30
Ca	95,71±9,65	92,5±16,87	100±0,00
Cd6	92,85±10,11	88±17,35	96,67±10,53
Ca+STD	98,57±4,52	96,67±10,53	100±0,00
Cd6+STD	98,57±4,52	97,5±7,91	100±0,00
Ca+Cd6	98,57±4,52	96,67±10,53	100±0,00

Table 8. ANN classification: Average and standard deviation evaluated on the test set, computed over 10 runs (Sensitivity: the true recognition of wakefulness).

AUC	
STD	0,9389±0,063
Ca	0,9986±0,003
Cd6	0,9967±0,006
Ca+STD	0,9960±0,012
Cd6+STD	0,9998±0,001
Ca+Cd6	0,9934±0,018

Table 9. Average and standard deviation of AUC of the NN outputs computed over 10 runs.

The joined application of connectivity and Wavelet analysis combined to ANN returned excellent results. Even though it must be noted that:

- the performed pre-processing was completely different, because we did not use a bipolar montage but we re-referenced with a common average;
- the channels selected for this work were different compared to the one used in connectivity analysis;
- methods employed were completely different

It is worth to underline that we obtained a common result between the connectivity analysis (described in Chapter 3) and the Wavelet/ANN study: data from subject 1 demonstrated a relevant role of the occipital/parietal area. In fact, in connectivity analysis the channel 4, positioned in occipital and parietal area, is a source channel in both Gamma and Delta bands. The information flow is directed from occipital/parietal to frontal area.

The result is consistent across Wavelet/ANN and connectivity studies, but the result is not consistent across patients: in Chapter 3 where the source channel is mainly positioned into the frontal area, as shown in Figure 14, subject 5 has the longest distance within the subject group.

4.2 How much the re-referencing style can affect the connectivity result? Comparison between three different styles

SEEG recordings were analysed with a referential montage in which every single intracranial channel was referenced to a single channels placed into the white matter (electrically inactive).

Bipolar re-referencing is not the only possible: Monopolar montage (without a re-referencing step) (MP) is preferred for evaluating possible connections between distant areas, in fact the spatial specificity of the recordings is preserved when using monopolar approach [85] [86] and this type of re-referencing highlights the absolute level of electrical activity underneath the active site. At the same time, its limitations is the fact that the referential montage can produce a spectral power map influenced by reference activity [87][87] even if iEEG data have excellent spatial resolution .

The assumptions on which this dissertation is based made it suitable to adopt the classical bipolar re-montage (subtraction of the signal from the adjacent contact) [21]: we applied this method to avoid additive variables. But we found of interest to explore different montages used in published papers.

The re-reference method mainly applied in literature is the bipolar one (BP)[88][89] because it minimizes common electrical noise and it maximizes spatial resolution [24][37]. But bipolar method has many limitations in time series analysis [90] due to: the introduction of unrelated information coming from the two referential time-series; the removing or the alteration of information common to the two referential time-series [90].

The potential pitfalls associated with the use of bipolar EEG for connectivity analysis (coherence analysis) is also recognized [91][90] due to phase distortion signals or to attenuation of coherent signals [48].

Another possible reference method is an independent montage: the common average [87] (MA) used as the reference for each individual reference of interest. In [92][93][94] ERP analysis, in ECOG (Electrocorticography) data, the mean value of every voltage from all channels is subtracted performing a spatial formatting to reduce differences in amplitude.

Another possible method consists of subtracting the signal from an electrode positioned on the scalp [95] [86], but many problems regarding the muscles activity contamination would be so introduced, above all muscle activity shows an important spectral activity in Gamma range.

Arnulfo et al. [48] proposed a novel reference method where electrodes into the grey-matter are referenced to the closest white-matter electrodes (CW), where the white contact is “silent”. CW montage has similar characteristics of MP but its limitation due to volume conduction seems to be overcome. Arnulfo et al. [48] research was focused on the invention of an automated identification technique able to distinguish electrode contacts in grey matter and the distance from contacts in white matter to the white-grey matter surface. G. Arnulfo, kindly, provided us the positions of the white contacts used in this thesis experiments.

We performed connectivity experiments with three re-referencing montages: bipolar (BP), moving average (MA) and closest white contact (CW). As exercise, we compared results of DTF analysis on Gamma band.

In Table 10 the main connection, over the threshold (95^opercentile) for each subject (1:5) are reported. Source and sink channels involved in each connection are also indicated. It is immediately observable that the connections involved in the three re-referencing styles are often not comparable. Results also varied in respect of the signal dataset of every subject (Table 10). The usage of a specific montage has to be selected according to the type of analysis to be performed [96]. These results corroborate the idea that the method re-referencing deeply influence the result.

It is to be noted that all three methods agree in NREM state about the number of main connections that is greater than in WAKE. CW and MA montages appear to provide more similar results with respect to BP.

Bipolar configuration may lead to mix the phases of the signals, and thus connectivity analysis should be performed using non-active reference electrodes. We have a better confidence in CW montage (published by Arnulfo et al. [48]) because it has the same benefits of the unipolar montage together with less drawbacks.

subject	min	max	threshold	main	source	sink
1	0	0,210214	0,199703	0,210214	4	2
2	0	0,301177	0,286118	0,301177	2	6
3	0	0,071934	0,068337	0,071934	7	8
4	0	0,190279	0,180765	0,190279	5	7
5	0	0,214859	0,204116	0,214859	5	7

A. BP montage in WAKE

subject	min	max	threshold	main	source	sink
1	0	0,173092	0,164437	0,173092	4	1
2	0	0,279753	0,265766	0,279753	6	7
3	0	0,366743	0,348406	0,366743	1	7
4	0	0,363329	0,345163	0,363329	6	4
5	0	0,26004	0,247038	0,26004	5	7
				0,251454	5	8

B. CW montage in WAKE

subject	min	Max	threshold	main	source	sink
1	0	0,468768	0,445329	0,468768	4	7
2	0	0,298803	0,283863	0,298803	8	7
3	0	0,500054	0,475051	0,500054	1	3
4	0	0,381167	0,362109	0,381167	5	1
5	0	0,380565	0,361536	0,380565	2	4
				0,37959	4	2

C. MA montage in WAKE

subject	min	Max	threshold	main	source	sink
1	0	0,625411	0,59414	0,624135	4	6
				0,625411	4	7
2	0	0,213903	0,203207	0,213903	8	3
3	0	0,627116	0,59576	0,627116	1	5
4	0	0,758964	0,721015	0,758964	3	5
5	0	0,315229	0,299468	0,315229	8	4

D. BP montage in NREM

subject	min	max	threshold	main	source	sink
1	0	0,49946	0,474487	0,49946	4	3
2	0	0,249817	0,237326	0,249817	6	1
				0,237893	6	4
3	0	0,66173	0,628644	0,66173	1	3
				0,635329	1	8
4	0	0,366152	0,347844	0,366152	3	1
5	0	0,451225	0,428663	0,451225	7	4

E. CW montage in NREM

subject	min	max	threshold	main	source	Sink
1	0	0,409052	0,3886	0,409052	2	7
2	0	0,277482	0,263608	0,270622	3	4
				0,277482	3	6
3	0	0,411662	0,391079	0,411662	1	6
				0,393232	3	1
4	0	0,309324	0,293858	0,309324	4	8

F. MA montage in NREM

Table 10. DTF analysis in three re-referencing styles BP, CW, MA. In Tables A, B, C results from the three re-referencing styles in WAKE condition. D, E, F results from the three re-referencing styles in NREM condition.

4.3 Conclusions

Studies from Connectivity and Wavelet/ANN are compared even if the pre-processing steps and channels involved are not the same. Interestingly, we showed a common result: channels positioned in occipital and parietal areas play a major role for conscious state detection and the information flow is directed from occipital/parietal to frontal area.

The evidence that different methods do not always produce similar results is a pitfall not sufficiently addressed in the literature that should be deeply studied and understood.

The same can be said about the different results due to the re-reference choice.

We discussed about three different re-reference styles: bipolar (BP), moving average (MA) and closest white contact (CW). We compared three methods and we got different connectivity information showing that the method deeply affects the result. The only common agreement is about the number of connections that is greater in NREM than in WAKE. CW and MA montages appear to provide more similar results with respect to BP. Bipolar montage is the most commonly used but we would have preferred not to use it. Bipolar montages could induce cancellation or distortion of the signal; our first choice was to use the monopolar montage (or unipolar, without performing the re-referencing step) that gives priority to connections between far cortex areas and it considers the entire activity of the system. Following discussions with colleagues and literature search we decided to adopt the re-referencing methods discussed in the dissertation: we have greater confidence in CW montage (published by Arnulfo et al.[48]) because it has the same benefits of the unipolar one.

In summary, comparing different signal pre-processing techniques (e.g. filters, different re-reference styles) and different causal directional estimators, we showed that it is not obvious to reach a common and universal result.

5 SUMMARY AND CONCLUSION

We explored and compared two different systems/conditions of the experiment: WAKE (conscious state) vs NREM, N3 (unconscious state).

Data used in the present study derived from a dataset of signals collected during the pre-surgical evaluation in epileptic patients. SPES-SEEG was performed five days after electrode implantation both during wakefulness and during NREM sleep.

This research covers more topics, aiming to:

1. Propose the directional connectivity method (DTF and ADTF) as a model to compare conscious states and as a way to capture information on network dynamics (Chapter 3);
2. Explore mechanisms of brain network able to add information on the differences between conscious and unconscious states (Chapter 3 and Paragraph 4.1);
3. Deal with the problem of finding the location of the cortical sources responsible of the induction of the CCEP (Chapter 3);
4. Show ways and methods for the extraction of features able to differentiate the two conscious states (Chapter 3 and Paragraph 4.1);
5. Explore the phenomena known from literature as down-state and re-activation (Paragraph 3.3);
6. Compare connectivity data obtained from two frequency ranges (Gamma and Delta) (Chapter 3);
7. Indicate a statistical approach for the evaluation of ADTF values (Paragraph 3.3.1);
8. Compare and discuss different re-montage methods (Paragraph 4.2).

In Chapter 3, Section 3.2, we adopted Directed Transfer Function as connectivity measure. We observed that in consciousness particular pathways of cortex areas were activated. We noted that in Gamma band the number of WAKE connections was greater, but the intensity of connection was higher in NREM, this result was also discussed in another our published work where we applied Granger Causality in a bivariate model [97]. We underlined that the main source channels in Delta band were positioned in the Brodmann area. We found that the information flow in the two conscious states have the same direction in

Gamma band, but opposite direction in Delta band. Due to the *inter*-patient variability it was not possible to define a common direction.

It is to be noted that, even if the number of NREM connections was lower, their intensity indicated an important activity during rest state, probably due to a restoration function or memory consolidation. Also the shown change in connectivity direction (NREM opposite to WAKE, only in Delta band) may be associated to some particular structure of the network during re-elaboration step: we can speculate that during NREM the connectivity inverts the direction with respect the activated connectivity during WAKE.

In Chapter 3, Section 3.3, an important part of this dissertation is dedicated to the time-varying Directed Transfer Function analysis of the signals to inquire about the down-state effect and re-activation phenomena. First of all, we observed that the information flow in Gamma band was fragmented compared to the one in Delta band: this effect could be explained by the rapid changes in time in functional end effective connectivity during WAKE. Analyzing ADTF values we observed that the WAKE network had strong connectivity activity, and every sink channel was influenced by many source channels, this effect was clear until 200 ms after the perturbation; the period after that time point showed a smaller amount of activity due to the lower number of influences caused by the source channels. In the same situation, NREM state showed a stable activity lasting all the period but due to few source channels. Furthermore, thanks to ADTF analysis, it was possible to distinguish the primary cortex areas (activated by the stimulus) from the secondary ones which corresponded to longer latencies after an ERP.

In Chapter 3, Section 3.3.1 we applied ANOVA and MANOVA test on ADTF values extracted before and after the expected down-state: we confirmed the presence of different behavior typical of re-activation phenomenon. In fact, we found out the presence of an effect (down-state), placed at a specific time point, able to make changes in the network, and interestingly, according to our data, this effect was not only related to Delta waves but also to Gamma ones. The down-state effect involved different frequency waves and, given that Delta band had the largest power in superficial layers and Gamma band in the deepest ones [48], we can speculate that the down-state affected different layers.

Massimini et al. [20] hypothesized that the presence of the down-state, observed during NREM, and not during WAKE, was not due to the interruption of structural cortico-cortical

and/or cortico- subcortico-cortical connections, but rather to changes in the dynamics of the neuronal responsiveness. We can confirm this hypothesis because we never observed a decrease or a cancellation in connectivity values after the down-state, as the information flow was always present.

As for the results reported in Section 3.3 we can affirm that time varying connectivity analysis was the right choice to reveal down-state presence. We observed that the signal filtering was also necessary to capture directionality and connectivity changes. In fact, the same result was not observable in raw data (Section 3.3.1.3).

Results from Connectivity and Wavelet/ANN analysis have been compared (Section 4.1) and, even if the preprocessing step and channels involved are not the same, interestingly they showed that a common channel, positioned in occipital and parietal areas, played a major role for conscious state detection; moreover, the information flow is commonly directed from occipital/parietal to frontal area.

We must outline that SPES-iEEG analysis, and EEG analysis in general, has some limitations:

1. Due to the data type:

CCEP could not correspond to a completely normal (physiological) network because data have been obtained from patients with intractable epilepsy. Ridley et al. [98] discussed the above mentioned problem, but also noticed that connectivity correlation in time is present between healthy areas and missing within epileptic areas. In the light of this study, the hypothesis is that working on selected, physiological channels the results obtained may be representative of a wider population.

2. Due to the experimental protocol:

The protocol was established for medical reasons. Different choices would give rise to different results, depending on:

- Type of electrode used. A 1 mm^2 electrode can record the activity of a modest number of neurons, while, with a few mm electrodes, such as those commonly used, the most general aspects of the brain's electrical or magnetic activity are captured. The spatial resolution obtainable by EEG electrodes and MEG sensors is around 1 cm^2 , corresponding to the average activity of about 10 million cortical neurons. In our experiment the electrodes had a diameter of 0.8 mm.

- Electrode implantation sites (e.g., implantation in only one hemisphere or in just some lobes)
- Stimulation site position and spatial relationships with other channels
- CCEP amplitude or morphology that may change depending on the patient conditions (e.g. the presence of pathology such as metabolic disorder, infections...)
- Data acquisition protocol such as stimulation session duration, intervals, sampling rate. (e.g. the analysis performed in the Delta frequency band can be problematic given the limited data length: the observed windows covered only some or very few cycles of the Delta oscillations.
- Patients were treated with antiepileptic therapies during iEEG recordings: drug effects could reflect on EEG activity and changed connectivity. In any case, the signals were processed *ceteris paribus*, so any change in connectivity would be present for all the patient. Given that the main issue of the thesis is to identify a method to distinguish between two different conscious states, a change in the connections configuration should not devalue our findings.

3. Due to the preprocessing step:

we compared three re-referencing methods, widely used in literature, and we obtained different connectivity information showing that the method deeply affected the results. We compared Bipolar Montage, Closest-White montage and Moving Averaging one, and we can confirm quite different results depending on methods and procedures (Section 4.2).

4. Due to non-stationarity of signals:

We are aware that the use of DTF is a critical issue, as it assumes data stationarity, whereas non stationary effects are present due to the evoked response. We decided to use DTF and ADTF in order to analyze two different aspects of the research project: DTF method was chosen to underline the network connectivity, comparing it between the two consciousness states; the ADTF method was chosen to shed light on the known down-state effect paying attention on a defined temporal slice. Due to the extreme sensitivity of the results to the choice of patients, analysis methods, preprocessing, re-reference, immediately evident from the first analyses and fully detailed in the thesis, the use of two procedures founded on the same theoretical bases appeared to us a valid precondition to create an analysis framework as homogeneous as possible.

Thus we limited the problem of non-stationarity through the segmentation of signals in windows (this step was applied in the toolbox eConnectome): AR models were estimated in every short temporal sliding windows where the process is assumed to be (locally) stationary: this is one of the possible methods to reach quasi-stationarity [60][61] (see also Section 2.1). Another approach to perform DTF would be analyzing the background EEG activity after removing the evoked response, and to perform ADTF analysis to the data containing both evoked and background activity.

5. Due to high *inter*-patient variability:

The main limitation is that it is not possible to generalize: *inter* individual variability. This is a known limit of many similar studies: but case reports are a typical way to add knowledge and useful considerations to a framework. We aim to reinforce and corroborate in future our results by increasing number of subjects, channels, sessions, stimulation points and preprocessing methods. A massive data analysis of such collection could be more indicative and useful for a hypothesis confirmation, allowing to increase the possibility to achieve a positive matching among patients' parameters.

The presented work offers a first step for a WAKE/NREM distinction and characterization using a physiologic human dataset that provides excellent spatial and temporal resolution.

The variability of the results, that depends on the *inter*-patients variability and on the methods used (both re-reference and analysis), showed that the path towards a satisfying understanding of brain connectivity and the ability to distinguish states of consciousness and unconsciousness is still far away. Not only connectivity and other studied parameters (e.g. down-state) depend on reference and method, but are clearly different from subject to subject.

This finding would be less severe if a unique criterion existed: the literature on this topic is extremely deficient, while researchers are more keen to choose a preferred method and conduct their analysis on the basis of this choice without applying other methods and trying to explain the differences that emerged.

In future works we would like to:

- 1.** Enhance data robustness: increasing the i) number of subjects and ii) number of channels under analysis;

2. Varying the time series length;
3. Considering also other frequency ranges;
4. Extract other characteristics from CCEP in order to find out new parameters to distinguish the two consciousness states.
5. Apply feature extraction methods for the identification of the down-state and re-activation effects

The problem of interpreting the meaning of different results from different analysis methods remains unchanged and pressing: but its solution passes through the progress of neuroscience and more accurate neurophysiological studies.

ACKNOWLEDGEMENTS

I would like to thank my supervisor, Prof.ssa Rita Pizzi, who suggested the Computer Science Ph.D. program to me, allowing me to specialize and improve my skills. I also wish to thank Prof.ssa Pizzi for her professional guidance as well as for her personal support.

I would like to thank Prof. Marcello Massimini, Dr. Andrea Pigorini, Dr. Simone Sarasso (Dept. of Biomedical and Clinical Sciences “L. Sacco”, University of Milan) and Gabriele Arnulfo (Dept. of Informatics, Bioengineering, Robotics, and System Engineering, University of Genova) for providing signal data set and for the technical discussions had.

I thank the Referees Prof. Luca Faes (Dept. of Energy, Information engineering and Mathematical models, University of Palermo), Prof. Ferruccio Panzica (Operative Unit of Neurophysiopathology and diagnostic epileptology, Istituto Neurologico C. Besta, Milano) and Prof. Jesus Gomez-Gardeñes (Dept. de Física de la Materia Condensada, Universidad de Zaragoza) for their precious remarks.

Above all, I want to acknowledge the invaluable contribution of Dr. Massimo Walter Rivolta and Prof. Roberto Sassi (Department of Computer Science, University of Milan), for their irreplaceable support, multiple technical suggestions and thoughtful encouragement.

Thanks to my friends, colleagues, supporters and coffee break buddies: Massimo Rivolta, Marco Casazza, Guido Lena Cota, Andrea Taverna e Marialessia Musumeci. Thank you for your professionalism and for always being there for me when I needed you.

A big thank you to my family, especially to my mother, Grandma, for her strength in my absence; and to my sister, Giorgia, for the late night thesis revisions. Thanks to my best friend, Ing. Valeria Festa, for the brainstorming sessions had.

All this work has been possible thanks to my mother, Massimo Rivolta and my determination. And I would like this to serve as a lesson for Matilda and Nicole: to persevere despite great many difficulties and obstacles.

REFERENCES

- [1] M. Di Luca, M. Baker, R. Corradetti, H. Kettenmann, J. Mendlewicz, J. Olesen, I. Ragan, and M. Westphal, “Consensus document on European brain research,” *Eur. J. Neurosci.*, vol. 33, pp. 768–818, 2011.
- [2] O. Sporns, *Discovering the Human Connectome*. MIT Press, 2012.
- [3] O. Sporns, *Networks of the Brain*. MIT Press, 2010.
- [4] O. Sporns, G. Tononi, and R. Kötter, “The human connectome: A structural description of the human brain,” *PLoS Comput. Biol.*, vol. 1, no. 4, pp. 0245–0251, 2005.
- [5] P. Hagmann, L. Cammoun, X. Gigandet, R. Meuli, C. J. Honey, J. Van Welden, and O. Sporns, “Mapping the structural core of human cerebral cortex,” *PLoS Biol.*, vol. 6, no. 7, pp. 1479–1493, 2008.
- [6] R. Gutiérrez, A. Amann, S. Assenza, J. Gómez-Gardeñes, V. Latora, and S. Boccaletti, “Emerging meso- and macroscales from synchronization of adaptive networks,” *Phys. Rev. Lett.*, vol. 107, no. 23, 2011.
- [7] K. J. Friston, “Functional and Effective Connectivity: A Review,” *Brain Connect.*, vol. 1, no. 1, pp. 13–36, 2011.
- [8] D. Zhou, W. K. Thompson, and G. Siegle, “MATLAB Toolbox for Functional Connectivity,” *Neuroimage*, vol. 47, no. 4, pp. 1590–1607, 2009.
- [9] K. J. Friston, L. Harrison, and W. Penny, “Dynamic causal modelling,” vol. 19, pp. 1273–1302, 2003.
- [10] R. Matsumoto, D. R. Nair, E. LaPresto, I. Najm, W. Bingaman, H. Shibasaki, and H. O. Lüders, “Functional connectivity in the human language system: A cortico-cortical evoked potential study,” *Brain*, vol. 127, no. 10, pp. 2316–2330, 2004.
- [11] J. Schrouff, V. Perlberg, M. Boly, G. Marrelec, P. Boveroux, A. Vanhaudenhuyse, M. A. Bruno, S. Laureys, C. Phillips, M. Péligrini-Issac, P. Maquet, and H. Benali, “Brain functional integration decreases during propofol-induced loss of consciousness,” *Neuroimage*, vol. 57, no. 1, pp. 198–205, 2011.
- [12] J. C. Mosher, L. Jehi, A. R. Antony, A. V Alexopoulos, J. A. Gonza, R. C. Burgess, N. K. So, and R. F. Gala, “Functional Connectivity Estimated from Intracranial EEG Predicts Surgical Outcome in Intractable Temporal Lobe Epilepsy,” *PLoS One*, vol. 8, no. 10, pp. 1–7, 2013.
- [13] A. Brovelli, M. Ding, A. Ledberg, Y. Chen, R. Nakamura, and S. L. Bressler, “Beta oscillations in a large-scale sensorimotor cortical network: directional influences revealed by Granger causality,” in *Proceedings of the National Academy of Sciences of the United States of America*, 2004, vol. 101, no. 26, pp. 9849–9854.
- [14] M. Boly, M. R. Coleman, M. H. Davis, A. Hampshire, D. Bor, G. Moonen, P. A. Maquet, J. D. Pickard, S. Laureys, and A. M. Owen, “When thoughts become action: An fMRI paradigm to study volitional brain activity in non-communicative brain injured patients,” *Neuroimage*, vol. 36, no. 3, pp. 979–992, 2007.

- [15] A. M. Owen and M. R. Coleman, “Detecting awareness in the vegetative state,” *Ann. N. Y. Acad. Sci.*, vol. 1129, pp. 130–138, 2008.
- [16] G. Tononi, “An information integration theory of consciousness.,” *BMC Neurosci.*, vol. 5, p. 42, 2004.
- [17] G. Tononi, “A Bit of Theory: Consciousness as Integrated Information,” *Encyclopedia of Consciousness*, vol. 2. pp. 8–10, 2008.
- [18] A. K. Seth, Z. Dienes, A. Cleeremans, M. Overgaard, and L. Pessoa, “Measuring consciousness: relating behavioural and neurophysiological approaches,” *Trends Cogn. Sci.*, vol. 12, no. 8, pp. 314–321, 2008.
- [19] G. Tononi and G. M. Edelman, “Consciousness and Complexity,” *Sci. Compass*, vol. 282, no. 5395, pp. 1846–1851, 1998.
- [20] M. Massimini, F. Ferrarelli, S. Sarasso, and G. Tononi, “Cortical mechanisms of loss of consciousness: Insight from TMS/EEG studies,” *Arch. Ital. Biol.*, vol. 150, no. 2–3, pp. 44–55, 2012.
- [21] A. Pigorini, S. Sarasso, P. Proserpio, C. Szymanski, G. Arnulfo, S. Casarotto, M. Fecchio, M. Rosanova, M. Mariotti, G. Lo Russo, M. J. Palva, L. Nobili, and M. Massimini, “Bistability breaks-off deterministic responses to intracortical stimulation during non-REM sleep,” *Neuroimage*, vol. 112, pp. 105–113, 2015.
- [22] A. Bartels and S. Zeki, “The chronoarchitecture of the cerebral cortex,” *Philos. Trans. R. Soc. B Biol. Sci.*, vol. 360, no. 1456, pp. 733–750, 2005.
- [23] a. G. Casali, O. Gosseries, M. Rosanova, M. Boly, S. Sarasso, K. R. Casali, S. Casarotto, M. -a. Bruno, S. Laureys, G. Tononi, and M. Massimini, “A Theoretically Based Index of Consciousness Independent of Sensory Processing and Behavior,” *Sci. Transl. Med.*, vol. 5, no. 198, p. 198ra105-198ra105, 2013.
- [24] S. S. Cash, E. Halgren, N. Dehghani, A. O. Rossetti, T. Thesen, E. Bromfield, and L. Ero, “The Human K-Complex Represents an isolated Cortical Down-State,” *Science (80-.)*, vol. 324, no. May, pp. 1084–1088, 2009.
- [25] M. Steriade and F. Amzica, “Intracortical and corticothalamic coherency of fast spontaneous oscillations.,” *Proc. Natl. Acad. Sci. U. S. A.*, vol. 93, no. 6, pp. 2533–2538, 1996.
- [26] D. Contreras, I. Timofeev, and M. Steriade, “Mechanisms of long-lasting hyperpolarizations underlying slow sleep oscillations in cat corticothalamic networks.,” *J. Physiol.*, vol. 494, no. 1, pp. 251–264, 1996.
- [27] S. Sarasso, M. Boly, M. Napolitani, O. Gosseries, V. Charland-Verville, S. Casarotto, M. Rosanova, A. G. Casali, J. F. Brichant, P. Boveroux, S. Rex, G. Tononi, S. Laureys, and M. Massimini, “Consciousness and complexity during unresponsiveness induced by propofol, xenon, and ketamine,” *Curr. Biol.*, vol. 25, no. 23, pp. 3099–3105, 2015.
- [28] A. Pigorini, A. G. Casali, S. Casarotto, F. Ferrarelli, G. Baselli, M. Mariotti, M. Massimini, and M. Rosanova, “Time-frequency spectral analysis of TMS-evoked EEG oscillations by means of Hilbert-Huang transform,” *Journal of Neuroscience Methods*, vol. 198, no. 2. pp. 236–245, 2011.

- [29] R. Peraita-Adrados, “Electroencephalography, polysomnography, and other sleep recording systems.,” in *The Physiologic Nature of Sleep*, 2005, p. 103–122.
- [30] M. H. Silber, S. Ancoli-Israel, M. H. Bonnet, S. Chokroverty, M. M. Grigg-Damberger, M. Hirshkowitz, S. Kapen, S. A. Keenan, M. H. Kryger, T. Penzel, M. R. Pressman, and C. Iber, “The visual scoring of sleep in adults,” *J. Clin. Sleep Med.*, vol. 3, no. 2, pp. 121–131, 2007.
- [31] H. K. Di Meir, T. Roth, and C. William, *Principles and practice of sleep medicine*, Sth. Philadelphia, PA: Elsevier Inc., 2017.
- [32] G. Orellana, C. M. Held, P. A. Estevez, C. A. Perez, S. Reyes, C. Algarin, and P. Peirano, “A balanced sleep/wakefulness classification method based on actigraphic data in adolescents,” in *Annual International Conference of the IEEE Engineering in Medicine and Biology Society.*, 2014, pp. 4188–4191.
- [33] W. Karlen, C. Mattiussi, and D. Floreano, “Sleep and wake classification with ECG and respiratory effort signals,” *IEEE Trans. Biomed. Circuits Syst.*, vol. 3, no. 2, pp. 71–78, 2009.
- [34] W. Hayet and Y. Slim, “Sleep-wake stages classification based on heart rate variability,” in *2012 5th International Conference on BioMedical Engineering and Informatics*, 2012, no. Bmei, pp. 996–999.
- [35] C. M. Reed, K. G. Birch, J. Kamiński, S. Sullivan, J. M. Chung, A. N. Mamelak, and U. Rutishauser, “Automatic detection of periods of slow wave sleep based on intracranial depth electrode recordings,” *J. Neurosci. Methods*, vol. 282, pp. 1–8, 2017.
- [36] T. Andrillon, Y. Nir, R. J. Staba, F. Ferrarelli, C. Cirelli, G. Tononi, and F. Itzhak, “Sleep spindles in humans: insights from intracranial EEG and unit recordings,” *J Neurosci.*, vol. 31, no. 49, pp. 17821–17834, 2011.
- [37] R. Gaillard, S. Dehaene, C. Adam, S. Clemenceau, D. Hasboun, M. Baulac, L. Cohen, and L. Naccache, “Converging Intracranial Markers of Conscious Access,” *PLoS Biol.*, vol. 7, no. 3, pp. 0472–0492, 2009.
- [38] L. N. and B. D. V. V. Jui-Yang Chang, Andrea Pigorini, Marcello Massimini, Giulio Tononi, “Multivariate autoregressive models with exogenous inputs for intracerebral responses to direct electrical stimulation of the human brain,” *Front. Hum. Neurosci.*, vol. 6, no. November, 2012.
- [39] M. J. Rasch, “Analysis of Neural Signals : Interdependence , Information Coding , and Relation to Network Models,” Graz University of Tecnology, 2008.
- [40] R. Matsumoto, D. R. Nair, E. LaPresto, I. Najm, W. Bingaman, H. Shibasaki, and H. O. Lüders, “Functional connectivity in the human language system: A cortico-cortical evoked potential study,” *Brain*, vol. 127, no. 10, pp. 2316–2330, 2004.
- [41] T. Kunieda, Y. Yamao, T. Kikuchi, and R. Matsumoto, “New Approach for Exploring Cerebral Functional Connectivity: Review of Cortico-cortical Evoked Potential,” *Neurol. Med. Chir. (Tokyo).*, vol. 55, no. 5, pp. 374–382, 2015.
- [42] M. Steriade, a Nuñez, and F. Amzica, “A novel slow (< 1 Hz) oscillation of neocortical neurons in vivo: depolarizing and hyperpolarizing components.,” *J. Neurosci.*, vol. 13, no. 8, pp. 3252–3265, 1993.

- [43] G. T. Neske, “The Slow Oscillation in Cortical and Thalamic Networks: Mechanisms and Functions,” *Front. Neural Circuits*, vol. 9, no. January, pp. 1–25, 2016.
- [44] M. Steriade, F. Amzica, and a Nuñez, “Cholinergic and noradrenergic modulation of the slow (approximately 0.3 Hz) oscillation in neocortical cells,” *J. Neurophysiol.*, vol. 70, no. 4, pp. 1385–1400, 1993.
- [45] B. He, Y. Dai, L. Astolfi, F. Babiloni, H. Yuan, and L. Yang, “EConnectome: A MATLAB toolbox for mapping and imaging of brain functional connectivity,” *J. Neurosci. Methods*, vol. 195, no. 2, pp. 261–269, 2011.
- [46] L. Astolfi, F. Cincotti, D. Mattia, C. Babiloni, F. Carducci, a. Basilisco, P. M. Rossini, S. Salinari, L. Ding, Y. Ni, B. He, and F. Babiloni, “Assessing cortical functional connectivity by linear inverse estimation and directed transfer function: Simulations and application to real data,” *Clin. Neurophysiol.*, vol. 116, no. 4, pp. 920–932, 2005.
- [47] E. Nyhus and T. Curran, “Neuroscience and Biobehavioral Reviews Functional role of gamma and theta oscillations in episodic memory,” *Neurosci. Biobehav. Rev.*, vol. 34, no. 7, pp. 1023–1035, 2010.
- [48] G. Arnulfo, J. Hirvonen, L. Nobili, S. Palva, and J. M. Palva, “Phase and amplitude correlations in resting-state activity in human stereotactical EEG recordings,” *Neuroimage*, vol. 112, pp. 114–127, 2015.
- [49] A. Sinai, “Electrocorticographic high gamma activity versus electrical cortical stimulation mapping of naming,” *Brain*, vol. 128, no. 7, pp. 1556–1570, 2005.
- [50] K. J. Blinowska, “Review of the methods of determination of directed connectivity from multichannel data,” *Med. Biol. Eng. Comput.*, vol. 49, no. 5, pp. 521–529, 2011.
- [51] M. Winterhalder, B. Schelter, W. Hesse, K. Schwab, L. Leistritz, D. Klan, R. Bauer, J. Timmer, and H. Witte, “Comparison of linear signal processing techniques to infer directed interactions in multivariate neural systems,” *Signal Processing*, vol. 85, no. 11, pp. 2137–2160, 2005.
- [52] Luca Faes and Giandomenico Nollo, “Multivariate Frequency Domain Analysis of Causal Interactions in Physiological Time Series,” in *Biomedical Engineering, Trends in Electronics, Communications and Software*, A. Laskovski, Ed. 2011, pp. 403–428.
- [53] L. Faes, S. Erla, and G. Nollo, “Measuring connectivity in linear multivariate processes: Definitions, interpretation, and practical analysis,” *Comput. Math. Methods Med.*, vol. 2012, 2012.
- [54] S. M. Kay, *Modern Spectral Estimation: Theory & Application*. NJ, USA: Englewood Cliffs, N.J Prentice Hall, 1988.
- [55] Hirotugu Akaike, “Autoregressive model fitting for control,” *Ann. Inst. Stat. Math.*, vol. 23, no. 1, pp. 163–180, 1971.
- [56] G. Schwarz, “Estimating the Dimension of a Model,” *Ann. Stat.*, vol. 6, no. 2, pp. 461–464, 1978.

- [57] C. W. J. Granger and P. Newbold, “Spurious Regressions in Econometrics,” *A Companion to Theor. Econom.*, vol. 2, pp. 557–561, 2007.
- [58] D. W. Gow and D. N. Caplan, “New Levels of Language Processing Complexity and Organization Revealed by Granger Causation,” *Front. Psychol.*, vol. 3, no. November, pp. 1–11, 2012.
- [59] M. Ding, S. L. Bressler, W. Yang, and H. Liang, “Short-window spectral analysis of cortical event-related potentials by adaptive multivariate autoregressive modeling: data preprocessing, model validation, and variability assessment,” *Biol. Cybern.*, vol. 83, no. 1, pp. 35–45, 2000.
- [60] I. Gath and G. F. Inbar, “Advances in Processing and Pattern Analysis of Biological Signals,” 1996.
- [61] L. A. B. Koichi Sameshima, *Methods in Brain Connectivity Inference through Multivariate Time Series Analysis*. 2014.
- [62] F. Babiloni, C. Babiloni, F. Carducci, P. M. Rossini, A. Basilisco, L. Astolfi, F. Cincotti, L. Ding, Y. Ni, J. Cheng, K. Christine, J. Sweeney, and B. He, “Estimation of the cortical connectivity during a finger-tapping movement with multimodal integration of EEG and fMRI recordings,” *International Congress Series*, vol. 1270, pp. 126–129, 2004.
- [63] L. Astolfi, F. Cincotti, D. Mattia, F. De Vico Fallani, A. Colosimo, S. Salinari, M. G. Marciani, M. Ursino, M. Zavaglia, W. Hesse, H. Witte, and F. Babiloni, “Time-varying cortical connectivity by adaptive multivariate estimators applied to a combined foot-lips movement,” *Annu. Int. Conf. IEEE Eng. Med. Biol. - Proc.*, pp. 4402–4405, 2007.
- [64] M. Arnold, W. H. R. Miltner, H. Witte, R. Bauer, and C. Braun, “Adaptive AR modeling of nonstationary time series by means of kaiman filtering,” *IEEE Trans. Biomed. Eng.*, vol. 45, no. 5, pp. 545–552, 1998.
- [65] T. Milde, L. Leistriz, L. Astolfi, W. H. R. Miltner, T. Weiss, F. Babiloni, and H. Witte, “A new Kalman filter approach for the estimation of high-dimensional time-variant multivariate AR models and its application in analysis of laser-evoked brain potentials,” *Neuroimage*, vol. 50, no. 3, pp. 960–969, 2010.
- [66] M. J. Kamifiski and K. J. Bfinowska, “A new method of the description of the information flow in the brain structures,” *Biol. Cybern.*, vol. 65, pp. 203–210, 1991.
- [67] S. Salinari, “Modelli autoregressivi per la connettività tra segnali biologici - Corso di Modelli di Sistemi Biologici,” Università di Roma “La Sapienza” -Fondazione S.Lucia IRCCS.
- [68] L. Astolfi and S. Salinari, “Modelli autoregressivi per la stima della connettività tra segnali biologici-Corso di Modelli di Sistemi Biologici,” Università di Roma “La Sapienza” -Fondazione S.Lucia IRCCS.
- [69] F. Babiloni, F. Cincotti, C. Babiloni, F. Carducci, D. Mattia, L. Astolfi, A. Basilisco, P. M. Rossini, L. Ding, Y. Ni, J. Cheng, K. Christine, J. Sweeney, and B. He, “Estimation of the cortical functional connectivity with the multimodal integration of high-resolution EEG and fMRI data by directed transfer function,” *Neuroimage*, vol. 24, no. 1, pp. 118–131, 2005.

- [70] C. Wilke, L. Ding, and B. He, “Estimation of time-varying connectivity patterns through the use of an adaptive directed transfer function,” *IEEE Trans Biomed Eng*, vol. 55, no. 11, pp. 2557–2564, 2008.
- [71] B. He, Y. Dai, L. Astolfi, F. Babiloni, H. Yuan, and L. Yang, “eConnectome: A MATLAB toolbox for mapping and imaging of brain functional connectivity,” *J Neurosci Methods*, vol. 195, no. 2, pp. 261–269, 2011.
- [72] C. Wilke, W. Van Drongelen, M. Kohrman, and B. He, “Neocortical seizure foci localization by means of a directed transfer function method,” *Epilepsia*, vol. 51, no. 4, pp. 564–572, 2010.
- [73] J. Theiler, S. Eubank, A. Longtin, B. Galdrikian, and J. Doynne Farmer, *Testing for nonlinearity in time series: the method of surrogate data*, vol. 58, no. 1–4. 1992.
- [74] L. Ding, G. A. Worrell, T. D. Lagerlund, and B. He, “Ictal Source Analysis: Localization and Imaging of Causal Interactions in Humans,” *Neuroimage*, vol. 34, no. 2, pp. 575–586, 2007.
- [75] Niedermeyer E. and F. L. da Silva, *Electroencephalography: Basic Principles, Clinical Applications, and Related Fields*. 2004.
- [76] C. Destrieux, B. Fischl, A. Dale, and E. Halgren, “Automatic parcellation of human cortical gyri and sulci using standard anatomical nomenclature,” *Neuroimage*, vol. 53, no. 1, pp. 1–15, 2010.
- [77] T. S. Arnold Neumaier, “Estimation of parameters and eigenmodes of multivariate autoregressive models.,” *ACM Trans. Math. Softw.*, vol. 27, no. 1, pp. 27–57, 2001.
- [78] T. Schneider and A. Neumaier, “Algorithm 808: ARfit---a matlab package for the estimation of parameters and eigenmodes of multivariate autoregressive models,” *ACM Trans. Math. Softw.*, vol. 27, no. 1, pp. 58–65, 2001.
- [79] R. E. Greenblatt, M. E. Pflieger, and A. E. Ossadtchi, “Connectivity measures applied to human brain electrophysiological data,” *J. Neurosci. Methods*, vol. 207, no. 1, pp. 1–16, 2012.
- [80] T. Rutigliano, M. W. Rivolta, P. Rita, and S. Roberto, “Composition of Feature Extraction Methods Shows Interesting Performances in Discriminating Wakefulness and NREM Sleep,” *IEEE Signal Process. Lett.*, 2017.
- [81] D. Senkowski, T. R. Schneider, J. J. Foxe, and A. K. Engel, “Crossmodal binding through neural coherence: implications for multisensory processing,” *Trends Neurosci.*, vol. 31, no. 8, pp. 401–409, 2008.
- [82] D. Senkowski, D. Saint-Amour, T. Gruber, and J. J. Foxe, “Look who’s talking: The deployment of visuo-spatial attention during multisensory speech processing under noisy environmental conditions,” *Neuroimage*, vol. 43, no. 2, pp. 379–387, 2008.
- [83] R. Campbell, C. A. Heywood, A. Cowey, M. Regard, and T. Landis, “Sensitivity to eye gaze in prosopagnosic patients and monkeys with superior temporal sulcus ablation,” *Neuropsychologia*, vol. Volume 28, no. 11, pp. 1123–1142, 1990.
- [84] C. Koch, M. Massimini, M. Boly, and G. Tononi, “Neural correlates of consciousness: progress and problems,” *Nat. Rev. Neurosci.*, vol. 17, no. 5, pp. 307–321, 2016.

- [85] N. Singer, I. Podlipsky, and F. Esposito, “Distinct iEEG activity patterns in temporal-limbic and prefrontal sites induced by emotional intentionality,” *CORTEX*, vol. 60, pp. 121–138, 2014.
- [86] S. Hu, Y. Cao, S. Chen, J. Zhang, and W. Kong, “A Comparative Study of Two Reference Estimation Methods in EEG Recording,” in *BICS 2012: Advances in Brain Inspired Cognitive Systems*, 2012, no. 2009, pp. 321–328.
- [87] D. Lehmann, *Principles of spatial analysis. Methods of Analysis of Brain Electrical and Magnetic Signals (Handbook of Electroencephalography and Clinical Neurophysiology, Rev Series)*. Methods of Analysis of Brain Electrical and Magnetic Signals, 1987.
- [88] M. Perrone-Bertolotti, J. Kujala, J. R. Vidal, C. M. Hamame, T. Ossandon, O. Bertrand, L. Minotti, P. Kahane, K. Jerbi, and J.-P. Lachaux, “How Silent Is Silent Reading? Intracerebral Evidence for Top-Down Activation of Temporal Voice Areas during Reading,” *J. Neurosci.*, vol. 32, no. 49, pp. 17554–17562, 2012.
- [89] H. Zaveri, R. Duckrow, and S. Spencer, “The effect of a scalp reference signal on coherence measurements of intracranial electroencephalograms,” *Clin Neurophysiol*, vol. 111, no. 7, pp. 1293–9, 2000.
- [90] H. P. Zaveri, R. B. Duckrow, and S. S. Spencer, “On the use of bipolar montages for time-series analysis of intracranial electroencephalograms,” vol. 117, pp. 2102–2108, 2006.
- [91] H. P. Zaveri, R. B. Duckrow, and S. S. Spencer, “The effect of a scalp reference signal on coherence measurements of intracranial electroencephalograms,” *Clin. Neurophysiol.*, vol. 111, pp. 1293–1299, 2000.
- [92] N. E. Crone, D. Boatman, B. Gordon, and L. Hao, “Induced electrocorticographic gamma activity during auditory perception,” *Clin. Neurophysiol.*, vol. 112, no. 4, pp. 565–582, 2001.
- [93] Boatman-Reich, “Quantifying auditory event-related responses in multichannel human intracranial recordings,” *Front. Comput. Neurosci.*, vol. 4, no. March, pp. 1–17, 2010.
- [94] D. B.- Sinaia A, Cronea N.E. , Wieda H.M., Franaszczuka P.J. , Migliorettib D. and Reicha D., “Intracranial mapping of auditory perception: Event-related responses and electrocortical stimulation,” *Clin Neurophysiol*, vol. 120, no. 1, 2009.
- [95] S. Hu, M. Stead, and G. a. Worrell, “Automatic identification and removal of scalp reference signal for intracranial eegs based on independent component analysis,” *IEEE Trans. Biomed. Eng.*, vol. 54, no. 9, pp. 1560–1572, 2007.
- [96] S. C. Ng and P. Raveendran, “Comparison of different Montages on to {EEG} classification,” *3rd Kuala Lumpur Int. Conf. Biomed. Eng. 2006*, vol. 15, pp. 365–368, 2007.
- [97] R. Pizzi, T. Rutigliano, M. Musumeci, and M. Pregolato, “Using Granger Causality to assess the interaction between brain areas during different consciousness states,” *Int. J. Biol. Biomed. Eng.*, vol. 10, pp. 241–247, 2016.
- [98] B. Ridley, J. Wirsich, G. Bettus, R. Rodionov, T. Murta, U. Chaudhary, D. Carmichael, R. Thornton, S. Vulliemoz, A. McEvoy, F. Wendling, F. Bartolomei,

J.-P. Ranjeva, L. Lemieux, and M. Guye, "Simultaneous Intracranial EEG-fMRI Shows Inter-Modality Correlation in Time-Resolved Connectivity Within Normal Areas but Not Within Epileptic Regions," *Brain Topogr.*, vol. 0, no. 0, p. 0, 2017.